APP Template V1.70 Article id: joptaa0bbf Typesetter: MPS Date received by MPS: 22/04/2016 PE: MAC003439 CE: LE:

IOP Publishing Journal of Optics

J. Opt. **00** (2016) 000000 (48pp)

Roadmap

Roadmap on optical energy conversion

Svetlana V Boriskina[1,25], Martin A Green[2], Kylie Catchpole[3], Eli Yablonovitch[4,5], Matthew C Beard[6], Yoshitaka Okada[7], Stephan Lany[6], Talia Gershon[8], Andriy Zakutayev[6], Mohammad H Tahersima[9], Volker J Sorger[9], Michael J Naughton[10], Krzysztof Kempa[10], Mario Dagenais[11], Yuan Yao[12], Lu Xu[12], Xing Sheng[13], Noah D Bronstein[14], John A Rogers[12,13], A Paul Alivisatos[14,4,24], Ralph G Nuzzo[12,13], Jeffrey M Gordon[15], Di M Wu[16], Michael D Wisser[17], Alberto Salleo[17], Jennifer Dionne[17], Peter Bermel[18], Jean-Jacques Greffet[19], Ivan Celanovic[20], Marin Soljacic[20], Assaf Manor[21], Carmel Rotschild[21], Aaswath Raman[23], Linxiao Zhu[23], Shanhui Fan[23] and Gang Chen[1]

[1] Department of Mechanical Engineering, Massachusetts Institute of Technology, Cambridge, MA, 02139, USA
[2] Australian Centre for Advanced Photovoltaics (ACAP), School of Photovoltaic and Renewable Energy Engineering, University of New South Wales, Sydney, Australia
[3] Centre for Sustainable Energy Systems, Research School of Engineering, Australian National University, Canberra, A.C.T. 2601, Australia
[4] Material Sciences Division, Lawrence Berkeley National Laboratory, Berkeley, CA 94720, USA
[5] Electrical Engineering and Computer Sciences Department, University of California, Berkeley, CA 94720, USA
[6] National Renewable Energy Laboratory, 15013 Denver West Pkwy, Golden, CO 80401, USA
[7] Research Center for Advanced Science and Technology, University of Tokyo, 4-6-1 Komaba, Meguro-ku, Tokyo, Japan
[8] IBM T J Watson Research Center, 1101 Kitchawan Rd, Yorktown Heights, NY 10598, USA
[9] Department of Electrical and Computer Engineering, George Washington University, 801 22nd Street NW, Washington, DC 20052, USA
[10] Department of Physics, Boston College, Chestnut Hill, MA 02467, USA
[11] University of Maryland at College Park, Department of Electrical Engineering, MD 20742, USA
[12] Department of Chemistry, Frederick Seitz Materials Research Laboratory, University of Illinois at Urbana-Champaign, Urbana, IL 61801, USA
[13] Department of Materials Science and Engineering, University of Illinois at Urbana Champaign, Urbana, IL 61801, USA
[14] Department of Chemistry, University of California, Berkeley, CA 94720, USA
[15] Department of Solar Energy & Environmental Physics, Blaustein Institutes for Desert Research, Ben-Gurion University of the Negev, Sede Boqer Campus 84990, Israel
[16] Department of Chemistry, Stanford University, 333 Campus Drive, Stanford, CA, USA
[17] Department of Materials Science and Engineering, Stanford University, 496 Lomita Mall, Stanford, CA, USA
[18] Purdue University, Electrical and Computer Engineering, Birck Nanotechnology Center, 1205 West State Street, West Lafayette, IN 47907, USA
[19] Laboratoire Charles Fabry, Institut d'Optique, CNRS, Université Paris-Saclay, 2 av Fresnel, 91127 Palaiseau, France
[20] Department of Physics, Massachusetts Institute of Technology, Cambridge, MA 02139, USA
[21] Russel Berrie Nanotechnology Institute, Technion-Israel Institute of Technology, Haifa 32000, Israel
[22] Department of Mechanical Engineering, Technion-Israel Institute of Technology, Haifa 32000, Israel
[23] Department of Electrical Engineering, Stanford University, Stanford, CA 94305, USA

[24] Department of Materials Science and Engineering, Kavli Energy NanoScience Institute, University of California, Berkeley, California 94720, USA
[25] Guest editor of the Roadmap

E-mail: sborisk@mit.edu

Received 17 August 2015, revised 18 November 2015
Accepted for publication 18 November 2015
Published DD MM 2016

Abstract

For decades, progress in the field of optical (including solar) energy conversion was dominated by advances in the conventional concentrating optics and materials design. In recent years, however, conceptual and technological breakthroughs in the fields of nanophotonics and plasmonics combined with a better understanding of the thermodynamics of the photon energy-conversion processes reshaped the landscape of energy-conversion schemes and devices. Nanostructured devices and materials that make use of size quantization effects to manipulate photon density of states offer a way to overcome the conventional light absorption limits. Novel optical spectrum splitting and photon-recycling schemes reduce the entropy production in the optical energy-conversion platforms and boost their efficiencies. Optical design concepts are rapidly expanding into the infrared energy band, offering new approaches to harvest waste heat, to reduce the thermal emission losses, and to achieve noncontact radiative cooling of solar cells as well as of optical and electronic circuitries. Light–matter interaction enabled by nanophotonics and plasmonics underlie the performance of the third- and fourth-generation energy-conversion devices, including up- and down-conversion of photon energy, near-field radiative energy transfer, and hot electron generation and harvesting. Finally, the increased market penetration of alternative solar energy-conversion technologies amplifies the role of cost-driven and environmental considerations. This roadmap on optical energy conversion provides a snapshot of the state of the art in optical energy conversion, remaining challenges, and most promising approaches to address these challenges. Leading experts authored 19 focused short sections of the roadmap where they share their vision on a specific aspect of this burgeoning research field. The roadmap opens up with a tutorial section, which introduces major concepts and terminology. It is our hope that the roadmap will serve as an important resource for the scientific community, new generations of researchers, funding agencies, industry experts, and investors.

Keywords: optical energy conversion, light harvesting, solar technology, photovoltaics, solar cell

SQ1 (Some figures may appear in colour only in the online journal)

Contents

PV and alternative technologies for the full spectrum harvesting

Thermal emission harvesting and radiative cooling for energy efficiency

1. Tutorial: thermodynamics of light and conventional limits of photon energy conversion

Svetlana V Boriskina

Massachusetts Institute of Technology

Thermodynamic properties of photon systems and their interaction with matter define efficiency limits of light energy-conversion schemes [1, 2]. Photons can be uniquely characterized by their energy $\hbar\omega = hc/\lambda$, momentum $\hbar\mathbf{k}$, and angular momentum, which, e.g., in the case of plane waves in free space, defines light polarization ($h = 2\pi\hbar$ is Planck's constant, λ, ω are the photon wavelength and angular frequency, and $\mathbf{k}$ is the wave vector) [3, 4]. In the interactions of photons with matter—such as light emission or absorption—the concept of temperature T is introduced to account for energy conservation. Some types of interactions, such as fluorescent emission or Bose–Einstein condensation [5], require adding a concept of photon chemical potential μ to account for the particle number conservation [6].

The photon density of states (DOS) defines the number of states in the momentum space between k and $k + \mathrm{d}k$ per unit volume and solid angle Ω that are available for a photon to occupy in 3D space as: $D(k)\mathrm{d}k = k^2\Omega\,\mathrm{d}k/(2\pi)^3$ (figure 1(*a*)). DOS as a function of photon energy is expressed via the photon dispersion relation: $D(\omega) = \Omega/(2\pi)^3 \cdot k^2(\omega) \cdot \mathrm{d}k/\mathrm{d}\omega$ [3, 4]. For plane waves of both polarizations in an isotropic bulk dielectric with refractive index n and $\Omega = 4\pi$, $D = \omega^2 n^3/\pi^2 c^3$, low bulk photon DOS is often a limiting factor in manipulating and enhancing absorption and emission processes. However, as the DOS is inversely proportional to the photon group velocity $v_g = (\mathrm{d}k/\mathrm{d}\omega)^{-1}$, trapped modes with flat dispersion can have DOS significantly exceeding that of bulk materials, especially in the near field (see section 16) [7–12].

As gauge bosons for EM, photons obey Bose–Einstein statistics with the mean occupation numbers in thermal equilibrium defined as $\tilde{N}(\omega, T, \mu) = (\exp((\hbar\omega - \mu)/k_B T) - 1)^{-1}$, where k_B is the Boltzmann constant and $\mu = 0$ for blackbody radiation (figures 1(*a*), (*b*)) [2–4]. The electromagnetic energy density of radiation in a material per unit time and angle is defined via the well-known Planck formula as $U = \hbar\omega \cdot N(\omega, T, \mu) \cdot D(\omega)\mathrm{d}\omega$ [1, 2]. It can be tailored not only just by the temperature as typical for the blackbody radiation, but also by the photon DOS and μ (see sections 13, 15–19). In turn, light intensity (power per unit area) is $I = v_g \cdot U$ [13] (figure 1(*b*)). Integration of I over the whole frequency and angular range yields optical energy flux through a unit surface area per unit time, which, for the blackbody source at temperature T in free space, equals σT^4 (σ is the Stefan–Boltzmann constant). The ratio of light intensities in an absorbing medium and free space defines the absorption limit, which, in the case of a bulk dielectric with a backreflector and isotropic light escape, has a well-known value of $4n^2$ [13, 14]. However, high-DOS (sub-) wavelength-scale absorbers can exceed this limit [10, 11]. They can have absorption cross sections larger than geometrical ones [9, 15] (see section 13) and, thus, feature higher than blackbody emittance [16].

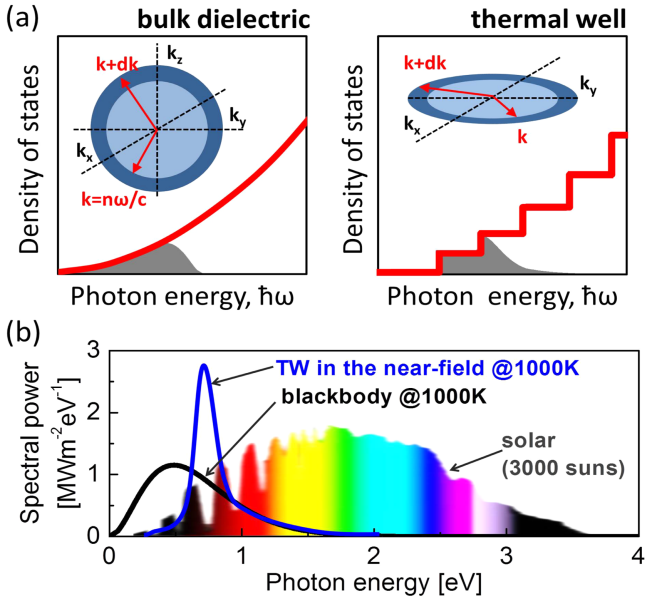

Figure 1. (*a*) Photon DOS (red lines) in isotropic bulk dielectrics (left) and dielectric thin films that act as thermal analogs of quantum wells [10] (right). Shaded gray areas: thermal distribution of photons shaped by the electromagnetic (EM) potential. Insets: isoenergy surfaces (contours) in the photon momentum space. Subwavelength-scale particles, thin metal films, photonic crystals (PhCs), and metamaterials also strongly modify the DOS [9], especially in the near field [12]. (*b*) Power flux spectra of solar photons as well as photons emitted by the 1000 K blackbody probed in the far field (black) and by a thin-film thermal well probed in the near field [10] (blue). Although the Sun emits as a blackbody at $T_s \sim 6000$ K, solar power flux is reduced due to the small angular range of terrestrial illumination and atmospheric attenuation.

Light can also be characterized by the entropy of photon gas with the entropy flux defined generally as $S(T, \mu) = k_B \iint v_g \cdot D(\omega) \cdot [(1 + N)\ln(1 + N) - N\ \ln\ N]\mathrm{d}\omega\,\mathrm{d}\Omega$ [2, 17]. At the thermal equilibrium, the entropy reaches its maximum, and the photon occupation numbers obey the familiar Bose–Einstein distribution, $N = \tilde{N}$. The entropy flux of a blackbody source equals $4\sigma/3 \cdot T^3$, and this value decreases if frequency and/or angular ranges shrink, tending to zero for a monochromatic directional radiation (e.g., laser beam). The introduction of the concept of photon entropy [17] helped to resolve the controversy about the thermodynamic second law violation in optical refrigeration (i.e., anti-Stokes fluorescent cooling) [18, 19]. It is also at the core of the efficiency limits of the photon energy conversion [20].

Fundamental efficiency limits for conversion of the photon energy into useful work stem from the laws of thermodynamics and quantum mechanics. The conversion efficiency of any photon energy-conversion platform (figure 2(*a*)) can be calculated in a general form by balancing the energy and entropy flows: $\eta = \frac{W}{I_s} = 1 - \frac{1}{I_s}[I_r(T_a) + T_c[S_s(T_s) - S_r(T_a) + S_g]]$. When both the source and the absorber emit as blackbodies with $\mu = 0$ and no entropy is generated in the engine, the above formula reduces to the Landsberg efficiency [21], which represents an upper

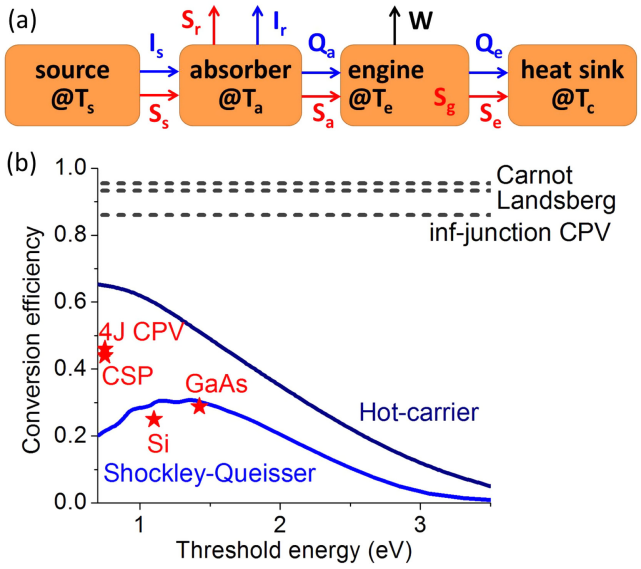

Figure 2. (*a*) A general schematic of a solar energy converter. Blue arrows—energy fluxes in the form of radiation (I) or heat (Q), red arrows—corresponding entropy fluxes through the converter. Irreversible entropy (S_g) can be generated in the engine. (*b*) Fundamental limits for photon energy-conversion efficiency. A Shockley–Queisser (SQ) limit is plotted for an ideal single-junction photovoltaic (PV) cell at $T = 300$ K under one-sun illumination. For the infinite number of PV junctions and full solar concentration, it reaches 86.6% (dashed line) [24] (see sections 11–13). The hot-carrier efficiency limit [25] is shown for an ideal cell with an electron (e) temperature of $T = 3000$ K and a lattice temperature of $T = 300$ K under one-sun illumination.

limit of the solar energy-conversion efficiency. Landsberg efficiency reaches maximum value at $T_a = T_e = T_c$ (93.3% if $T_a = 300$ and $T_s = 6000$ K). A more conventional Carnot efficiency [22] $\eta = 1 - T_c/T_a$ is obtained if there is no radiative energy exchange between the source and the absorber (95% if $T_a = T_s$ and $T_c = 300$ K). Both Landsberg and Carnot limits assume complete reversibility, while operation of realistic photon-conversion platforms involves irreversible thermodynamic processes, such as photon absorption and charge carrier thermalization, and is accompanied by entropy creation (see section 20). Absorption and emission properties of realistic converters may also differ significantly from those of a blackbody. Finally, operation at the efficiency limit typically means that the power is extracted infinitely slowly, while the maximum-power-out efficiency can be found by solving $\mathrm{d}W(\eta)/\mathrm{d}\eta = 0$.

For example, maximum-power-generation efficiency of a PV cell can be obtained from the general formula by assuming entropy production in the cell due to charge carrier thermalization with the crystal lattice as well as particle number conservation and fluorescent emission with the chemical potential equal to the applied voltage ($\mu = \mathrm{eV}$). The resulting limiting efficiency is known as the SQ limit [23, 24], which is shown in figure 2(*b*) for the case of a single-junction power-conversion (PC) cell with a threshold absorption energy corresponding to the width of the e band gap of the cell material. It is also known as the detailed balance limit. Higher efficiency has been theoretically predicted [25] for the regime of operation when the photoexcited charge carriers are extracted after they thermalize between themselves yet prior to their thermalization with the lattice, which reduces entropy creation (figure 2(*b*)). While hot-carrier photon energy converters with high efficiencies have not yet been realized, there is promising ongoing work in this direction that focuses on quantum confinement effects and plasmonics (see sections 5, 6, 9, 13).

Concluding remarks

All practical realizations of photon energy converters operate at lower efficiencies than their theoretical limits [26] due to design and material imperfections (figure 2(*b*)). However, a deep understanding of the origin and constraints of fundamental limits guides future research and development in the area of light–energy conversion [27]. In particular, advanced material developments and optimized optical designs have recently propelled some technologies (e.g., GaAs PV cells [28]) to the brink of reaching their theoretical limits of operation (sections 2–5), and there is still plenty of space at the top of the efficiency scale (figure 2(*b*)). Many opportunities still exist not only for material designers (see sections 3, 5–10, 14), but also for optical scientists and engineers to reach and to overcome the efficiency limits (see sections 2–4, 9–19). Novel optical concepts and schemes for light concentration, photon trapping, optical spectrum splitting, and material emittance modification offer new insights and yield new technological solutions for solar and thermal energy harvestings. These insights will also benefit other fields, such as solid state and advanced incandescent lighting, optical refrigeration, waste heat harvesting, and radiative cooling just to name a few.

Acknowledgments

The author thanks G Chen, W-C Hsu, and J K Tong for helpful discussions.

2. The commercial push of silicon PVs to high efficiency

Martin A Green

University of New South Wales

Status

Solar cells (SCs) seem destined to play a large role in the future energy supply due to cell prices decreasing by a factor of 8 since 2008 and the installed PV system capacity increasing by a factor of 50 over the last decade. Overall manufacturing costs are continuing to decrease by ~10%/year due to a combination of decreasing prices of purified polysilicon (Si) source material and Si wafers, increased manufacturing volumes, and increasing energy-conversion efficiency [29]. Increasing the latter efficiency not only reduces costs per unit power rating by increasing power output for a given investment in material and processing costs, but also it similarly leverages transportation and installation costs when the solar modules are subsequently put into use.

The cell structure that has been produced in the highest volume, to date, is the aluminum backsurface field (Al-BSF) cell shown uppermost in figure 3 [29, 30]. A boron-doped, *p*-type wafer presently about 180 μm thick is the starting point in the manufacture of these cells. After cleaning and surface texturing, these wafers are diffused with phosphorus to form the n^+ region of a *p*–*n* junction. The metal contacts are then screen printed with most of the rear covered by a screened Al-based paste. During firing, this layer alloys with the silicon to form an Al-doped p^+ region at the rear, known as the Al-BSF.

This fabrication sequence became the standard production approach in the 1980s with over 200 GW of cells based on this approach now deployed. Ongoing improvements in the pastes and processing sequences used in cell fabrication have seen steady increases in cell performance to the stage where manufacturers can routinely manufacture cells in the 17%–18% efficiency range on multicrystalline substrates in 2015, increasing to 18%–19% on better quality monocrystalline substrates [29].

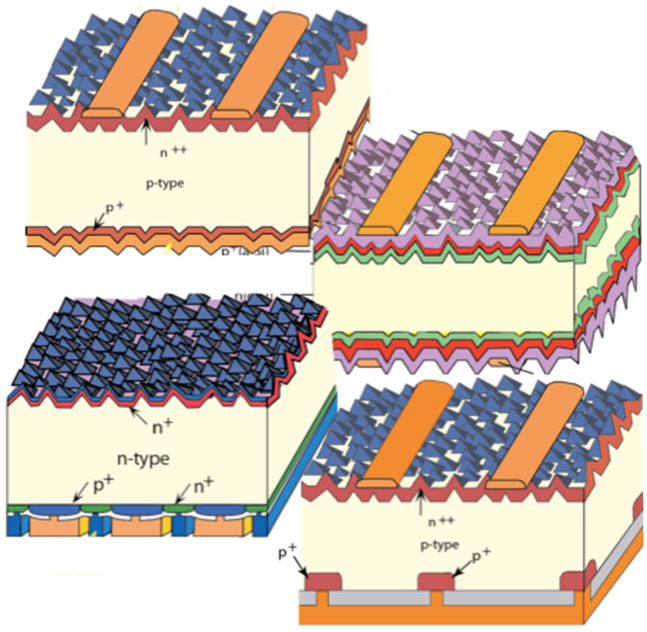

Figure 3. Commercial Si SCs. From top to bottom are shown the standard Al-BSF cell, the heterojunction (HJT) cell, the rear-junction (rear-J) cell and the passivated emitter and rear cell (PERC).

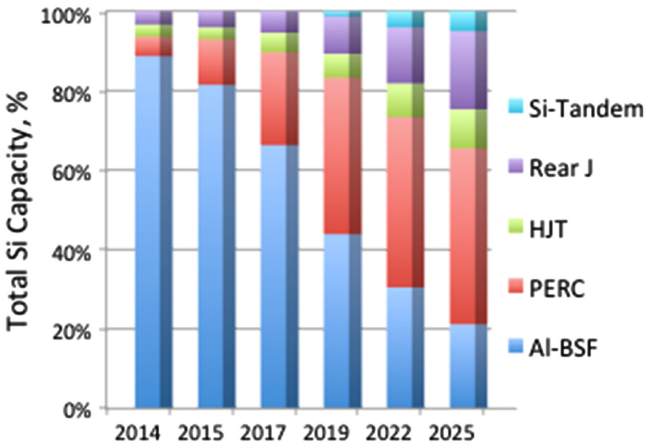

Figure 4. Industry consensus on the present and future market share of the different Si cell technologies of figure 3 (data extracted from [29]).

Current and future challenges

The performance-limiting feature of the cell has now become the Al-BSF region. To progress past the 20% efficiency mark in production, manufacturers are looking to high-efficiency cell structures that overcome this limitation.

Advances in science and technology to meet challenges

The challenge of increasing cell efficiency considerably above 20% has been met by three vastly different cell structures also shown in figure 3 that have all now demonstrated efficiencies of 25% or higher in the laboratory [31] and are being fabricated commercially in increasing volume.

The first to reach 25% efficiency [32] was the PERC shown lowermost in figure 3, first reported in 1989 [33]. Although the most recent to be introduced into large-scale commercial production, PERC cells have already established the strongest commercial position (figure 4). In the structure, the Al-BSF is replaced by a more sophisticated rear contacting approach that not only reduces detrimental carrier recombination at the cell rear, but also improves reflection of weakly absorbed light reaching this surface. Industry consensus is that, by 2020, the PERC cell will displace the Al-BSF approach as the dominant commercial technology [29] as indicated in figure 4. The strength of the technology is its robustness, being suitable for improving performance of both

low- and high-quality Si wafers, giving it an advantage over the other two technologies to be described.

The second cell structure, reaching 25% efficiency in 2014 [31], is the rear-J SC, shown second lowermost in figure 3. This structure was first suggested in 1977 [34] with the first efficient devices reported in 1984 [35]. Close to 1 GW of these cells were sold in 2014 representing about 2.3% of the total market. The industry consensus is that this market share is poised to increase, although this likely depends upon the availability of high-quality monocrystalline *n*-type wafers at lower cost than presently available [29]. The cells have an unusual geometry where both polarity contacts are located on the rear unilluminated cell surface. This has the advantage of avoiding metal contact shading the front surface, eliminating one of the obvious losses of traditional cells. Since most light is absorbed close to entry at the top surface, photogenerated carriers have to diffuse across the wafer to be collected at the rear, making the structure suitable only for good quality wafers.

The final cell structure to have given efficiency close to 25% is the HJT cell approach pioneered by Sanyo (now Panasonic) [36], taking advantage of the company's considerable prior experience with hydrogenated amorphous Si (a-Si:H) thin-film cells. The high atomic percentage of H in the a-Si:H imparts properties completely different from crystalline Si (c-Si) including a wider band gap (1.7 versus 1.1 eV) and electron affinity about 0.1–0.2 eV lower. An important feature is the inclusion of a very thin layer of undoped intrinsic a-Si:H between the c-Si wafer and the oppositely doped a-Si:H layers deposited on either side of the wafer. Given the higher band gap of the a-Si:H regions, essentially all recombination occurs in the pristine c-Si wafer or at its interfaces with the intrinsic a-Si:H layer. The latter turns out to be very low, resulting in the highest open-circuit (OC) voltage of any c-Si cell technology. Combining with the rear-J approach recently increased record Si-cell efficiency to 25.6% [31, 37].

Concluding remarks

These high-efficiency cell technologies will enable the ongoing incremental improvement in commercial Si-cell efficiency to the best laboratory values of ~25%, with 29% a fundamental limit. The most likely route to allow significant progress beyond this point is by going to a tandem cell approach where a higher-band-gap cell is monolithically integrated on top of the c-Si cell. Some recent success in this direction has been obtained by combining with perovskite SCs [38] (see section 3), although the present lack of perovskite cell stability prevents serious consideration for commercial use. Some industry participants, however, rather optimistically believe that such tandem technology may be ready for commercial application by 2019 (figure 4).

Acknowledgments

The author acknowledges support by the Australian Government through the Australian Renewable Energy Agency (ARENA), although the Australian Government does not accept responsibility for the views, information, or advice expressed herein.

3. Optics and nanophotonics for Si cells and Si-based tandem cells

Kylie Catchpole

Australian National University

Status

Currently, about 90% of the PV market is based on c-Si SCs. Si is the third most abundant element on Earth and has a near ideal band-gap energy for maximizing the efficiency of a single-junction SC. c-Si SCs have now exceeded efficiencies of 25% in the laboratory, and Si modules have reached an efficiency of over 22% (see section 2). In order to take advantage of the decades of development of Si and massive economies of scale that have been achieved, it makes sense to push the technology to the highest efficiencies possible. To do this, it is essential that optical losses are minimized. Even when this has been achieved, however, Si SCs are limited to an efficiency of about 27% by Auger recombination. Because of this, there has been increasing interest in combining emerging materials, such as perovskites with Si to form high-efficiency tandems (see also sections 11, 13). For such tandems, sophisticated designs that minimize optical loss are crucial in order to go beyond the break-even point and to realize the potential of the high-band-gap material.

Optical loss mechanisms in SCs are due to reflection from the front surface, incomplete absorption, escape from the SC, and parasitic absorption. All of these need to be addressed in order to reach the maximum efficiencies. Incomplete absorption is important when the SC is thin compared to the absorption length of light. This is relevant as Si wafers become thinner in order to reduce costs and for perovskite materials, which can have relatively low diffusion lengths. Reflection control is necessary for all types of SCs but is particularly important for multi-c cells where anisotropic wet etching cannot be used to create pyramids.

Nanophotonics, which involves structures on the scale of the wavelength of light, is an important approach in the optical engineering of SCs because it allows a level of control that cannot be achieved with conventional geometrical optics. Nanophotonic techniques can be large area and potentially cheap. To date, many different approaches have been used for reducing reflection and increasing light trapping in SCs, including etched surfaces, plasmonic nanoparticles and reflectors, diffuse reflectors, and PhCs. For a more detailed overview of this work, see [39].

Current and future challenges

The emergence of the perovskites has led to the possibility of cheap tandem SCs with efficiencies higher than the limit for single crystal Si.

In order to reach the potential of perovskite/Si tandems, it is important to consider optical losses very carefully

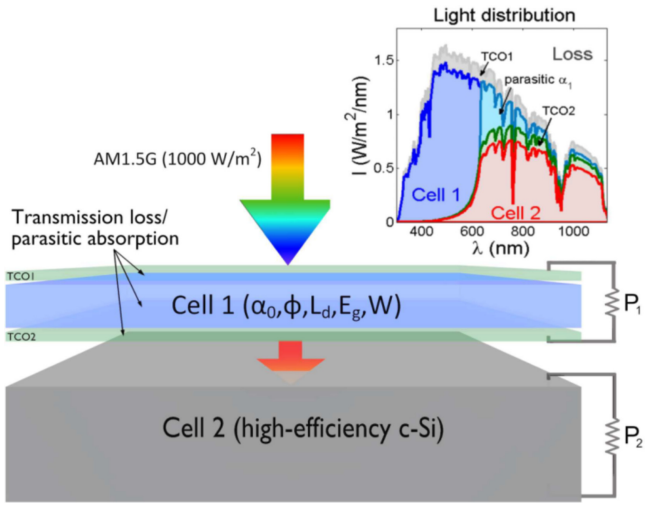

Figure 5. Schematic of a four-terminal tandem cell on Si. (Inset) Optical distribution of absorbed sunlight (AM1.5G) through the complete tandem structure. From [43], reproduced with permission from IEEE.

(figure 5). A perovskite/Si tandem consists of a perovskite SC with a top transparent conducting oxide (TCO) layer and either a rear transparent conducting layer (for a four-terminal tandem) or a tunnel junction (for a two-terminal tandem). Currently, parasitic absorption in the TCO layer is about 10% per layer. Together with reflectance losses, this means that we can expect a loss of about 20% of sub-band-gap light with the present technology. This leads to required top-cell efficiencies of 18% at a band gap of 1.5 eV just to break even and 23% to reach tandem efficiencies of 30% [40]. Reduction of these losses would increase the efficiencies that are achievable, making the technology more attractive for commercialization.

Current challenges for the optical engineering of single-junction Si cells are reflection control and incomplete light absorption due to nonideal light trapping. Theoretically, isotropic Lambertian light trapping can increase the current density for a 100 μm thick Si SC from about 38 to 43 mA cm^{-2}. Light trapping can also increase V_{oc} by increasing the internal intensity of light. However, improvements in the randomization of light and surface passivation are necessary before these improvements can be fully realized. One promising approach for extremely low reflectance is 'black Si,' produced by reactive ion etching or femtosecond laser texturing. Achieving low reflectance together with low recombination is generally a challenge, although, recently, effective surface recombination velocities of less than 10 cm s^{-1} and 1% solar weighted reflectance have been reported [41].

A further challenge is integration of novel structures into high-efficiency cells as cell fabrication has many interdependent processes, and it is necessary that they be optimized simultaneously.

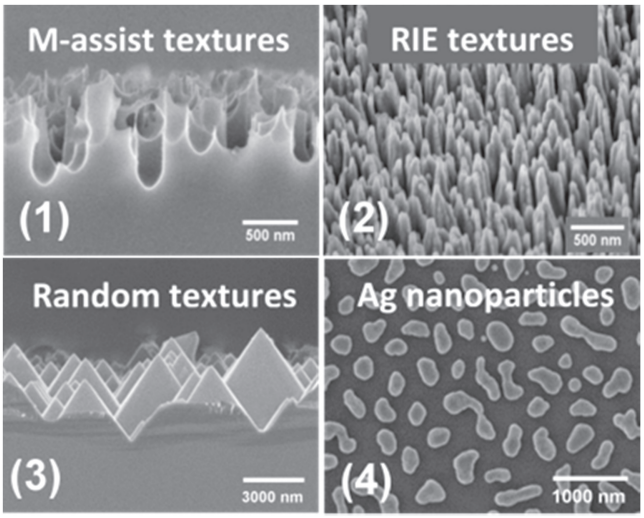

Figure 6. SEM images of various types of texture structures on Si: (1) metal-assisted etched texture (side view); (2) reactive ion etched texture (angle view); (3) random pyramid texture (side view), and (4) plasmonic Ag nanoparticles on Si wafers (top view). Adapted from [45], with permission from the Optical Society of America.

Advances in science and technology to meet challenges

There are several major areas where advances in optics are important in order to improve Si cells and Si/perovskite tandems.

The first is the development of low-loss transparent conductors. Candidate materials for reducing the loss are graphene and nanophotonic structures (see section 8). There has been some work done here with silver (Ag) nanowires [42], but there is a great deal of scope for improvement using controlled designs and different materials. Also note that often the optimum combination of transparency and low resistance loss can be achieved with a grid combined with a transparent conductor, rather than a transparent conductor alone [43].

For perovskite tandems, wavelength-selective light trapping may provide a route to high efficiency as tandem efficiencies greater than 30% are potentially possible with diffusion lengths less than 100 nm. At an optimal top-cell band gap of 1.7 eV, with diffusion lengths of current $CH_3NH_3PbI_xCl_{1-x}$ perovskites, tandem efficiencies beyond 35% are potentially achievable, but this will require low-loss TCOs and highly effective wavelength-selective light trapping [44].

A third major area for improvement is light trapping for Si cells. It is incomplete light trapping and reflection, rather than parasitic loss, that are limiting current in Si SCs. Figure 6 shows some of the structures that have been used to provide light trapping and reflection control in Si SCs. Metal nanoparticles in combination with a diffuse reflector can give comparable light trapping to pyramids [45]. Both pyramids and plasmonic particles give light trapping that is compatible with currents of over 42 mA cm^{-2}, but there is still scope for an extra 1 mA cm^{-2}. Even with plasmonic particles, improving light trapping is more important than reducing loss (see sections 9, 13).

It is also worth pointing out what we do not need for these particular applications. For example, there has been quite a bit of work on exceeding the Lambertian limit for light trapping. However, this is only of interest for very thin structures (see section 8). For a 100 μm or thicker Si SC and for perovskite SCs, there is no significant benefit in above Lambertian light trapping.

Concluding remarks

The global PV market is worth about $100 billion and is completely dominated by Si. The challenge here for optics is to use our greatly improved ability to understand and to engineer optical structures on the nanoscale to improve the efficiencies of Si-based SCs to levels never before seen. There are important near-term and longer trajectory opportunities for both standard Si cells and the rapidly emerging Si-based tandems as SCs continue to play an ever-increasing role in our energy future.

Acknowledgments

I would like to thank my colleagues at ANU and, in particular, T White, N Lal, and C Barugkin for their contributions to the work described in this paper.

4. Photon recycling versus luminescence extraction for record PV efficiency

Eli Yablonovitch

University of California, Berkeley

Status

There has been great progress in SC efficiency by the recognition of the need for luminescent extraction from SCs, which now reach 28.8% efficiency [26] in the flat-plate single junctions. (This is to be compared [46] with the SQ [23] limit, 33.5% efficiency (see section 1).) The improvement is often mistakenly attributed to photon recycling, but that is only a special case of the real mechanism, luminescence extraction, which can be present with or without photon recycling.

Challenges and advances in science and technology

The idea that increasing light emission improves OC voltage seems paradoxical as it is tempting to equate light emission with loss. Basic thermodynamics dictates that materials that absorb sunlight must emit in proportion to their absorptivity. At an OC, an ideal SC would, in fact, radiate out from the SC, a photon for every photon that was absorbed. Thus, the external luminescence efficiency is a gauge of whether additional loss mechanisms are present. At the power-optimized operating bias point, the voltage is slightly reduced, and 98% of the OC photons are drawn out of the cell as real current. Good external extraction at the OC comes at no penalty in current at the operating bias point.

On thermodynamic grounds, Ross derived [47] that the OC voltage is penalized by poor *external luminescence efficiency* η_{ext} as

$$qV_{\text{OC}} = qV_{\text{OC-ideal}} - kT\,|\ln \eta_{\text{ext}}|, \tag{1}$$

where η_{ext} is the probability of an internally radiated photon eventually escaping from the front surface of the cell. Equation (1) can be derived through the detailed balance method [46] of SQ. Green already inferred [48] the external luminescence yield η_{ext} of all the different historical SC materials from their respective record $\{V_{\text{OC-ideal}}—V_{\text{OC}}\}$, employing equation (1).

As solar efficiency begins to approach the SQ limit, the internal physics of a SC transforms. SQ showed that high solar efficiency is accompanied by a high concentration of carriers and by strong fluorescent emission of photons. Photons that are emitted internally are likely to be trapped, reabsorbed, and re-emitted, i.e., photon recycling, which can assist the external luminescent emission at the OC. Alternately, surface texture on the SC, often added for absorption enhancement, equally will lead to external luminescence extraction by random scattering, not requiring photon recycling at all. These two distinct mechanisms were first identified by Lundstrom [49].

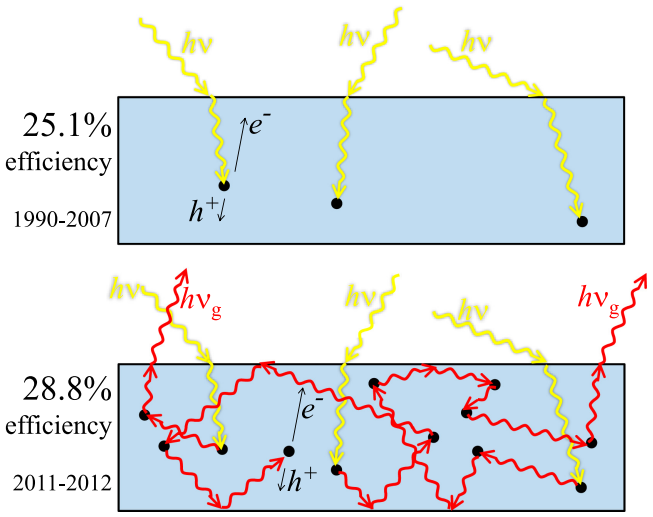

Figure 7. The physical picture of high-efficiency SCs, compared to conventional cells. In high-efficiency SCs, good luminescent extraction is a requirement for the highest OC voltages. One-sun illumination is accompanied by up to 40 suns of trapped infrared (IR) luminescence, leading to the maximum external fluorescence efficiency. Reproduced from [46] with permission of IEEE.

The requirement for efficient luminescence extraction is accompanied by many suns of trapped internal luminescence in high index, high-efficiency SCs, and >26% efficiency as illustrated in figure 7:

To resolve the paradox of why external luminescence is good for SC efficiency, there are a number of different explanations:

1. Good external luminescence is a gauge of few internal loss mechanisms. At an OC, an ideal SC radiates a photon for every absorbed photon. When e–hole (e–h) pairs recombine nonradiatively or when photons are absorbed without generating photocarriers within the active part of the device, both the external luminescence efficiency and the cell efficiency decrease.
2. In a rate equation analysis, external emission of photons into free space is unavoidable. All other losses can, in principle, be eliminated. Thus, the total losses are at their very least when external emission is the only loss mechanism. Maximum external emission is minimum total losses, which leads to the highest efficiency.
3. In untextured cells, good external luminescence requires recycled photons and reabsorption. Internal reabsorption recreates the e–h pair, effectively extending the minority carrier lifetime. The longer lifetime leads to a higher carrier density. Free energy, or voltage, increases with the logarithm of density.
4. The SC and the light-emitting diode are equivalent but reciprocal devices. Just as external emission leads to the most efficient light-emitting diode, the reciprocal device also benefits when there are no other loss mechanisms.

5. External luminescence is sometimes used as a type of contactless voltmeter, indicating the separation of quasi-Fermi levels in the solar material. This is sometimes employed as a contactless, quality-control metric in SC manufacturing plants. In this viewpoint, it is tautological: Good external luminescence actually IS good voltage and, therefore, good efficiency.

This is the preferred explanation for the paradox: *Good external luminescence IS good voltage.*

Concluding remarks

Counterintuitively, efficient external luminescence is a necessity for achieving the highest possible SC efficiency. Why would a SC, intended to absorb light, benefit from emitting light? Although it is tempting to equate light emission with loss, paradoxically, light emission actually improves the OC voltage and the efficiency. The voltage boost generally arises from luminescence extraction for which photon recycling is only one possible mechanism, or extraction by surface texturing is the other possible mechanism, [49].

5. Quantum-confined semiconductor nanostructures for enhanced solar energy photoconversion

Matthew C Beard

National Renewable Energy Laboratory

Status

New PV technologies should have the potential to achieve PC efficiencies (PCEs) beyond ~33% as well as to reduce module costs. In 1982, Ross and Nozik determined that the PCE of unconcentrated solar irradiance into electrical or chemical free energy could be as high as ~66% for a single-junction solar converter when the excess kinetic energy of photogenerated e–h pairs is harnessed without allowing it to dissipate as heat [25]. Excess energy arises from carriers that are generated with photon energies greater than that of the semiconductor band gap. Semiconductor nanostructures where, at least, one dimension is small enough to produce quantum confinement effects, provide new pathways for energy management and have the potential to increase the efficiency of the primary photoconversion step so as to approach the Ross–Nozik limit (see sections 6, 8, 9, 13).

Multiple exciton generation (MEG), also called carrier multiplication, is a process where charge carriers with sufficient excess kinetic energy expend that energy via excitation of additional e–h pairs instead of dissipating the excess energy as heat. In bulk semiconductors, the latter process is limited by both momentum and energy conservation. In quantum-confined nanocrystals, or quantum dots (QDs), it is only limited by energy conservation. Thus, a MEG-active SC with nanocrystals could achieve a PCE of ~44% at one sun and ~85% under full concentration [50].

In 2004, Schaller and Klimov developed a method of measuring the number of e–h pairs produced per absorbed photon in colloidal QD samples using ultrafast transient absorption spectroscopy [51]. The QD system of PbSe and PbS has received the most attention and is used to benchmark the prospects for quantum-confined nanostructures. The MEG process is enhanced by a factor of ~3 going from bulk PbSe to quasispherical PbSe nanocrystals (figure 8). Further enhancements have been observed with more complex nanostructures, such as quantum rods (QRs) [52], quantum platelets (QPs) [53], and nanoheterostructures [54].

Incorporating QDs into solar energy-conversion architectures is an active area of research [55] with current efforts now approaching a PCE of 10%. These approaches employ electronically coupled QDs in films, allowing for transport of electrons and holes within QD layers to their respective electrodes. In 2011, Semonin *et al* fabricated a PbSe QD SC that achieved an external quantum efficiency (QE) exceeding 100% for high-energy photons [56]. This result demonstrated that QD-based SCs have the potential to bypass the SQ limit and to approach the Ross–Nozik limit.

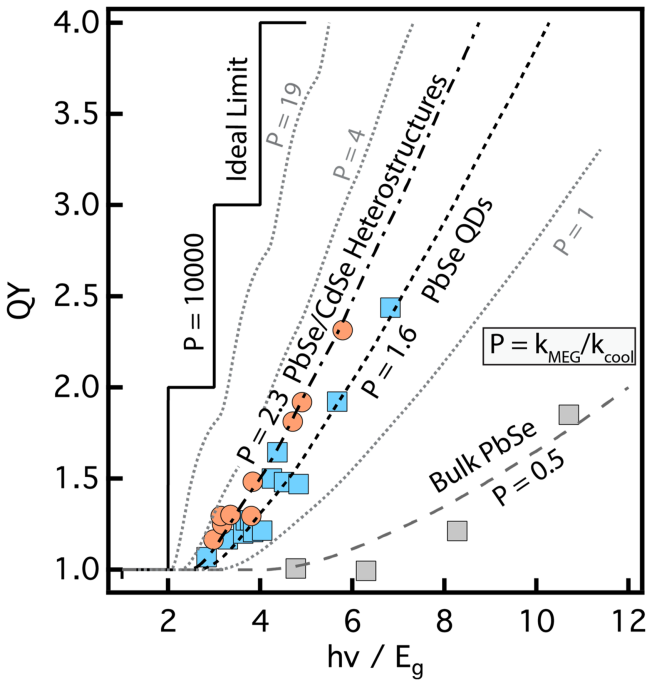

Figure 8. Case study for PbSe (bulk versus nanostructured components). The number of e–h pairs produced from absorption of a single photon at a scaled energy. The gray squares are for bulk PbSe, the blue squares are for PbSe QDs, and the orange circles are for PbSe/CdSe hetereostructures.

Current and future challenges

When MEG is in competition with other exciton cooling mechanisms, the number of e–h pairs generated per absorbed photon (QY) can be expressed as [57]

$$QY = 1 + \frac{k_{\mathrm{MEG}}^{(1)}}{(k_{\mathrm{MEG}}^{(1)} + k_{\mathrm{cool}})} + \frac{k_{\mathrm{MEG}}^{(1)} k_{\mathrm{MEG}}^{(2)}}{(k_{\mathrm{MEG}}^{(1)} + k_{\mathrm{cool}})(k_{\mathrm{MEG}}^{(2)} + k_{\mathrm{cool}})} + \cdots,$$

where $k_{\mathrm{MEG}}^{(i)}$ is the rate of producing $(i + 1)$ excitons from (i) hot excitons and k_{cool} is the exciton cooling rate via heat generation. The ratio of k_{MEG} and k_{cool} can be characterized by a parameter P (figure 8). P increases from ~0.5 for bulk PbSe to 1.6 for PbSe QDs and further increases to ~2.3 for nanoheterostructures [54] and QRs [52].

In the case where only energy conservation limits MEG and P is large, two e–h pairs could be produced with photons, whose energy is twice the semiconductor band gap ($2E_g$), three at $3E_g$, four at $4E_g$, etc (black staircase line in figure 8). In bulk PbSe, the onset for producing multiple carriers per absorbed photon is ~$6.3E_g$ and to produce two e–h pairs requires ~$11.5E_g$ (figure 8, gray squares). The onset energy and the QY are related and can be combined to calculate an MEG efficiency. For bulk PbSe, the MEG efficiency is ~0.19. For PbSe QDs, the MEG efficiency increases to ~0.5, showing a decrease in the onset energy to ~$3E_g$ and production of two e–h pairs when the photon energy reaches ~$6E_g$ (figure 8, blue squares). Future research should

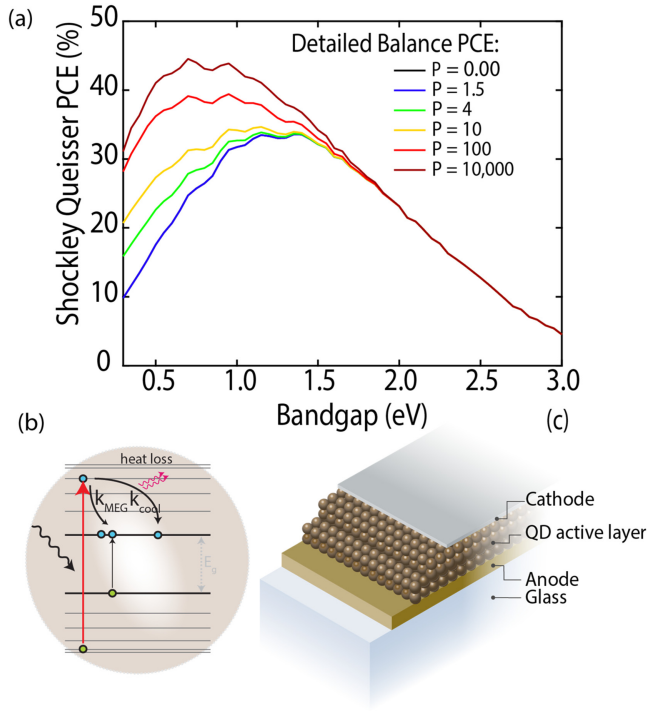

Figure 9. (*a*) Detailed balance calculations for various values of *P*. (*b*) Nanostructures allow for control of various relaxation channels. (*c*) QD SC illustration. Reprinted with permission from Acc. Chem. Res., 2013, 46, 1252–1260, Copyright 2013 American Chemical Society.

determine systems that can further approach the staircase characteristics.

The thermodynamic PCE limit of SCs is a function of *P* (figure 9). For example, the PCE limit is ~44% when *P* is large and 39% with a *P* of 100. These conditions should be achievable within suitably designed quantum-confined nanostructures. For example, recent efforts within Si nanostructures suggest that such high MEG efficiencies are achievable [58].

Advances in science and technology to meet challenges

Semiconductor nanocrystals offer many avenues toward increasing the MEG yields through internal and external modifications. To achieve the largest benefit, one should either look for systems that can reduce k_{cool} or can increase k_{MEG}. Within the Fermi-golden-rule approximation, k_{MEG} depends upon two factors: (1) the density of final biexciton states ρ_f and (2) the Coulomb matrix element W_c. To achieve improvements in these characteristics, researchers are exploring several options: (1) multicomponent systems where either the e or the h experience slowed cooling that allows for a greater probability of undergoing MEG. Multicomponent systems may also increase W_c by breaking the spherical symmetry and, thereby, decreasing carrier screening effects. Enhanced MEG in QRs and QPs can also be ascribed to such a breaking of spherical symmetry. (2) New low-band-gap semiconductor systems. A good place to start is those systems with known low e–phonon coupling strengths and/or are semimetals in bulk form (such as HgTe, graphene, and β-Sn) but whose band gap can be tuned via quantum-confinement effects. (3) Matrix-QD coupling effects that can achieve slowed cooling and/or higher W_c [59].

In order to identify new systems with enhanced MEG characteristics, researchers should develop new faster and more robust means of testing for MEG as well as a theory to predict promising systems for exploration. Currently, the most used approach for measuring carrier yields is based upon ultrafast transient absorption or photoluminescence (PL) spectroscopy [51, 57]. Both techniques are laborious and are prone to experimental errors, and, thus, great care must be taken in order to extract the photon-to-carrier quantum yield [57]. SC architectures where current is measured are preferable [56]. Developing a QD SC from QD systems can be time consuming, and, thus, knowing whether high MEG yields are possible prior to undertaking such an endeavor is necessary.

Developing device current-based approaches for measuring enhanced light to current yields but which are less complex than a SC should be pursued. For SCs, the basic strategy is to sandwich a QD layer between an *n*-type window layer, which accepts electrons while blocking holes, and a metal electrode that accepts holes. Light is absorbed in the QDs, and excitons separate to form free electrons and holes. Critical issues that need to be addressed are robustness of QD-layer formation and optimization of the front and back interfaces. Adapting such architectures for fast and reliable MEG measurements would benefit the search for systems with enhanced MEG characteristics.

Concluding remarks

QD SCs remain a promising technology for inexpensive, scalable, and efficient SCs. Such semiconductor nanostructures are synthesized in solution phase chemical reactions where the reaction conditions can be modified to produce a variety of shapes, compositions, and structures. Thanks to their size, surface tunability, and solution processing, it should be possible to find systems that enable inexpensive and highly efficient devices from QD-based inks. Surpassing the SQ limit for a single-junction solar converter system is a scientific and technological challenge with a significant benefit to society. The challenge is to increase the MEG efficiency to approach the energy conservation limit.

Acknowledgments

Support from the Solar Photochemistry program within the Division of Chemical Sciences, Geosciences, and Biosciences in the Office of Basic Energy of the Department of Energy is acknowledged. DOE funding was provided to NREL through Contract No. DE-AC36-086038308.

6. Challenges and advances in the fabrication of QD intermediate band SCs

Yoshitaka Okada

The University of Tokyo

Status

The QD intermediate band SCs (QD-IBSCs), which commonly suffer from small absorption and low density of QDs, result in a drop of V_{OC}. However, V_{OC} and, hence, the efficiency recover fast, and cell performance improves with concentrated illumination of sunlight [60]. Current QD-IBSCs require light concentration to ensure that the photogeneration rate outperforms the recombination rate *via* IB states. The areal density of QDs has a direct influence on the generation and recombination processes *via* the IB because the DOS of the IB (N_{IB}) is linked to the areal density as $N_{IB} = N_{areal} \times N_{stacks}/W$, where N_{areal} is the areal density of the QD array, W is the intrinsic QD region width, and N_{stacks} is the number of QD stacks.

Assuming an energy band gap of $E_g = 1.40$ eV for the GaAs host material, the generation and recombination rates for the widely studied InAs/GaAs QD-IBSC with different positions of the IB can be calculated based on the detailed balance theory as shown in figure 10 [61]. Here, the QD areal density corresponds to the total QD density given by $N_{areal} \times N_{stacks}$. The absorption cross sections are taken as $3 \times 10^{-14}\,cm^2$ for both optical transitions between the valence band (VB) to the IB and the IB to the conduction band (CB). It can be clearly seen that, if the QD areal density is below $1 \times 10^{16}\,cm^{-2}$, the net generation rate G_{net} becomes *negative* with deepening the location of the IB in the QD region.

The highest areal density of InAs QDs on GaAs experimentally demonstrated, to date, is $\sim 1 \times 10^{12}\,cm^{-2}$ [62], which means that the recombination rate would dominate over the photogeneration rate under one sun as from figure 10. However, the situation will significantly improve if the cell is under light concentration. Figure 11 shows the dependence of net generation rate G_{net} on the concentration ratio for the case of the IB being located at 0.2 eV below the CB edge. It shows that G_{net} turns *positive* after 10 suns. When the concentration exceeds 1000 suns, a positive G_{net} value can be expected even for the QDs areal density of $1 \times 10^{12}\,cm^{-2}$, and the simulation results are consistent with the experimental results reported in literature [63, 64].

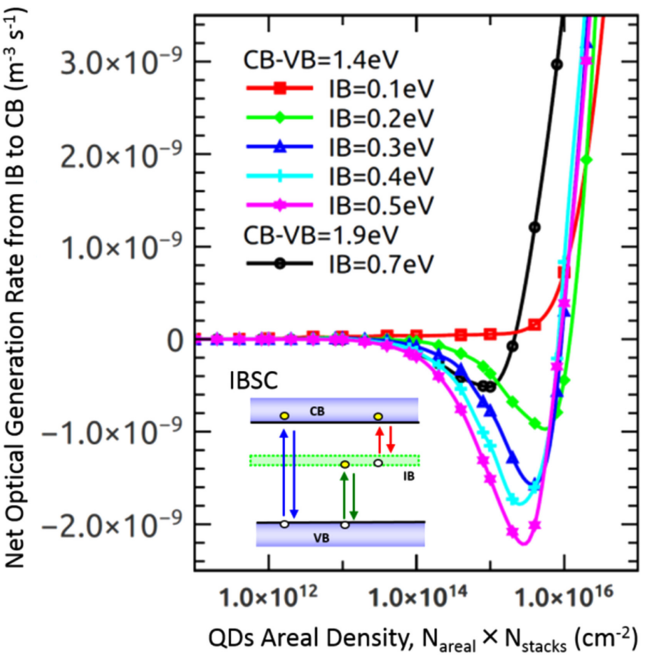

Figure 10. Detailed balance calculation of the dependence of net generation rate from the IB to the CB, G_{net} on InAs QDs density, and the IB energy position relative to the CB band edge. Reproduced with permission from [61].

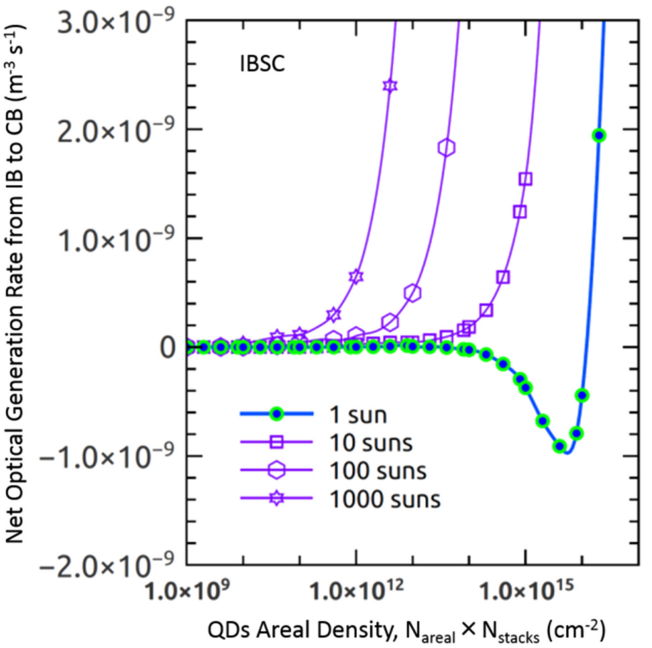

Figure 11. Detailed balance calculation of the dependence of G_{net} on concentration ratio. The IB is located at 0.2 eV below the CB edge. Reproduced with permission from [61].

Current and future challenges

In the last decade, there has been an extensive effort to demonstrate QD-IBSCs with high efficiency. The QDs are required to be homogeneous and small in size and to be regularly and tightly positioned in the active region of the cell in order to form an IB or a superlattice miniband that is well separated in energy from the higher-energy states [65]. Furthermore, dense QDs arrays are required to achieve sufficient photoabsorption resulting in a positive G_{net}. The most commonly used fabrication method of QD structures is to utilize spontaneous self-assembly of coherent 3D islands in lattice-mismatched heteroepitaxy, the Stranski–Krastanov (S–K) growth mode in molecular beam epitaxy or metal organic vapor phase epitaxy. The InAs/GaAs material system has a lattice mismatch of 7.2%, and the strain induced by this lattice

mismatch drives into 3D coherent S–K growth after formation of a thin 2D InAs wetting layer in the initial growth stage. The typical areal density of InAs QDs achieved by the S–K mode is $N_{areal} = 10^{10}$–$10^{11}\,cm^{-2}$ grown on the GaAs (001) substrate. However, the size is still large, and the density is much less than what is required. The QD sizes and density are dependent on the growth conditions, such as the V/III flux ratio, substrate orientation, growth temperature, and material used for the buffer layer. The areal density of the QDs is increased by irradiating Sb to the buffer or wetting layer, and Sakamoto *et al* have recently demonstrated $N_{areal} = 1 \times 10^{12}\,cm^{-2}$ [62].

For further increasing in the total QDs density, the fabrication of a multistacking configuration is necessary. One has to consider that a gradual buildup of internal lattice strain with an increased number of stacking leads to an increase in both the size and its fluctuation for the multistacked QDs grown by S–K growth. In addition, the strain accumulated above the critical thickness generally results in a generation of misfit dislocations, which occurs typically after 15–20 layers of stacking in the case of InAs/GaAs QD growth. Recently, Sugaya *et al* have demonstrated stacking of $In_{0.4}Ga_{0.6}As$/GaAs QDs fabricated by an intermittent deposition technique [66]. The critical thickness of the $In_{0.4}Ga_{0.6}As$/GaAs system is much thicker than that of the InAs/GaAs system, and no dislocations are generated even after stacking up to 400 $In_{0.4}Ga_{0.6}As$ QD layers.

Meanwhile, tensile-strained barriers have been studied in order to compensate for the compressive strain induced by the QD layers. This growth method is called the strain-compensation or strain-balanced technique, and, to date, InAs QDs in an AlGaInAs matrix on an InP substrate, InAs QDs in GaAsP, in a GaP matrix on a GaAs substrate, and InAs QDs in GaNAs on GaAs (001), and on (311)B substrate of high material quality have been reported [67].

Advances in science and technology to meet challenges

The IBSC concept shown in the inset of figure 10 represents the optimal cell configuration under maximum solar concentration. However, practical SCs operate at lower solar concentrations, usually below ~1000 suns, and there is an efficiency advantage to be gained by introducing a relaxation stage. The principle is that the optical transitions between this relaxed IB, or so-called ratchet band (RB) and a VB are critically forbidden, hence, the only route for relaxation *via* the IB now involves surmounting a potential barrier from the RB to the VB. The fundamental efficiency benefit of relaxation has also been recognized in up-converting (UC) systems that rely upon sequential absorption. To date, a molecular system [68] and a ferromagnetic dilute magnetic system [69] promoting this scheme have been proposed.

The carrier lifetime in the IB also directly influences the conversion efficiency of QD-IBSCs. The detailed balance calculations for the case of ideal IBSCs often neglect the effect of nonradiative lifetime. However, QDs have a finite nonradiative lifetime and could affect the photogeneration rate because they act as recombination centers just as absorption levels. The carrier lifetime and, hence, the efficiency is influenced by the carrier recombination strength, thermal escape, and the tunneling escape rates out of QDs. A long carrier lifetime is obtained by controlling the recombination rate using a type-II QD heterostructure, using a high potential barrier preventing the thermal carrier escape from QDs, and by introducing an electric field damping layer preventing the field-assisted tunneling out of the QDs. Furthermore, introducing a RB into the SC assists with the problem of maintaining long carrier lifetime. Assuming that the VB–IB transition is direct and allowed, a typical carrier lifetime in an IB on the order of 10 ns can be assumed. Assuming a Boltzmann statistics for the carrier distribution, introducing the relaxation step of ΔE (between the IB and the RB) could increase the lifetime by a factor of exp ($\Delta E = k_B T$). This effect is responsible for intermediate-state lifetimes on the order of 100 μs measured in some molecular UC systems.

Concluding remarks

Significant effort and rapid progress have been made in the device physics as well as practical demonstration of high-efficiency IBSCs. These achievements have been possible due to mature and highly uniform III–V QDs, nanostructure material growth, and processing technology. For this, the demonstration of QD-based IBSCs is presently undergoing three main stages. The first is to develop technology to fabricate high-density QD arrays or superlattices of low defect densities and long carrier lifetimes. The strain-compensated or strain-balanced growth technique significantly improves the QD material quality and characteristics of SCs even afterthe stacking of 100 QDs layers or more in S–K growth. The second is to increase the carrier lifetime in IB states by controlling the recombination rate using a type-II QD heterostructure, a high potential barrier preventing the thermal carrier escape from QDs, and an electric field damping layer preventing the field-assisted carrier escape. Furthermore, introducing a RB into the SC assists with the problem of maintaining long carrier lifetime. The last is to realize ideally half-filled IB states to maximize photocurrent generation by two-step photon absorption. The doping of the IB region, photofilling by light concentration, and photon confinement structures are all considered important.

In addition to further improvements in the material quality, the control of absorption matching in IB materials is expected to improve the efficiency of QD-IBSCs in the near future (see also sections 5, 14).

7. Advanced materials for solar energy conversion

Stephan Lany[1], Talia Gershon[2], and Andriy Zakutayev[1]

[1]National Renewable Energy Laboratory
[2]IBM T J Watson Research Center

Status

The PV market, dominated by c-Si technologies, has seen remarkable cost reductions in recent years. The current module cost of 0.5–0.7 \$/W should translate into 5–10 ¢ kWh^{-1} electricity prices after further reductions in the balance of system and soft costs. However, recent macroeconomic analysis [70] suggests that the scaling to and beyond the terawatt (TW) level will depend strongly on the rate of future capital investment in manufacturing capacities (see section 2). Potential barriers toward multi-TW-scale PV include the relatively large capital expenditures (capex) for PV grade Si production as well as supply limitations of Te and In for CdTe and Cu(In,Ga)Se_2 beyond the TW scale. The scalability challenge becomes an even bigger one if aiming for both electricity and fuel generation by solar energy conversion.

The development of new PV technologies based on novel advanced materials could create a new industry with independent supply chains, foster market diversification, and attenuate market volatility and, thereby, enhance the odds for beyond-TW scaling of solar energy production (see also section 8). Such *disruptive* PV technologies must be competitive with current technologies in efficiency, cost, and reliability, and they must use readily available elements [71], but they also have to be compatible with low-capex production processes to ensure rapid industry growth after initial commercialization.

Over the past decade, considerable research effort has addressed alternative approaches, including dye sensitized cells and organic and inorganic PVs. Particularly noteworthy are the $Cu_2ZnSn(S,Se)_4$ kesterites [72] as well as the hybrid methylammonium lead-halide perovskites that have reached SC efficiencies above 20% in just a few years of research and development [73]. We note, however, that both systems must still overcome significant hurdles (e.g., performance and stability) before they will become commercial. Beyond the further development of such individual materials systems, the Materials Genome Initiative provides a framework for broader search, design, and discovery of materials for PVs, solar fuel generation, and a wide range of other applications [74].

Current and future challenges

In order to identify promising and under-explored PV materials worthy of future development, the band gap and the optical absorption strength are often used as a first selection criterion [71]. Despite being good screening metrics to quickly winnow out unfeasible candidates, there are many additional material criteria needed to be fulfilled beyond the band gap and optical properties. The absorber material must have high carrier mobilities, particularly for minority carriers,

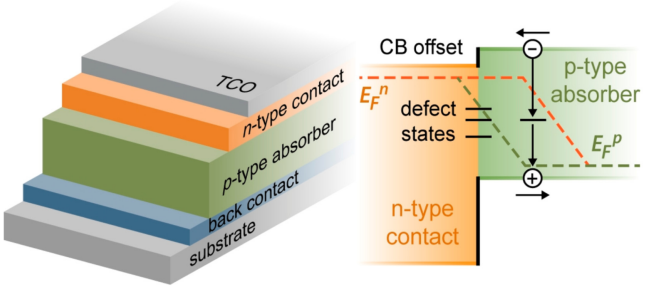

Figure 12. (*a*) Schematics of a SC structure; (*b*) band diagram illustrating some of the material issues, i.e., doping, band offsets, and defect states.

low densities of detrimental point or extended defects (e.g., grain boundaries) that can accelerate recombination and can limit minority carrier lifetimes, as well as a high level of control of the electrical doping to enable formation of *p–n* junctions with a suitable depletion width.

Besides Si and epitaxial III–V systems, there are few known bipolar dopable semiconductors that could be suitable for *p–n* homojunction PVs. Therefore, most thin-film SCs use a HJT with two different materials (see figure 12): typically, a *p*-type absorber and an *n*-type contact. In this configuration, the quality of absorber/contact heterointerface becomes crucial for achieving high-efficiency cells, i.e., it should have low interface defect densities and a small CB offset. Considering that the interface at the backcontact can also play a role in device performance, it is clear that the development of a new PV technology must address the entire device structure, not just individual absorber and contact materials.

A significant number of potential inorganic absorber materials has been suggested and has been studied in recent years, including Zn_3P_2, Cu_2SnS_3, WSe_2, Cu_2S, $ZnSnN_2$, FeS_2, $BiFeO_3$, Cu_2O, SnS, and Sb_2Se_3. However, solving all of the above-mentioned bulk transport and interface issues under the constraints of a limited choice of elements (availability, cost, and toxicity), processing considerations, and anticipated production cost, remains a huge challenge. In particular, this task requires a balance between sufficient breadth and depth; we must address all requirements on the materials' bulk and interface properties while, at the same, time screening a large number of materials including unconventional and unsuspected candidates that might have been overlooked before. Furthermore, the search should not only enumerate the possible stoichiometric binary, ternary, and multinary compounds, but also include the possibility to design desirable properties through deliberate variation of the composition, such as in the case of semiconductor alloys. Considering the vastness of the full phase space of compositions and process parameters, it is clear that the traditional way of case-by-case studies is too time consuming. Thus, new research approaches (outlined below), and arguably new funding mechanisms are needed to bridge the wide gap between basic materials science and the commercialization of new TW-scalable PV technologies.

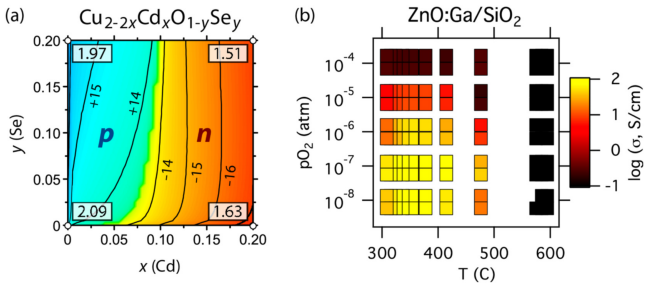

Figure 13. (*a*) Calculated composition dependence of band gaps and doping in Cu_2O-based alloy absorbers [77]. (*b*) Measured electrical conductivity of combinatorial libraries for a ZnO:Ga contact as a function of temperature and O partial pressure [78].

Advances in science and technology to meet challenges

In order to be successful, the research has to span the entire PV development cycle: from broad materials exploration, to targeted research on individual materials, and to device integration and testing. This formidable task can be accomplished by the complementary use of computational materials science and synthesis/characterization/analysis. Besides accelerating the development cycle of investigations via high-throughput and combinatorial approaches for both computations and experiments, the research strategy should also include in-depth studies of the underlying materials science to distill composition–structure–property relationships and to formulate design rules. For example, the need for low-cost synthesis routes increases the need for 'defect tolerant' materials, i.e., materials that maintain favorable electronic properties, despite the presence of structural defects, disorder, or impurities [75].

Computational advances

High-throughput computing has enabled the creation of databases for structural, mechanical, thermodynamic, magnetic, and electronic properties [76]. The capability of quasiparticle energy calculations in the GW approximation is now implemented in several electronic structure codes. Although limitations and challenges remain, particularly, for more complex systems, the reliable GW prediction of band gaps and optical properties is now in reach for a broad range of materials. Supercell calculations, which are traditionally employed to describe doping and defects in the dilute limit, can now be extended to the case of aliovalent alloys, allowing the prediction of both band gaps and doping as a function of composition [77], as illustrated in figure 13(*a*) for the case of Cu_2O-based alloy absorbers.

Experimental advances

Combinatorial experiments have traditionally been used to screen large elemental composition variations for their intrinsic properties, such as crystal structure and absorption spectra. Recent advances in the combinatorial methods allow the deposition and analysis of 'libraries' with a gradient in both composition and growth temperature, thereby enabling a high-throughput exploration of the phase space (see figure 13(*b*) as an example for ZnO:Ga contact [78]). Finally, combinatorial optimization of multilayer PV devices is now possible [79], implicitly taking into account the interaction effects of individual material layers at their interfaces, including band offsets and interdiffusion.

Future needs

Further development of computational capabilities would be desirable for the routine calculations of electron and hole mobilities and minority carrier lifetimes, which would enable device modeling based on computational parameters. In order to assess the electronic properties of the interface at HJTs, it would be of high importance to establish theoretical methods for generating structural models of nonepitaxial interfaces. Development of faster and more accurate experimental methods for measuring the lifetimes of the photoexcited charge carriers and for determining band offsets at heterointerfaces is equally important. Additional research needs are the improved understanding of nonequilibrium effects in thin-film deposition and the implications on the defect densities.

Concluding remarks

Many promising PV materials remain undiscovered or underexplored due to the lack of information regarding their optoelectronic, structural, and intrinsic defect properties. Individual experiments exploring one composition at a time could consume years of effort before the system is fully understood. Reducing this time is, therefore, of paramount importance. Improvements in computational and experimental techniques are accelerating the screening of the fundamental optoelectronic and defect tolerance characteristics at the individual material level. This information is invaluable for down-selecting systems worthy of a more targeted development. Future approaches for developing new PV technologies will consider more specifically kinetic limitations during deposition and the structure and electronic properties of interfaces, which are crucially important for integrating individual materials into high-efficiency devices. The feedback between computational and experimental approaches will significantly reduce the time needed to achieve disruptive materials discovery for TW-level PV production in the future.

Acknowledgments

S.L. and A.Z. are supported by the U.S. Department of Energy, Office of Energy Efficiency and Renewable Energy (DOE-EERE) under Contract No. DE-AC36-08GO28308 to NREL. T.G. is supported by DOE-EERE under Award No. DE-EE0006334.

8. Going thin: atomic-layered 2D materials for photon conversion

Mohammad H Tahersima and Volker J Sorger

George Washington University

Status

The field of atomically thin 2D materials has grown rapidly over the last few years since it exhibits nonclassical phenomena. The field of atomically thin 2D materials has grown rapidly over the last few years since they exhibit non-classical phenomena, diverse electronic properties, and can cover a wide range of electromagnetic spectrum (see figure 14). The well-studied carbon material, graphene, is characterized by an absence of a band gap (for monolayers) [80]. This is relevant for photon absorption since, unlike semiconductor materials, this band structure is spectrally not band-edge limited, thus, enabling broadband absorption. Transition-metal-dichalcogenides (TMDs), however, do have a band gap and have been found to be stress and composition band-gap tunable [81]. The band gap (0.8 eV) of black phosphorous matches that of the telecom c-band (1550 nm) and, hence, could find applications in photoreceivers [82].

Taking a closer look at one material system (MoS_2) reveals some unexpected properties relating to interactions with light; the band structure of MoS_2 transforms from being an indirect band gap (1.2 eV) for bulk material to a direct band gap (1.8 eV) for single layers, which is accompanied by a 10^4-fold PL enhancement [81]. Unlike in classical physics where the optimum thickness of an absorber is given by the imaginary part of the permittivity, 2D materials behave quite differently. For instance, the photodetection can be tuned for different wavelengths where single- and double-layer MoS_2 absorbs green light, while triple-layer MoS_2, which is less than a nanometer thicker absorbs in the red visible spectrum [83]. Such thickness-modulated absorption in conjunction with their relative earth abundance open up prospects for atom-thin 2D material-based multijunction (MJ) SCs that capture photons from the visible to the near IR.

Heterostructures, such as MoS_2/graphene or MoS_2/WS_2, have shown that a layer as thin as 1 nm is able to absorb 5%–10% of the incident light [84]. This is an order of magnitude higher compared to the same thickness of GaAs or Si and might translate into 1–3 orders of magnitude higher power densities than the best existing ultrathin SCs. The origin for this is found in the electronic DOS, which exhibits peaks known as Van Hove singularities.

With intriguing prospects for 2D material-based photon-conversion applications, a variety of fundamental challenges need to be overcome and to be investigated as discussed next.

Current and future challenges

For instance, these atom-thin materials are rather sensitive to surface charges, neighboring materials, and stresses. While such sensitivity can be exploited (if properly controlled) to achieve higher functionality, the field is still in the exploratory phase. Improvements are needed from fundamental band structure engineering to control of chemical synthesis and material processing.

Although semiconducting TMDs exhibit high absorption coefficients, TMD-based PV cells with superior PV performance have yet to be demonstrated. This is because a monolayer material has obvious physical thickness limitations and is mostly transparent at visible frequencies. Furthermore, in order to obtain a reasonable photocurrent and voltage for PV applications, stacked multilayer devices might be needed. This, however, demands a clear understanding and control of the interface physics and might encompass novel structures to increase the light–matter interaction or processing approaches to create built-in potential in multilayers, such as via plasma doping.

An exciting avenue for 2D materials is the controlled introduction of strain, which offers the flexibility in controllable and potentially tunable functionality for device engineering; strain reduces the crystal symmetry, leading to significant shifts in the energy band edges, which changes the electronic and optical properties of the material.

Regarding e transport and field effect transistor devices, monolayer TMDs have shown low electronic mobility. For instance, the value for single-layer MoS_2 is about 2 orders of magnitude lower compared to that of bulk. In this regard, a complete understanding of the microscopic picture for the e transport in monolayer or few-layer TMD films remains unclear.

Regarding the synthesis of TMD sheets, low-temperature approaches and catalyst-free synthesis are highly desirable for practical applications. However, to date, no practical method for the large-scale, defect-free, and scalable production of TMD sheets with fine control over the number and the structure of the layers over the entire substrate has been developed. If successful, however, it would dramatically accelerate the production and deployment of these materials in photon-conversion industries, such as for PV. However, even if the synthesis is mastered, techniques for transferring large-scale TMD sheets also need to be developed since direct growth often conflicts with temperature budgets.

Advances in science and technology to meet challenges

Addressing the low photon absorption of 2D materials can be met by deploying light–matter interaction enhancement techniques. Here, three options are possible; (a) enhancing the optical DOS via incorporating optical cavities, (b) designing momentum-bending options that feed waveguidelike structures that allow for lateral (versus normal) absorption, and (c) field density enhancements using metal-optics approaches, such as found in plasmonics if loss management can be achieved.

Furthermore, physical strain creates an opportunity to create multiband-gap designs within one material system. For instance, the induction of periodic changes in strain values could lead to advanced PV cells. Regarding the electrical

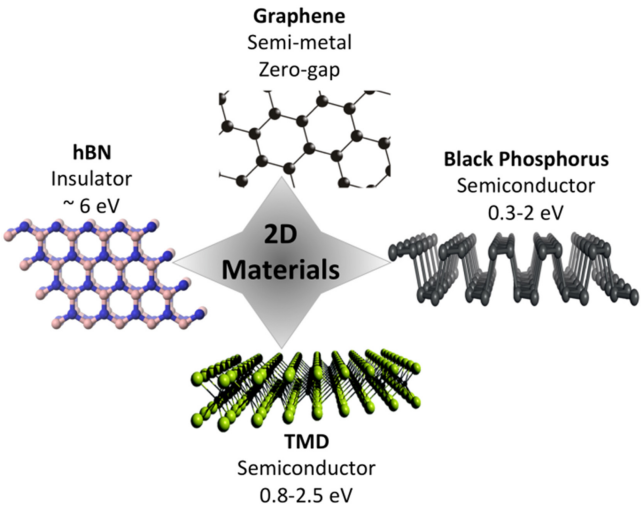

Figure 14. The 2D atomic-layered materials offer a variety of band structures toward designing highly functional photon absorption devices. While this emerging material class exhibits some non-classical band structures, more research is needed to fully understand the interplay among transport, light–matter-interaction properties, and mechanical properties, such as stress. Abbreviations: see the main text.

transport, Lee *et al* [85] reported that, although Van der Waals HJTs exhibit both rectifying electrical characteristics and PV responses, the underlying microscopic processes differ strongly from those found in conventional devices in which an extended depletion region plays a crucial role. In atomic heterostructures, the tunneling-assisted interlayer recombination of the majority carriers is responsible for the tunability of the electronic and optoelectronic processes.

Interestingly, the combination of multiple 2D materials has been shown to provide high photon-conversion performance; for instance, sandwiching an atomic *p–n* junction between graphene layers enhances the collection of the photoexcited carriers [85]. Hexagonal boron nitride (h-BN) was shown to be a promising substrate (improved 2D material mobility) for high-quality 2D electronics due to its atomically smooth surface that is relatively free of dangling bonds and charge traps [86].

On the processing side, plasma-assisted doping can serve as a reliable approach to form stable *p–n* junctions in multilayer MoS_2 resulting in a significant enhancement of the PV response, such as a higher OC voltage and a lower dark current [87]. Applying field enhancement techniques via using plasmonic resonances in nanoparticles can improve absorption; Britnell *et al* placed gold nanospheres on top of the 2D heterostructures showing a tenfold photocurrent increase [88]. Rolling a stacked heterolayer of semiconducting, metallic, and insulating 2D materials in a core–shell fashion allows for broadband photoabsorption up to 90% due to a broadband nanocavity and an opportunity for strain engineering for multiband-gap PV cells [89].

Concluding remarks

Although still at an early stage of development, the known properties of atomically thin material systems for photon conversion are motivating for ongoing research. Together with graphene and insulating materials, such as h-BN, 2D semiconducting materials are an attractive choice for constructing SCs on flexible and transparent substrates with ultrathin form factors and potentially even for mid-to-high-efficiency SCs. While some fundamental and practical challenges are still present, the field of nanophotonics has a wide variety of toolkits available toward handling these challenges. In addition, 2D materials show a decent potential for highly functional and tunable material platforms if synthesized and controlled properly. Incidentally, the latter is the aim of the Materials Genome Initiative and the DMREF program of the National Science Foundation of the United States (see also section 7). In conclusion, the rapid progress of this field might overcome control and design challenges in the near future.

Acknowledgments

We thank the National Science Foundation and the Materials Genome Initiative for support under Award No. NSF DMREF 14363300.

9. Plasmonics for optical energy conversion

Michael J Naughton and Krzysztof Kempa

Boston College

Status

Plasmonics is the study of plasmons, quasiparticles associated with collective oscillations of e density in a metal. Plasmon waves can exist and can propagate within the bulk or at the surface of a metal and can be generated by interactions of EM radiation or an e beam with the metal. Most of the phenomena associated with waves, in general, apply to plasmons, perhaps most importantly that of resonance. The energy-momentum dispersion relation for plasmons also differs greatly from that of EM radiation in vacuum or air, a fact that affords numerous routes to manipulating light–matter interactions. For example, surface-bound plasmons can be localized on size scales far smaller than the wavelength of light in free space and can propagate (as surface plasmon polaritons (SPPs)) along channels of comparable small size. In addition, structured media forming metamaterials can be fabricated that incorporate plasmonics to enable new functionalities in nanophotonics and electronics.

Numerous applications have been envisioned and have been implemented that take advantage of this light confinement and light waveguiding with plasmons. These include molecular and neurosensing, color filtering, nanoscale lithography, lasing, imaging, waveguiding, and the topic of this contribution, energy conversion. The ability to excite plasmons with light means that the energy in light can be transformed and can be manipulated in tailorable and potentially useful ways [9].

Current and future challenges

It can be said that the most significant scientific challenges to increased optical energy-conversion efficiency, especially in PVs, are color matching and the 'thick–thin' conundrum. The former refers to the spectral nature of sunlight versus the single energy (band-gap) nature of semiconductors, and the latter refers to a thick SC being required to maximize optical absorbance, while a thin one is advantageous for e–h extraction. To date, the series MJ cell is the only proven solution to the spectral issue (see sections 11, 13). As also described elsewhere in this roadmap, there are several alternative concepts proposed to deal with the problem, from carrier multiplication to hot e extraction (see sections 5, 13), to a parallel MJ (as in a prism) (see sections 11, 13), and to a thermal PV (see sections 15–20). Likewise, for the optical absorber thickness issue, various light-trapping innovations are being conceived and are being implemented to enable high absorption in ultrathin media. These include textured front and/or back electrodes, radial-junction architectures that strive to decouple the optical and electronic pathlengths by orthogonalizing their respective directions, periodic back-reflectors that channel, or waveguide light along the plane of a film, thus, extending the optical path length, and others. One of the most interesting and perhaps promising new routes to increased light trapping involves plasmonics.

Atwater and Polman [90] gave a thorough review of plasmonics for PV in 2010, discussing how plasmonic metallic nanoparticles/nanostructures could be used to scatter light at oblique angles into a PV absorber, as nanoantennas to enhance near-field scattering within an absorber, or as waveguides supporting SPP modes at the backreflector with the evanescent EM wave in the semiconductor at the metal interface that enhances carrier generation.

In 2011, a review of plasmonics by Wang *et al* [91] included a chapter that described key plasmonics concepts in solar plasmonics, including Mie resonance, nanotransmission lines, metamaterials for light trapping, as well as plasmon-induced charge separation for a novel class of SCs.

In 2012, Green and Pillai [92] also briefly summarized the prospects for plasmonics in SCs but added to the discussion mentions of possible roles of plasmonic metamaterials and for hot es which, in concert, could potentially yield conversion efficiencies well in excess of the SQ limit.

Each of these schemes can be advantageous for reducing the thickness of a PV absorber while maintaining or even increasing optical absorbance. Independently, a great deal of research is underway that uses plasmonics for photocatalytic (water splitting) and photoelectrochemical optical energy conversion. It remains a challenge, however, to successfully implement an energy-conversion scheme, aided by device architecture, plasmonic interactions, or a yet-to-be-discovered method that yields energy conversion greater than that of conventional devices and of the scale needed to address the global energy challenge.

Advances in science and technology to meet challenges

A great deal of research is ongoing to improve light collection/trapping in materials and to use that optical energy for the purpose of energy conversion. An increasing amount of those efforts is devoted to exploiting plasmonics in this realm. Much of the pioneering work of the 19th and early 20th centuries on EM from the origins of the diffraction limit to light scattering in the Mie and Rayleigh regimes to waveguiding and radio technology is being revisited on smaller spatial dimensions and optical frequencies in nanostructures with plasmonic interactions playing a leading role.

Ongoing developments in metamaterials are bringing novel concepts to the field, wherein optical constants (e.g., refractive index) are tailorable not only by material composition, but also by architecture. The combination of plasmonics and metamaterials affords new opportunities for creative nanoscale manipulation of light and the conversion of EM energy into usable thermal, electrical, or chemical forms.

The various plasmonics concepts can lead to greatly improved photon management materials, including in SCs where they address the thick–thin issue. However, the main challenge of solar PVs still remains the color matching problem, i.e., the recovery of the energy of hot es. This energy is

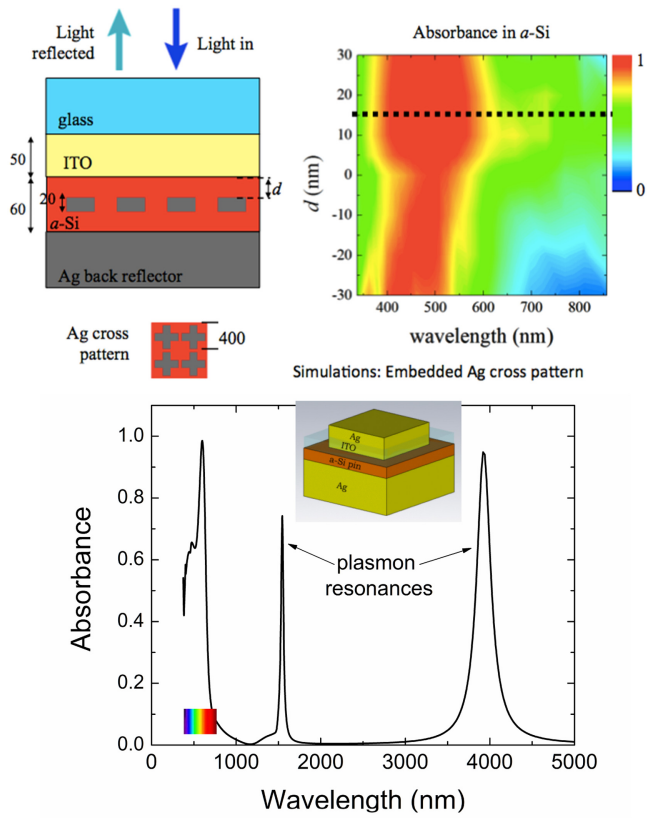

Figure 15. Examples of plasmonic energy-conversion schemes. Top: Plasmonic metal nanopattern embedded in a semiconductor enhances near-field scattering [98]; Bottom: Plasmonic metal–insulator–metal (MIM) structure where excess energy from hot es resonantly couples to IR plasmon modes [97].

typically lost to heat due to the rapid times scale of e–phonon scattering. The expensive MJ scheme is the only working scheme today and aims at eliminating hot es altogether by capturing multiple parts of the light spectrum in successively higher-band-gap semiconductor.

Hot es have very short mean-free paths due to phonon emission on the order of 1 nm. Various schemes have been proposed to recover this hot e energy. For example, narrow band energy filters at the absorber–electrode contacts were proposed to facilitate the needed isoentropic cooling of the hot es, while semiconducting QDs were proposed as an active medium of a SC to create a phonon bottleneck to slow down phonon emission [93]. In a recent paper [94], a small voltage increase due to the direct recovery of hot es was demonstrated in ultrathin a-Si PV junctions, illuminated by laser light at different frequencies in the visible range. Plasmonics could enhance this effect [95, 96].

A specific approach to accomplish this task has been recently proposed [97], based on the fact that e–*plasmon* scattering can be much faster than e–*phonon* scattering. Thus, by providing conditions for the former, the hot e energy could be protected from the latter, and it would remain in the electronic degree of freedom for an extended amount of time. Such hot e plasmonic protection (HELPP) could be enabled by plasmonic resonators. In one version, these could be embedded directly in a PV junction [98] as shown in figure 15 (top). In another, a planar array of plasmonic resonators could be adjacent to a junction as shown in figure 15 (bottom). Here, the planar plasmonic resonators also become a part of a metamaterial light-trapping structure, which facilitates broadband absorption in the ultrathin absorber. This dual function is evident from the simulated absorption spectrum shown in figure 15 (bottom), which consists of two sharp plasmonic peaks in the IR range for the HELPP and a broadband feature in the visible range for light trapping. HELPP effectively increases the lifetime of hot es and, thus, increases the probability of their arrival at the collector in the hot state. Successfully implemented, this scheme would lead to increased OC voltage with no loss of current.

Concluding remarks

While most proposed plasmonic energy-conversion concepts focus on light trapping, leading to a significant improvement in, e.g., solar performance, the main challenge is to solve the color matching problem: recovery of the energy of hot es usually lost to heat. Novel plasmonic concepts, such as the HELPP mechanism, offer possible solutions.

10. Light rectification using an optical antenna and a tunneling diode

Mario Dagenais

University of Maryland

Status

The integration of an optical antenna with a tunneling diode with proper impedance matching leads to what is now called a rectenna [99]. This device allows the capture of an optical signal falling on an optical antenna and the efficient rectification of this signal by the tunneling diode. The demodulator of choice for the rectenna is the MIM tunnel diode [100]. Schottky diodes are also a candidate for the rectifier, but they typically operate at lower frequencies than MIM diodes. The response time of the rectenna consists of several contributions: (1) the collective response of the conduction e that establishes the AC bias, which extends to frequencies well beyond the UV, (2) the tunneling time for es to cross the gap region before field reversal, and (3) the electrodynamical (parasitic) response of the junction to the changing field, in particular, the resistance and capacitance (RC) response time.

The antenna is modeled as a voltage source V_A in series with a resistance R_A, and the MIM diode is modeled as a resistor R_D in parallel with a capacitor C_D. Efficient transfer of power from the antenna to the load R_D requires matching R_A with R_D and keeping the time constant $\tau = (R_A \parallel R_D)C_D$ much below the time period of the source V_A [101]. For a parallel plate capacitor, the time constant $\tau = R_D C_D$ is independent of the diode area and is determined by the composition of the MIM diode. Assuming a breakdown current density of 10^7 A cm^{-2} at 0.1 V and a dielectric constant $\varepsilon = 1$ at a thickness of 10 nm, a time constant of $\tau = 10^{-15}$ s is extracted, which is too large for coupling at a visible wavelength. It is, then, concluded that a planar MIM diode, represented by a parallel plate capacitor, would operate well in the IR, say up to 30 THz, but would not operate in the visible. The extension of the planar MIM diode to the visible wavelength is a challenge. By contrast, point-contact devices (i.e., whisker diodes) have demonstrated frequency responses up to frequencies in the green part of the visible spectrum, but they are very irreproducible and are hard to use. The asymmetrical nonplanar geometry of the whisker, together with the flat anode, are essential requirements for increasing the cutoff frequency of the diode. The present challenges include realizing these structures in a reproducible and stable way, using well-established nanofabrication techniques, and scaling up these structures to large arrays.

Current and future challenges

It was recently demonstrated that the response time for a point contact with a spherical tip is proportional to $A^{-1/4}$, where A is the area of the junction [102]. This implies that it is possible to decouple RC and to appreciably improve the response time of the diode, possibly to the visible frequencies of the solar

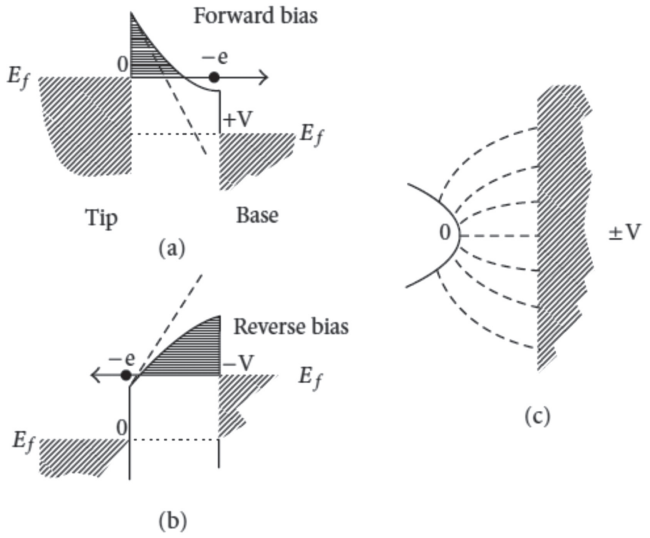

Figure 16. The (*a*) forward and (*b*) reverse asymmetric potential barriers for a geometrically asymmetric point-contact diode structure. Figure taken from [4].

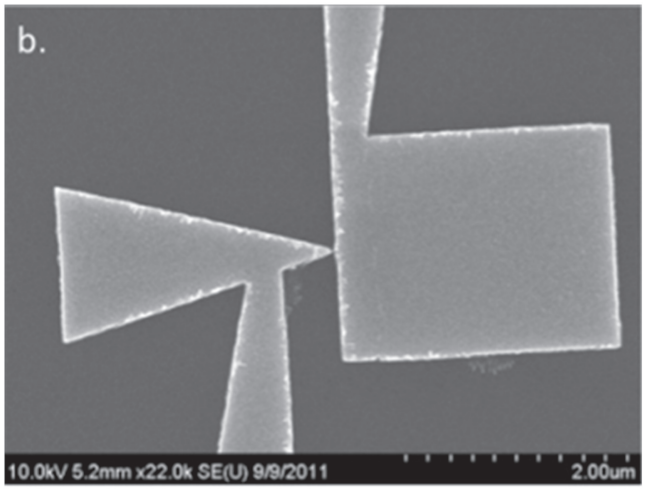

Figure 17. SEM micrograph of Ni/NiO_x/Ni geometrically asymmetric tunneling diode/nanoantenna.

spectrum. Rectification requires an imbalance between the forward and the reverse currents circulating during the positive and negative cycles of the AC potential at the junction. An electrical asymmetry in the *I–V* characteristics can be obtained using various approaches including material asymmetry, thermal asymmetry, and geometric asymmetry. By applying a bias, efficient rectification can be realized for detector applications. However, for energy harvesting applications, it is necessary to operate the diode at zero external bias. The geometric asymmetry diode (see figure 16) was demonstrated in [104], and it allowed energy harvesting at zero external bias. A sharply pointed planar triangular tip emitter incident on the boundary of a square receiver provides electric field asymmetry (see figure 17) [100]. When the square is biased positively, the electric field line density incident on the triangular tip is enhanced by the lightning rod effect. The inverse tunneling current is very reduced because

of the lower electric field at the surface of the flat electrode. Four parameters are typically used to characterize the rectification efficiency. They are: (1) the differential junction resistance $R = \mathrm{d}V_{\mathrm{DC}}/\mathrm{d}I_{\mathrm{DC}}$, (2) the nonlinearity $I'' = \mathrm{d}^2I_{\mathrm{DC}}/\mathrm{d}V_{\mathrm{DC}}^2$, (3) the sensitivity or responsivity $S = \frac{1}{2}\frac{\mathrm{d}^2I_{\mathrm{DC}}/\mathrm{d}V_{\mathrm{DC}}^2}{\mathrm{d}I_{\mathrm{DC}}/\mathrm{d}V_{\mathrm{DC}}}$, and (4) the QE $\eta_q = \frac{\hbar\omega}{e}S$. The equations for R and S are altered in a quantum description of the photon-assisted tunneling. This is required when the incident optical photon energy on the antenna corresponds to $V_{\mathrm{nonlinear}}$ on the order of 100 meV, typical of low-barrier MIM diodes and is typical of MIM barrier height. In this quantum description, the classical values of resistance and the responsivity decrease as the photon energy increases [105]. The maximum achievable conversion efficiency (ratio of output DC power to the input AC power) for monochromatic illumination is 100%. For broadband illumination, the diode operating voltage plays the role that the band gap plays in conventional SCs and efficiencies approaching the SQ limit are expected [106]. Furthermore, because sunlight is spatially coherent only over a limited area, concentration of the incident light is limited (see section 12). A coherence of 90% for a broadband solar spectrum is reachable only for a circle of radius 19 μm [107].

Advances in science and technology to meet challenges

The power-conversion efficiency in a rectenna depends on: (1) the efficiency of the coupling of incident radiation to the antenna, which depends on the antenna radiation pattern as well as its bandwidth and the coherence of the light, (2) the efficiency with which the collected energy propagates to the junction and is governed by resistive losses at high frequencies in the antenna, (3) the coupling efficiency between the antenna and the diode, which depends on impedance matching, and (4) the efficiency of rectifying the power received in the diode, which is related to the diode responsivity. It is also important to consider the use of noble metals and plasmonic resonances on the field enhancement and rectification properties on a tunneling junction (see section 9). Recent results demonstrate the importance of the plasmon frequency on both the material and the geometry of the tip, which could be used to control the frequency at which the junction is most efficient for the rectification of optical signals [102]. At optical frequencies, the classical skin depth in metals is on the order of 30 nm, and optical losses can be very large. Characterization of nanojunctions as a function of wavelength, polarization, and materials is required for optimizing the rectenna. The difficulty of producing arrays of nanometer gap junctions over areas of order cm^2 has to be studied. By using constructive interference, it is possible to coherently combine the electric fields from the different antennas of an array. This would allow the control of the antenna array far field. This needs to be studied in more detail. Tips of radii of a few nanometers have to be produced in order to get very high frequency responses. Ultimately, the junctions will be limited by dielectric breakdown. More research needs to focus on this issue.

Concluding remarks

Rectennas have the potential for converting solar energy to electrical power all the way from the IR to the visible using arrays of potentially low-cost devices with conversion efficiencies similar to PV devices. As discussed, geometrically asymmetric diodes can rectify radiation all the way to the visible and, therefore, appear most promising. Rectennas can also be used for beaming monochromatic IR and visible power with detection efficiencies approaching 100%. Another potential application of this technology is for waste heat harvesting in the IR if the coherence area of the IR radiation is appropriately selected. Rectennas can use nanoimprints and roll-to-roll technologies for reducing the manufacturing cost. So far, low-efficiency rectennas (on the order of 1%) have been demonstrated in the IR. Much work obviously remains to be done to demonstrate the full potential of this technology.

11. Full solar spectrum conversion via MJ architectures and optical concentration

Yuan Yao[1], Lu Xu[1], Xing Sheng[1], Noah D Bronstein[2], John A Rogers[1], A Paul Alivisatos[2,3], and Ralph G Nuzzo[1]

[1]University of Illinois at Urbana-Champaign
[2]University of California, Berkeley
[3]Lawrence Berkeley National Laboratory

Status

Significant advances have been made in research to improve the performance of single-junction PV devices. Currently, the best Si and GaAs devices have achieved efficiencies of 25.6% and 28.8%, respectively [26] (see sections 2, 4). The realization of significant further enhancements in the efficiencies of PV energy conversion, however, resorts to MJ architectures using semiconductor materials with subcell band gaps tuned to target different portions of the solar spectrum in order to minimize carrier thermalization losses and to increase spectrum coverage to exceed the SQ limit [24]. In theory, a MJ cell can achieve an efficiency as high as 86.8% with an infinite number of junctions [108] (a value lower than the Landsberg limit [21] due to entropy losses), and a number of different cell designs have been intensively explored by the PV research community as a means through which such forms of performance enhancement can be realized. These include, most notably, devices that embed the semiconductor elements in the form of MJ SC stacks [109] and, to a lesser degree, optical approaches involving various forms of spectrum splitting [110] (see also section 13). In the first design, the subcells are either epitaxially or mechanically stacked together in the order of decreasing band gaps to divide the incident sunlight using the absorption of the subcells (see also section 3). In the second approach, separate optics (e.g., prisms, holograms, and dielectric bandpass filters) are used to split the solar spectrum and to direct different portions to the relevant subcell. It has been persuasively argued that both designs would benefit from high geometric concentration of the solar irradiance as one means to both offset the high material costs encumbered by the III–V semiconductor device elements and to enhance the system power-conversion efficiency. To date, cell stacking designs have achieved the highest benchmark performances in solar energy conversion with world-record efficiencies of MJ cells reaching 46.0% with a four-junction design (InGap/GaAs/GaInAsP/GaInAs) under 508 suns [26]. Exemplary recent progress includes a report from our group of 43.9% efficient quadruple-junction four-terminal microscale SCs that were fabricated by mechanical stacking of a top 3-J device onto a bottom Ge cell via transfer-printing-based assembly [111].

Current and future challenges

For epitaxially grown MJ devices, the difficulty of sustaining lattice matching through multiple layers of growth limits the material selections that are available for use in each subcell and, thus, directly restricts achievable limits for device performance. Mechanically stacked devices, on the other hand, can be fabricated via high-temperature wafer bonding [112] to circumvent this issue but still carries a requirement for current matching at the electrically conducting interfaces, which is difficult to realize as the number of subcells increases to subdivide the solar spectrum. Alternatively, insulating adhesives can be used between mechanically stacked subcells to enable multiterminal connections and, in this way, to avoid the need for current matching. These interfaces need to be carefully designed to minimize reflection losses as well as to manage heat flow and thermal-mechanical stresses at high optical concentration [111]. Additional electro-optical challenges exist for the material used in each subcell. For example, a top wide-band-gap subcell (i.e., $E_g > 1.4$ ev) generally cannot be doped to a sufficiently high level to enable efficient carrier collection under high-irradiance concentration; it requires incorporation of highly doped low-band-gap materials that either degrade its optical transparency for low-energy photons or complicate backcontact grid configurations [109].

It has been noted that the limitations associated with stacked MJ devices can be tackled, in principle, by employing external optical components to split and to distribute the solar radiation to an array of spatially separated subcells [113]. By decoupling material compatibility from band-gap optimization, this approach also enables MJ designs with larger numbers of subcells and, thus, higher theoretical efficiencies. As the cell fabrication steps are reduced to provide a set of single-junction devices, simplified process flows for the semiconductor components are possible (see sections 2, 7). The commonly proposed optical designs include holographic gratings and wavelength-selective mirrors (e.g., multilayer dielectric Bragg stacks). Their practical use, however, is hindered by the formidable requirements for high-optical quality as well as the complexity of the optical designs needed to achieve competitive system-level efficiencies.

The high cost of III–V materials, especially in MJ cell contexts, likely necessitates a high-optical-concentration design to achieve commercial viability (see section 12). Optical losses figure importantly in all forms of concentrator PV designs. Stacked cells, for example, are subject to significant Fresnel losses (e.g., 12% of incident photons are lost to reflection before reaching the SCs for a system with three glass/air interfaces) that limit their optical (and, thus, power-conversion) efficiencies. Broadband antireflection (AR) coatings would afford an ideal solution, but materials that can span the refractive index range needed to mitigate these effects have yet to be developed. The use of common light-trapping designs on the PV cells also become more complex as they can scatter light and, otherwise, limit the broad-spectrum performance of high-concentration optics (see section 3). Geometric solar concentrators (GSCs) also require

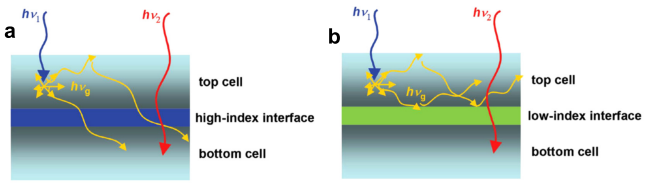

Figure 18. Illustrations demonstrating photon dynamics in a MJ device (reproduced from [117]). (*a*) No photon recycling: the radiative emission from the top cell is coupled to the bottom cell. (*b*) With photon recycling: using a low index interface as an intermediate reflector, the ERE and V_{OC} of the top cell are enhanced.

solar tracking and, even more significantly, do not utilize diffuse light—a significant component of the solar spectrum. (The diffuse component is 10% in AM1.5G illumination; most locations in the United States having 24% to 50% diffuse sunlight [114].)

Advances in science and technology to meet challenges

Light management within and between subcells

It has been shown in single-junction devices that high external radiation efficiencies (EREs), as achieved by luminescence extraction enhanced by photon recycling, are crucial for high PV performance (as demonstrated by the world-record GaAs device where the radiatively emitted photons are reflected by a metal backsurface rather than absorbed by the substrate) [46, 115] (see section 4). Likewise, MJ devices with intermediate reflectors that enhance ERE with photon recycling would improve the V_{OC} for each subcell (figure 18), although these reflectors also need to transmit sub-band-gap photons for the next cell. Different designs have been examined theoretically that provide such effects, such as stacks spaced by an air gap coupled with AR coatings as the intermediate reflector in-between subcells [116]. The elements of this design have been demonstrated experimentally using microscale SCs stacked onto prepatterned air gap spacers using a soft-transfer-printing technique [117]. The opportunities for progress have also been demonstrated theoretically in the design of a high-performance spectrum-splitting PV system that uses polyhedral specular reflectors coupled to spatially separated devices to enhance both photon recycling within a subcell and radiative coupling between them [118].

Improving the optical efficiencies of GSCs

There exist numerous opportunities to improve the performance of concentrator PV systems. Providing improved broadband AR coatings (e.g., porous films with sub-wavelength features to avoid scattering) forms one obvious direction in research to reduce the Fresnel losses associated with concentrating optics. The development of strategies that would allow the utilization of diffuse light within a concentrator PV design is also of significant interest. We might envision, for example, the coupling of a GSC with a luminescent solar concentrator (LSC), wherein, diffuse radiation striking the backplane can be absorbed by the luminophore

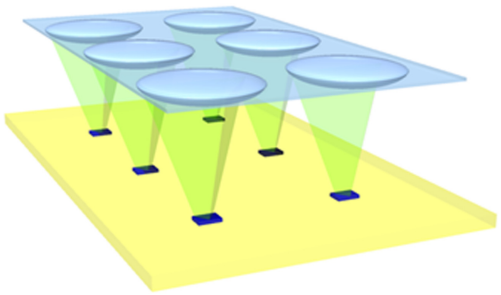

Figure 19. Schematic of a hybrid concentration system with an embedded microscale SC module, both the device and the luminescent waveguide can be configured as a MJ architecture for full spectrum conversion.

and can be down-converted into total internal reflection modes that are directed to the embedded PV device elements. A possible geometry for such a system suggested by elements of our past work is one of embedding arrays of microscale SCs directly in the LSC waveguide (figure 19) such that, in addition to diffuse light conversion, the direct illumination from the Sun can be concentrated at the top surface of the devices using a GSC with a higher concentration ratio and optical efficiency [119, 120]. We have shown that QD luminophores (see also sections 5, 6) are particularly advantageous for use in such microcell LSC arrays as compared to traditional organic dyes as they have high quantum yields, large (and tunable) Stokes shifts for reduced reabsorption losses, and better long-term photostability. Their narrow emission peaks also facilitate photonic designs to better trap/manage the luminescent photons to improve optical efficiency [120, 121]. It is also of particular interest to note that high-optical efficiency LSCs may engender specific capabilities for high-performance concentrator PV designs that would be transformational, specifically to obviate the need for solar tracking as well as the intriguing possibility that they might enable new approaches to spectrum splitting using discrete subcell arrays that can achieve efficiencies approaching those associated with monolithic MJ cell stacks.

Concluding remarks

MJ architectures are required to achieve full spectrum conversion and to surpass the SQ limit. Concentration is advantageous in a MJ system in both improving their efficiency and reducing their cost. This perspective outlines new materials, optical integration strategies, and approaches to spectrum splitting that beget new opportunities through which the grand challenge of full-spectrum conversion might be realized.

Acknowledgments

This work is part of the 'Light-Material Interactions in Energy Conversion' Energy Frontier Research Center funded by the U.S. Department of Energy, Office of Science, Office of Basic Energy Sciences under Award No. DE-SC0001293.

12. Advanced solar concentrators

Jeffrey M Gordon

Ben-Gurion University of the Negev

Status

Concentrating sunlight has fascinated people since time immemorial [122]. Heat production and electricity generation comprise the main current applications (unorthodox uses include nanomaterial synthesis [123] and medical surgery [124]). Generally, solar concentration is motivated by cost and efficiency. Cost because expensive receivers are largely replaced by inexpensive optics. Solar-*thermal* efficiency benefits from markedly reducing heat-loss area. PV-conversion efficiency can increase linearly with the logarithm of the concentration at low series resistance.

'Advanced' refers to concentrators that approach the thermodynamic limit for the relation between flux concentration C and acceptance half-angle θ_a *at high collection efficiency*: $C\ \sin^{d-1}(\theta_a) \leqslant n^{d-1}\ \sin^{d-1}(\theta_e)$, where n is the refractive index in the concentrator (air but, occasionally, a transparent dielectric for PVs), θ_e is the maximum half-angle irradiating the absorber, and d is the dimensionality [125–127]. Minimally, θ_a is the convolution of the Sun's angular radius (0.27°) with manufacturing, installation, and tracking imperfections. Maximally (for static low-concentration collectors), θ_a is the angular range from which beam radiation is collected over the day. The familiar solutions of spherical-cap or Fresnel lenses and parabolic or Fresnel mirrors that have dominated solar technologies, to date, fall far short of the thermodynamic limit [125–127].

Advanced concentrators range from static 2D systems ($\theta_a \approx 25°$–$90°$), to single-axis tracking line-focus systems ($C \approx 5$–100), and dual-axis tracking point-focus systems ($C \approx 100$–$100\,000$). Nonimaging optics uniquely provides static designs that approach the thermodynamic limit [125–127]. Some enjoyed commercial realization (figure 20(*a*)). The higher concentration domain is still dominated by parabolic and Fresnel mirrors and Fresnel lenses, although a variety of advanced nonimaging second-stage concentrators have been developed [125–127]. The simultaneous multiple surface (SMS) method [125, 126] was the first to spawn advanced concentrators that both were ultracompact and could accommodate a sizable gap between the absorber and the optic. The nonimaging strategy maps incident extreme rays to the extremes of the absorber [125, 126].

Advanced aplanatic concentrators [128] opened new vistas, recently adopted for PVs (figure 20(*b*)). The *imaging* aplanatic strategy (viable for $\theta_a \leqslant \sim 2°$) completely eliminates spherical aberration and coma [128] while admitting ultra-compact pragmatic optics.

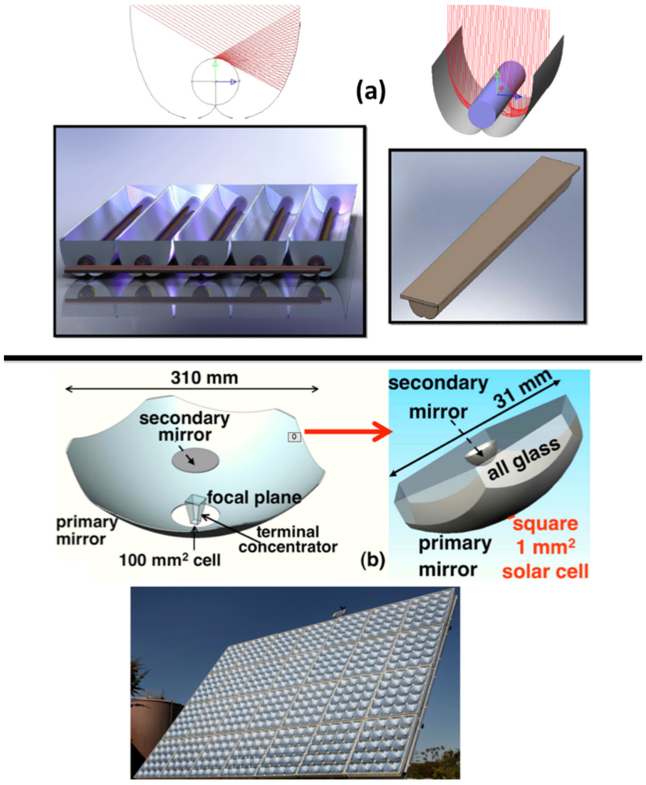

Figure 20. (*a*) Sample advanced *static* nonimaging concentrator with an evacuated tubular absorber for steam production. (*b*) Two generations of advanced aplanatic concentrators for PVs, first air-filled for 1 cm^2 cells, then, transitioning to glass-filled for 1 mm^2 cells plus a photograph of an installed 15 kW_{peak} array comprising the former.

Current and future challenges

For PVs, current challenges subsume (a) ultraminiaturization that enhances the feasibility of SMS and aplanatic concentrators (especially, dielectric-filled units), and (b) spectrum splitters that take better advantage of the spectral conversion of separate SCs. Another tack is quasistationary high-concentration optics that would markedly simplify and downsize solar trackers via the use of either: (1) light guides (that have remained at the developmental level due, in part, to substantial optical losses), and (2) *spherical* gradient-index (GRIN) lenses (figure 21(*a*)) that await accurate high-volume fabrication methods. A recent GRIN advance demonstrated lens refractive index profiles for off-the-shelf solar-transparent materials with efficient performance that approaches the thermodynamic limit [129]. The prior conventional wisdom had been that only the refractive index profiles of eponymous Luneburg lenses (with refractive indices for solar frequencies for which no materials have yet been identified) could achieve the objectives [129].

Another tantalizing new direction is solar aperture rectifying antennas (rectennas), predicated on exploiting the partial spatial coherence of sunlight with microconcentrators, nanoantennas, and ultrafast rectifiers (AC to DC conversion) (see section 10) [130]. The topic of light rectification is elaborated in section 08b of this article. Solar aperture rectennas have been shown to possess fundamental limits (for

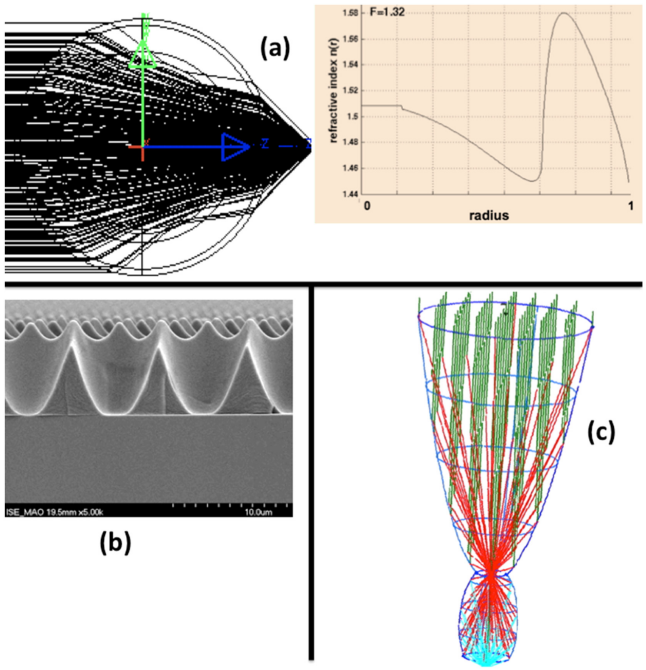

Figure 21. (*a*) Illustration of new solutions (for refractive index as a function of radius) for spherical GRIN lenses accommodating refractive indices available for off-the-shelf materials that are transparent in the solar spectrum. The substantial constant-index core region facilitates lens fabrication [129]. This unit-radius ultrahigh-concentration $f/0.66$ lens was ray traced for the full solar spectrum and the extended solar disk. (*b*) E micrograph showing current state-of-the-art fabrication for microconcentrators. (*c*) A candidate high-concentration aplanat [128] that could be used in solar aperture rectennas [130]. The aplanat can be dielectric filled and satisfies total internal reflection.

conversion efficiency) that exceed those of solar-thermal and concentrating PVs but require microconcentrators within the spatial coherence area of solar beam radiation, to wit, radii on the order of tens of micrometers [130] (figure 21(*b*)), such that C is on the order of 10^3. Because phase-conserving optics are needed, devices should approach perfect imaging and, hence, the thermodynamic limit (figure 21(*c*)).

Advances in science and technology to meet challenges

The technological advances needed to address these challenges fall mainly into two categories: microfabrication and materials. For the latest miniaturized concentrator SCs with linear dimensions of ~0.5 mm, all-dielectric optics that are unfeasible for conventional cells with linear dimensions on the order of a centimeter (simply due to the mass per aperture area) present promising alternatives. This will require integrated production methods (micromodularity) with SCs, micro-optics, wiring, bypass diodes, and heat sinks comprising a single manufactured unit. Accurate micro-optical fabrication both for lenses and for highly reflective specular mirrors will be essential. This also necessitates the precise and reproducible fabrication of sheets comprising thousands of PV miniconcentrators per m^2 of collection area.

For solar rectennas, this will correspond to the order of 10^9 aperture rectennas per m^2 of collection area. These units will require the development of efficient *broadband* nanoantennas and broadband ultrafast rectifiers (a bandwidth on the order of 10^6 GHz).

Although viable spherical GRIN lenses have been produced by the trillions for millions of years (chiefly fish eyes), the development of accurate, robust, and affordable fabrication procedures has proven elusive, albeit with recent encouraging progress [131]. The newly discovered GRIN solutions for available materials can also be tailored to fabrication constraints, such as an extensive constant-index core and constant-index shell regions [129]. Lens diameters will vary from the order of centimeters (for concentrator PVs) to tens of micrometers for solar aperture rectennas.

Finally, specifically for the *optical* aspects of solar-thermal power conversion, the challenge shifts to the development of superior (and robust) selective coatings (i.e., high solar and low IR emissivity) at progressively higher temperatures that give rise to higher turbine efficiencies. This relates both to line-focus (evacuated) receivers in the quest for efficient operation above ~700 K as well as to point-focus (nonevacuated) receivers aiming to operate at temperatures exceeding 1000 K.

Concluding remarks

Achieving ultraefficient solar conversion could basically be solved if *efficient and feasible* methods could be found to convert broadband solar to narrow band radiation, which could then be exploited by a plethora of radiation converters (including those from physical optics, such as diffractive and holographic elements, rectifying antennas, etc., that are insufficiently efficient due to the narrow spectrum they can accommodate). Proposals of PV UC and down-conversion notwithstanding (see sections 13–18), current proposals are far below the required performance. Hence, in the foreseeable future, the focus will likely be on the types of nonimaging and aplanatic optics, GRIN optics, and micromodularity (permitting optics precluded by common large-absorber collectors) that not only can raise solar-conversion efficiency, but also can render them more practical and amenable to large-volume production.

13. Spectral splitting and nonisothermal solar energy conversion

Svetlana V Boriskina

Massachusetts Institute of Technology

Status

The broadband nature of thermal radiation—including sunlight and that of terrestrial thermal sources—imposes limitations on the light-to-work efficiency of the whole-spectrum energy converters [27]. Quantum-conversion platforms, such as PV cells are unable to harvest the low-energy photons and to convert the high-energy ones very inefficiently (see sections 2, 3). In turn, thermal energy converters with blackbody receivers suffer from re-emission losses at high temperatures and require high levels of solar concentration to overcome such losses (see section 12). Achieving high optical concentration (e.g., by using a large heliostat field) may not only be costly, but also introduces additional loss mechanisms that negatively impact overall system efficiency.

Sorting photons by their energies and processing them separately helps to increase the light-to-work-conversion efficiency. The most explored approach to spectral splitting is based on using MJ PV cell stacks (figure 22(*a*)) where the wide-band-gap top cells absorb high-energy photons, while the lower-energy ones are transmitted through to the narrow-band-gap cells at the bottom of the stack (see section 11). The stacked spectral splitters/converters can also incorporate catalytic platforms to harvest UV light and thermal receivers to absorb low-energy IR photons. Yet, efficient stacking and electrical wiring of several converters is challenging, especially in hybrid configurations that include converters with different operating temperatures, which might require thermal insulation between the PV and the thermal receivers.

To address these issues, cascade reflection and external spectrum splitting schemes are being actively explored, which make use of perfect and dichroic mirrors, holograms, dielectric prisms, polychromats, etc [132, 133]. (figures 22(b), (c)). This shifts the R&D focus from the PV material design and fabrication issues to the development of efficient optical elements. Even traditional stacked PV configurations can benefit from adding photon-management elements, such as embedded wavelength-selective filters for photon trapping and recycling [134].

Current and future challenges

The solar radiation is dilute and is even further diluted by spectral splitting, which, in turn, reduces the energy-conversion efficiency, especially for the solar-thermal converters. Although spectral splitters can be combined with external solar concentrators, fully integrated platforms may help to reduce optical losses and to provide cheaper and more compact technological solutions. Spectral-splitting holograms can simultaneously provide some optical concentration. Higher concentration can be achieved with planar light guides either passively (by light trapping and guiding) or actively—by down-converting photon energy by embedded luminescent

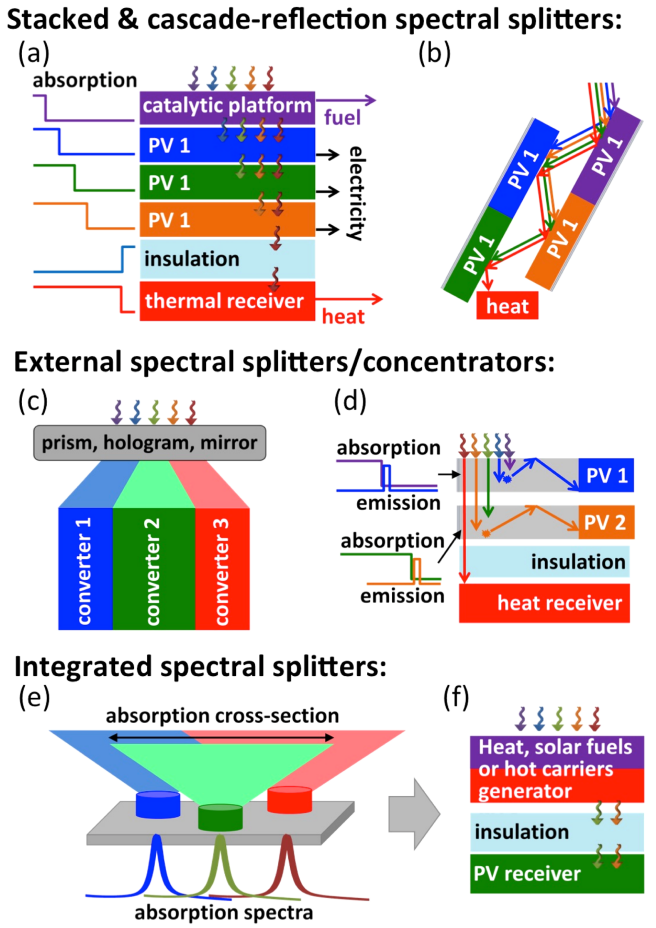

Figure 22. Various types of spectral splitters.

material (figure 22(d)), yet the optical efficiencies of such schemes need to be improved (see section 11).

Light-conversion platforms would greatly benefit from the development of integrated elements that simultaneously provide spectral and spatial selectivities, which translates into optical concentration [135] (see section 9). This approach is schematically illustrated in figure 22(*e*) and makes use of wavelength-scale selective absorbers with large overlapping absorption cross sections. Spectral selectivity of individual absorbers can be governed by their localized optical resonances [9, 135] and/or via long-range interactions that form quasilocalized lattice modes at different wavelengths [136]. Although challenging, this scheme can be realized with resonant plasmonic and dielectric nanoantennas. Photons not captured by localized absorbers are harvested in the bottom layer. Such a scheme makes possible designing inverted stacks with PV receivers as the bottom converter, and the top layer selectively harvesting shortest- and longest-wavelength photons, which are not efficiently converted by the PV cells (figure 22(*f*)).

Advances in science and technology to meet challenges

The MJ stacked PV is the most mature spectral-splitting technology. Despite reaching impressive 46% efficiency, it still falls below the theoretical limits (figure 23(*a*)) [26]. Additional external spectrum-splitting elements can further

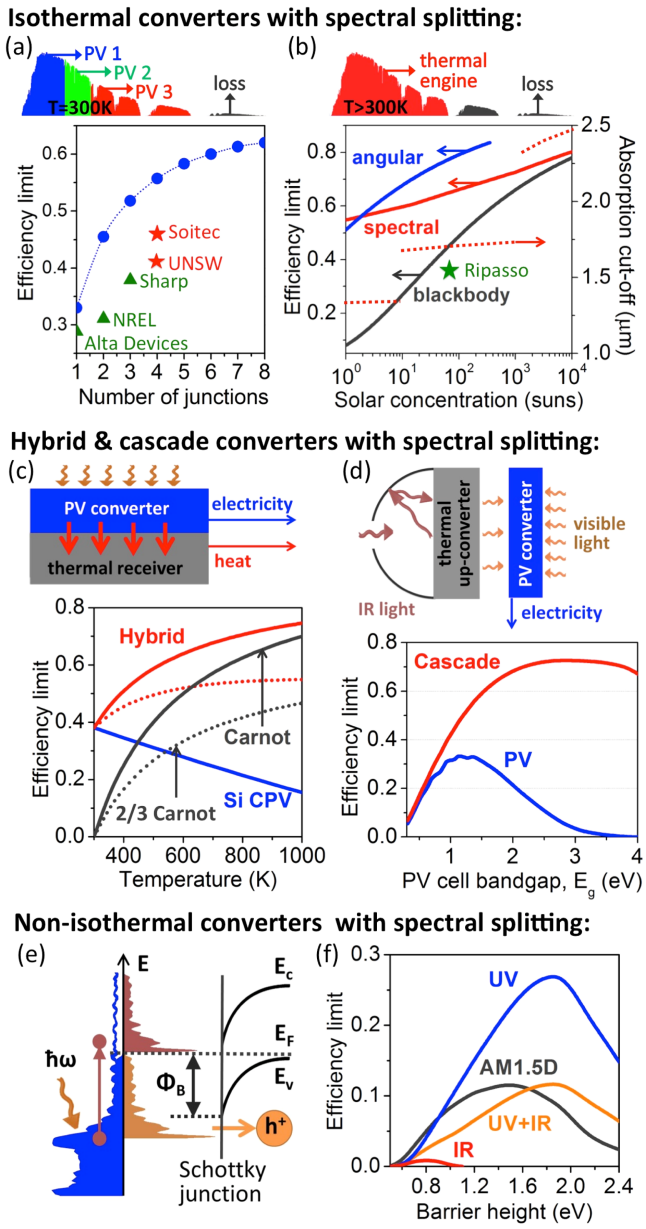

Figure 23. Predicted and achieved efficiencies of solar-conversion platforms with spectral splitting. In theoretical limit calculations, thermal engines are assumed to be operating at Carnot efficiency and PV cells—at SQ efficiency; solar concentration: (*a*), (*d*) one sun, (*c*), (*f*) 100 suns.

improve the efficiency of PV stacks (e.g., in University of New South Wales cells). In turn, solar-thermal converters rely on high concentration to compensate for the radiative losses at high temperatures. This technology can significantly benefit from the development of selective absorbers [10, 137], which suppress emission at longer wavelengths and can operate at high temperatures (see section 17). Absorbers with angular selectivity (i.e., those that can only absorb/emit light within a narrow angular range to match that of incoming sunlight [138]) can offer even higher efficiency (figure 23(*b*)). Spectral and angular selectivities can be achieved via external filters or by designing the absorber itself to be selective.

Another important issue in the solar energy conversion is the intermittent nature of the sunlight, which calls for the development of the energy storage solutions. The high cost of electrical storage and a possibility of combining PV and solar-thermal engines in hybrid platforms fueled interest in the thermal storage [139]. Efficiency of the PV cells degrades if they operate at high temperatures matching that of the heat receiver (figure 23(*c*)). This calls for the development of transparent thermal insulators and integrated spectral splitters to further boost the hybrid device efficiency. External spectrum splitting also alleviates thermal issues, and—in combination with spectral and angular selectivities of the thermal emitter—is predicted to offer promise of achieving thermal UC of photon energy (figure 23(*d*)) [140]. Another way to reduce radiative losses can be by topping thermal absorbers with transparent thermal insulators, creating nonisothermal (i.e., externally cool internally hot) converters [141, 142].

Another type of nonisothermal converter—known as the hot-carrier converter—is based on harvesting photoexcited charge carrier before they thermalize to the temperature of the crystal lattice (see also sections 5, 9, 14). Despite high predicted efficiency limit [143], development of such converters has been stymied by the difficulties in efficient extraction of hot carriers. Not only the carriers need to be harvested within an ultrashort time period (below a picosecond), but also the efficiency of commonly used filters, such as, e.g., Schottky barriers is low (figure 23(*e*)). Furthermore, large enough population of carriers hot enough to pass through the energy filter cannot be easily created by sunlight in conventional materials, such as noble metals [144]. Our calculations predict that material engineering (see sections 5–8) to tailor the e DOS in combination with spectral-splitting schemes can boost efficiency of hot-carrier converters (figures 23(*e*), (*f*)) [145]. Hot-carrier converters that make use of plasmonic nanoelements naturally benefit from high spectral and spatial selectivities and can make use of the integrated spectral-splitting scheme shown in figure 22(*f*).

Concluding remarks

Spectral selectivity can be achieved by the choice of the receiver material, which calls for the development of high-quality PV materials and heat absorbers stable at high temperatures (see sections 7–9, 15–17). The use of external splitters shifts the emphasis to the design of optical elements, which ideally combine selectivity, high concentration, and low losses. Non-isothermal energy converters are promising but call for significant advances in material design and integration. Hybrid schemes with energy storage in the form of heat or fuels are highly desirable.

Acknowledgments

The author thanks G Chen, B L Liao, W-C Hsu, J K Tong, Y Huang, J Loomis, L Weinstein, and J Zhou for discussions. This work was supported by DOE-BES Award No. DE-FG02-02ER45977 (for thermal emission tailoring) and by ARPA-E Award No. DE-AR0000471 (for full spectrum harvesting).

14. A path upward: new upconversion schemes for improving PVs

Di M Wu, Michael D Wisser, Alberto Salleo, and Jennifer Dionne

Stanford University

Status

Thermodynamic considerations limit PV efficiency to a maximum of 30% for single-junction SCs under one-sun illumination. The Carnot limit, however, sets the maximum for terrestrial SC efficiencies at 95% (see section 1, 20). To close the efficiency gap between these limits, MJ cells (see sections 3, 11), thermo-PV (TPV) cells (see sections 15–17), and solar concentrators (see sections 10–13) are each promising approaches. UC can complement these strategies. As illustrated in figure 24(*a*), UCs convert sub-band-gap solar photons to above band-gap photons, increasing the cell's short-circuit current. Modeling predicts that UC could increase the theoretical maximum efficiency of a single-junction SC from 30% to 44% for nonconcentrated sunlight [146]. An important advantage of UC is electrical isolation from the active layer of the cell, eliminating the need for current or lattice matching.

In recent years, UC materials have been used to bolster the performance of photoelectrochemical cells, c- and a-Si cells, organic cells, and dye-sensitized SCs [147]. The record improvement was demonstrated this year with lanthanide UC applied to a bifacial c-Si cell under 94-sun concentration, resulting in a 0.55% increase in cell efficiency [148].

Current and future challenges

While the performance of solar UC devices has been steadily improving, a substantial gap remains between theoretical cell improvements and experimental realizations. Three major challenges include: (1) increasing the efficiency of UC; (2) ensuring spectral overlap with SCs; and (3) increasing the UC absorption bandwidth.

The limitations on UC efficiency are rooted in the UC mechanism. Generally, UC of incoherent low-power light requires a metastable intermediate state for the first excited e to populate until a second photon is absorbed as highlighted in yellow in figure 24(*b*). Two material systems that have the requisite energy levels include lanthanide ion systems and bimolecular systems. In lanthanide ions, the long-lived state is an *f*-orbital with parity-forbidden decay to the ground state; in bimolecular systems, it is a long-lived triplet state populated through intersystem crossing. Lanthanide UC is often less efficient than bimolecular UC, in part, because in the former, both absorption and emission occur between weak *f*–*f* transitions, limiting both the light absorbed and the efficiency with which it is emitted. In bimolecular UC, absorption and emission occur between bright singlet states and, with the proper selection of sensitizer and emitter dyes, the major bottleneck to efficiency is the energy transfer between triplet states. The UC emission from both material systems has a quadratic dependence on incident power in low-flux illumination conditions, and efficiency typically increases with incident power density. Consequently, all demonstrations of effective UC-enhanced SCs, to date, have been performed under laser or concentrated solar illumination.

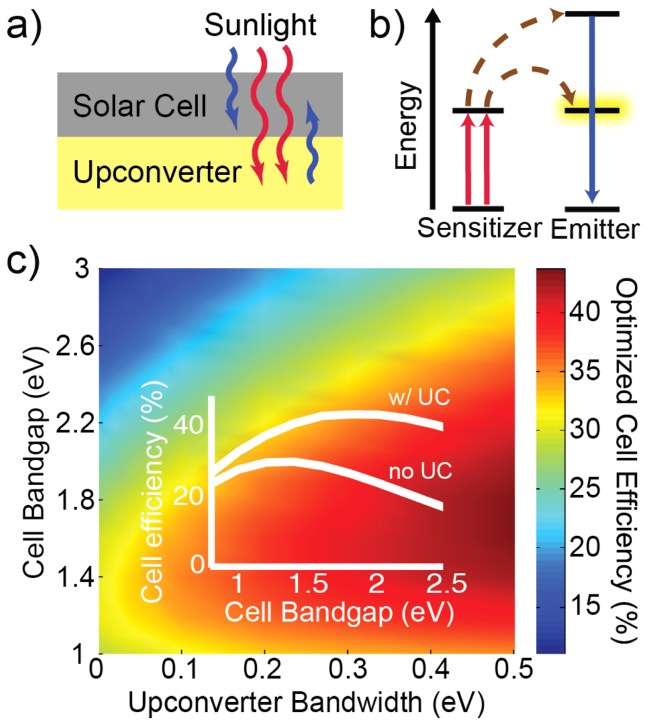

Figure 24. (*a*) UC-enhanced PV device. (*b*) Simplified UC mechanism highlighting the metastable intermediate state. (*c*) Effect of the cell band gap and UC bandwidth on cell efficiency [146].

The second challenge is tuning the spectral position of UC absorption and emission to make optimal use of sub-band-gap light. For example, the energy levels of lanthanide ions allow absorption of low-energy light below the Si band gap and re-emission above it, but the *f*-orbital energies can only be slighted tuned with the host lattice and are effectively fixed. Bimolecular UCs have synthetically tunable absorption but often operate above the band gap of many SC materials. Continued exploration of IR-absorbing triplet sensitizers will increase the relevance of these materials for PV.

A final challenge is extending the absorption bandwidth. As shown in figure 24(*c*), the potential cell-efficiency improvements increase with UC bandwidth [146]. Most studies, to date, have examined the performance of an individual UC; combining sensitizers to increase the absorption bandwidth for both lanthanide and molecular UCs is a direction that merits further exploration.

Advances in science and technology to meet challenges

Two approaches to address these challenges include: (1) improving existing lanthanide and bimolecular systems, and (2) exploring radically new UC schemes. Extensive investigations of the host lattice for lanthanide UC have yielded

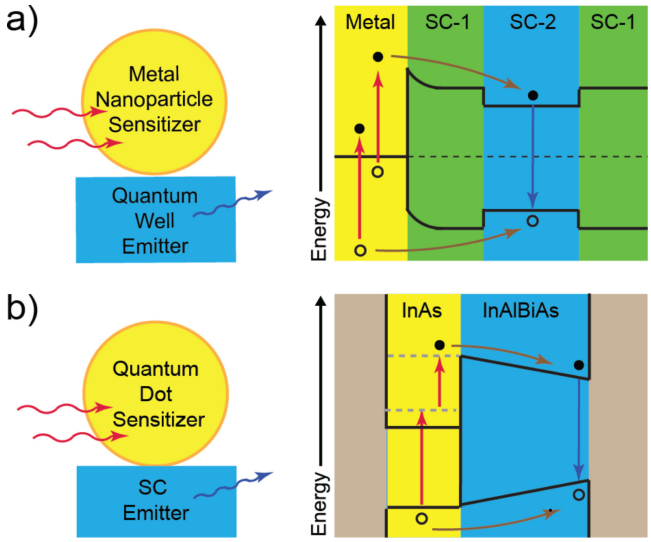

Figure 25. New UC schemes: (*a*) hot-carrier UC using metals near quantum wells [149] and (*b*) photon ratchet UC using graded band-gap semiconductors [150].

many key design principles, including low phonon energy, optimized interion spacing, and minimization of defects. New host lattices, such as Gd_2O_2S, that fulfill these requirements have demonstrated lanthanide UC quantum yields exceeding 15% (with a theoretical maximum of 50%) [151]. While bimolecular UC in solids is often limited by intermolecular energy transfer, novel matrices have efficiencies approaching those in solution with up to 17% reported in a polymer [152].

To address spectral considerations for solar energy conversion, design of new IR absorbing supramolecular dyes and hybrid UC-nanoantenna materials are promising approaches. For example, adsorbing of IR dyes to the surface of UC nanoparticles led to a 3300× increase in UC emission relative to the bare nanoparticle [153]. Plasmonic nanoantennas can increase the UC absorption bandwidth while also increasing the radiative rate of emission (see sections 9, 13) [154].

An emerging approach that could revolutionize the efficiency and spectral tunability of UCs is the use of hybrid semiconductor materials. Semiconductors generally absorb light with greater bandwidth than molecules or ions. Furthermore, their band gaps can be tuned with composition over the energy range most relevant for PV (see sections 7, 8). This tunability can be used to craft a potential energy landscape allowing sequential absorption of low-energy photons in one material followed by radiative recombination in a neighboring semiconductor.

For example, figure 25(*a*) illustrates hot-carrier UC in plasmonic materials interfaced with semiconductors. Here, a hot h and a hot e are independently created through absorption of light in a metallic nanostructure. These hot carriers are injected into a semiconductor quantum well where they are trapped until radiatively recombining with the corresponding carrier. Judicious selection of plasmonic materials and semiconductors leads to light emitted with higher energy than that absorbed. This scheme has a theoretical UC efficiency of 25% using 5 nm Ag nanocubes with absorption and emission tunable through geometry and material (see sections 9, 13) [149].

A second approach to semiconductor UC is shown in figure 25(*b*) (see also sections 5, 6). Here, light absorption occurs in QDs with VB edges matched to a neighboring semiconductor with a graded band gap. After a low-energy photon is absorbed by an InAs QD, exciting an e into the CB, the h is rapidly injected into the InAlBiAs layer. As in hot-carrier UC, the energy barrier back into the InAs is high enough to prevent the reverse process, establishing a long-lived intermediate state. A second low-energy photon excites the intermediate-state e above the CB edge of the neighboring material. The e is injected into the InAlBiAs where the h and e can radiatively recombine, emitting a photon of higher energy than either of those absorbed [150].

Finally, research on triplet energy transfer between organic dyes and SC nanostructures is another promising development for UC. For example, a recent study has shown that a semiconductor QD can serve as a triplet sensitizer for dyes attached to its surface [155]. The QDs can absorb near-IR light, improving spectral overlap with the needs of PVs. Design of hybrid UCs that selectively incorporate the best properties of each material is a strategy that merits further attention.

Concluding remarks

UC holds significant potential as an inexpensive and generalizable way to improve the efficiency of any SC. Existing UCs, however, lack the efficiency or optimal spectral characteristics for integration into commercial SCs. The study of canonical UC materials, including lanthanide and bimolecular systems, has provided key insight into the UC process and the limiting factors at play. Design of radically new materials and new UC schemes—including those based on semiconductors—is rapidly moving the field forward (and upward).

Acknowledgments

This work is part of the ‘Light Material Interactions in Energy Conversion’ Energy Frontier Research Center funded by the U.S. Department of Energy, Office of Science, Office of Basic Energy Sciences under Award No. DE-SC0001293. D.W. acknowledges support from the Gabilan Stanford Graduate Fellowship and the National Science Foundation Graduate Research Fellowship.

15. TPVs: an alternative strategy for converting heat to electricity

Peter Bermel

Purdue University

Status

TPVs convert heat into electricity by using thermally radiated photons to illuminate a PV cell as shown in figure 26 [156]. In comparison with alternative strategies for converting heat into electricity, TPVs have the potential for a quiet, compact, reliable, and highly efficient operation, although several barriers to widespread adoption remain. The original demonstration of TPVs at Lincoln Laboratories in 1956 used a camping lantern to illuminate a Si-based 'solar battery' to generate electricity [157]. However, compared to a solar PV, a TPV thermal emitter is much colder, emitting predominantly in the IR. Thus, within a decade, work began on TPV systems with smaller band-gap PV cells.

Initial work focused on germanium, but more recent work has included higher-efficiency gallium antimonide (GaSb) [158] as well as ternary and quarternary III–V materials, such as InGaAs and InGaAsSb [159]. Nonetheless, the broad bandwidth of thermal radiation gives rise to a great deal of wasted midwavelength and long-wavelength IR radiation [156]. To address this problem, optical short-pass filters have been placed on the front or back side of PV cells to reflect otherwise unused light back to the emitter. This approach constitutes external photon recycling and has been demonstrated to improve overall efficiencies [159, 160] (see also sections 4, 13). Combining these innovations has led to conversion efficiencies of radiated power into electricity as high as 23.6% [159].

Nonetheless, theoretical calculations have shown that there is room for a great deal of further improvement in TPV efficiencies (see also sections 16, 20). In particular, several theoretical studies have shown that ultimate efficiencies are highly dependent on the maximum emitter temperature and emitter designs and that, in some scenarios, the efficiency of the overall TPV system can exceed 50% [156] as shown in figure 27. By creating structures with emissivity concentrated primarily at wavelengths matching the regions of high external QE for the PV cells utilized, selective emission can be a key driver of improved performance. Specific structures with the potential for high efficiencies that have been proposed and have been built, to date, include 1D multilayer stacks [161], 2D metallic arrays of holes [162], and 3D woodpile PhCs [163].

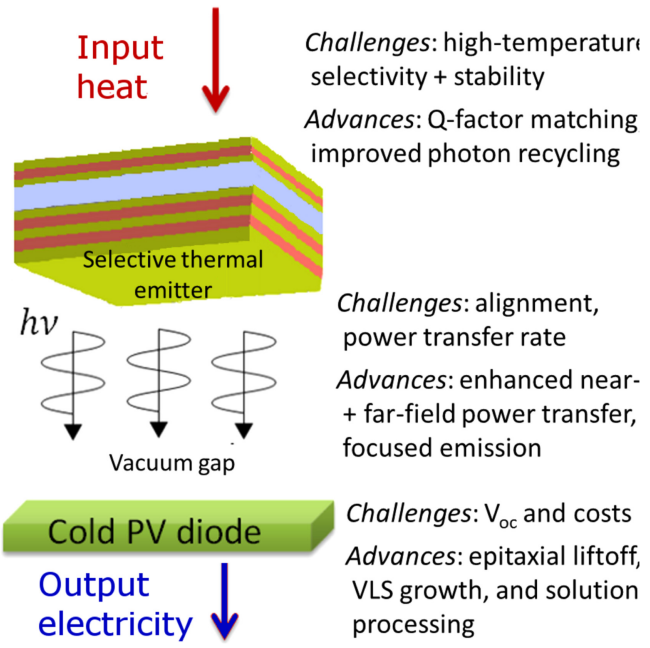

Figure 26. Overview of TPV operation along with a summary of the remaining challenges and possible advances to help address them.

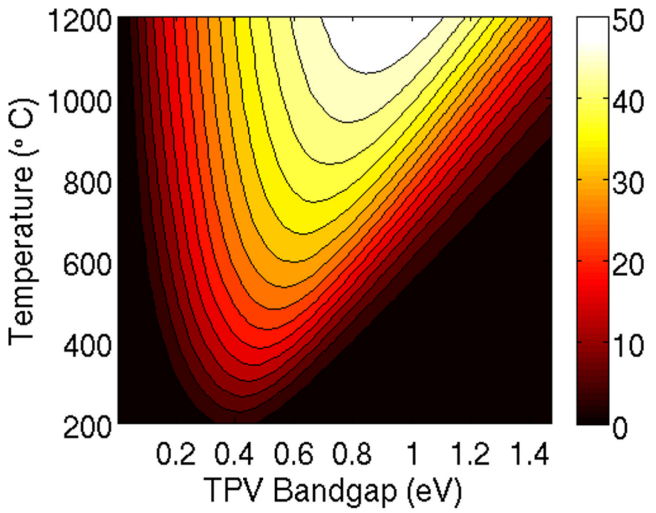

Figure 27. Illustration of the potential of TPVs. Using an integrated selective emitter structure can shape thermal radiation to match the PV cell band gap. Efficiency is plotted as a function of band gap and temperature. Maximum efficiencies may reach up to 50% for PV cell band gaps of 0.7–1.1 eV at 1200 °C.

Current and future challenges

In order for the TPV to approach its theoretical limits and to make the transition to a practical technology, there are a number of challenges that must first be overcome.

First, it is critical to further improve the theoretical design and experimental fabrication of selective emitters to offer greater high-temperature stability and performance (see also section 17). Many simpler emitter structures, such as metallic sheets, inevitably experience significant degradation in wavelength selectivity at high temperatures. More complex nanostructures can avoid some of these challenges but are more vulnerable to structural degradation even at temperatures well below the bulk melting point of the underlying elements (e.g., refractory metals, such as tungsten).

Second, it is important to consider strategies for reducing the need for precise alignment between emitters and receivers.

High-performance external photon-recycling strategies, in particular, generally require precise alignment, yet have zero tolerance for direct mechanical contact because of the thermal gradient. This combination may be experimentally unrealistic to achieve, so more straightforward alternatives would be highly beneficial.

Third, it is crucial to achieve improved understanding of novel physical phenomena in thermal radiation and to develop appropriate strategies for harnessing them. One particular emerging topic concerns the potential to achieve thermal radiation power levels that appear to exceed the common understanding of Planck's blackbody law (see section 1) through alternative geometric surfaces with increased surface area offering improved impedance matching between high DOS materials and air [164]. Another promising approach uses subwavelength gaps between emitter and receiver structures to transfer power in the near field exceeding that of a blackbody (see section 16). However, alignment of macroscopic plates at nanometer-scale distances without physical contacting would seem to be an even more prohibitive experimental challenge than discussed previously.

Finally, reducing the cost and improving the performance of the low-band-gap PV cells is often a challenge. Even for relatively expensive GaSb cells ($E_g = 0.7$ eV), this difficulty manifests primarily in low OC voltages (typically 250 mV or less), which has follow-on effects for the fill factor and overall efficiency of the TPV system, even in the presence of an ideal thermal emitter with excellent photon recycling.

Advances in science and technology to meet challenges

To surmount the challenges discussed above, a number of promising approaches are under active investigation at this time. To improve the selectivity and thermal stability of emitters, a couple of key strategies are emerging. First, quality factor matching approaches that combine naturally selective, albeit, weak emitters, such as rare-earth-doped crystals (e.g., erbium aluminum garnet), with PhCs having resonant modes at the same key wavelengths [165]. Second, next-generation photon-recycling approaches that sharply reduce the effective emissivity observed from outside the photon-recycling system. With sufficient selectivity, additional benefits can be realized, such as dielectric waveguides for increasing separation between emitters and receivers—particularly useful for maintaining large thermal gradients outside of ultra-high vacuum.

In parallel, advances are needed in terms of reliability and stability of selective thermal emitters (see section 17). For example, work has recently been performed to fill in the voids for 2D and 3D PhC structures with optically transparent diffusion barrier materials to greatly improve thermal stability. With the appropriate choice of materials, transparent encapsulation can be performed to package the high-temperature emitters against softening and oxidation, which are often difficult to avoid. This also offers the possibility of heterogeneous integration with other types of structures that promote photon recycling without mechanical failures from large thermal gradients.

In terms of realizing new physical mechanisms for TPVs, one promising approach would be to develop and to use angle-selective thermal emitters to more naturally concentrate light on a distant receiver, which would reduce the need for precise alignment between emitter and receiver. For near-field thermal transfer, promising alternative strategies include using an array of sharp tips (as in transmission e microscopy) to achieve precise alignment and sufficient power transfer.

Another needed advance would be improvements in both efficiency and manufacturability for low-band-gap PV diodes. Here, several possibilities could be considered. First, epitaxial liftoff of high-quality direct band-gap III–V materials on reusable substrates could allow for record efficiencies at much more reasonable costs. Second, *in situ* vapor–liquid–solid growth from metallic precursors should be considered as recently demonstrated for indium phosphide PVs. Third, solution-processed low-band-gap materials could be used in TPVs, such as perovskites for PVs.

Concluding remarks

In conclusion, TPVs is a technology that has the proven capability of quietly converting heat into electricity without moving parts [156]. The best designs, to date, have combined high-temperature operation, high-performance InGaAs PV cells, and long-pass filters to achieve up to 23.6% conversion of thermal radiation into electricity [159]. TPVs also has the potential for even higher performance in the future, potentially exceeding 50% [156] as shown in figure 27 (see also sections 13, 16) as well as lower costs. Achievement of such metrics could be enabled by future advances in selective emitter or PV technology, which may include the exploration of novel materials as well as the incorporation of novel physical phenomena, such as enhanced out coupling for thermal emitters in the near or far fields as summarized in figure 26.

16. Near-field radiative transfer in the energy-conversion schemes

Jean-Jacques Greffet

Institut d'Optique, CNRS, Université Paris-Saclay

Status

The field of radiative heat transfer on the nanoscale started with the experimental observation [166] that the flux exchanged between two metallic plates separated by a sub-micrometer gap d could be larger than the Stefan–Boltzmann law (figure 28). We now have a simple picture that explains the reason for this extraordinary flux [167] as depicted in figure 29(a). The radiative flux is given by the sum of the intensity over all angles from normal incidence to grazing incidence. Let us, instead, adopt an electromagnetic point of view and sum over all parallel wave vectors of the electromagnetic fields on the (k_x, k_y) plane. For parallel wave vectors with a modulus $k_p < \omega/c$, where ω is the frequency and c is the light velocity, the waves are propagating (figure 29(*b*)), and there is no difference with summing over all angles.

The additional heat flux can be partly attributed to additional modes that are propagating in the medium but not in the air with k_p in the range $[\omega/c, n\omega/c]$ producing the so-called frustrated total internal reflection (figure 29(*c*)). A more complete theoretical explanation provided by Polder and van Hove [168] clarified the role of the evanescent modes with arbitrary large wave vectors (figure 29(*d*)) (see also section 1). The transmission factor associated with each mode decays exponentially as $\exp(-k_p d)$ and introduces a cutoff: only modes with $k_p < 1/d$ contribute to the heat flux. Hence, the heat flow increases as $1/d^2$ because the number of modes increases as the area of the disk is limited by $k_x^2 + k_y^2 = 1/d^2$.

Experimental observation of this enhanced flux appeared to be extremely difficult at ambient temperatures [169] so that this effect remained a physics peculiarity until it was discovered [170] that the heat flux can be much larger for dielectrics than for metals. This is due to the fact that the transmission factor associated with each mode is very low for metals but close to 1 for dielectrics at a particular frequency in the IR due to the resonant excitation of gap modes produced by surface phonon polaritons. It follows that *the flux is quasimonochromatic*. Large heat fluxes have been observed [171, 172] confirming theoretical predictions. As shown in figure 29(*e*), *the flux is expected to be orders of magnitude larger than in the far field* so that there is a potential gain for energy-conversion devices.

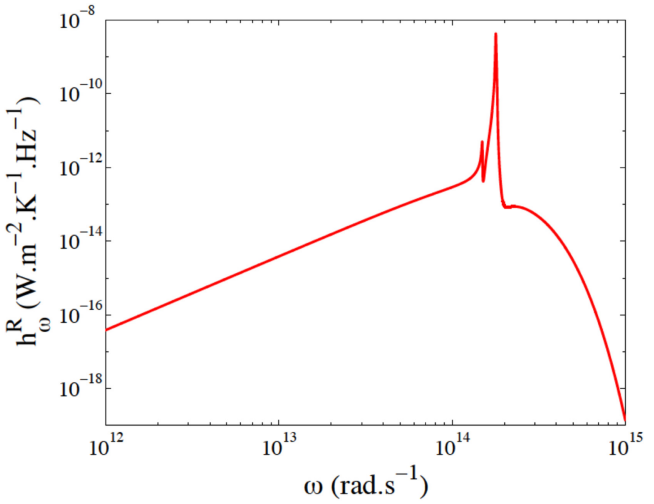

Figure 28. Spectral density of the heat transfer coefficient h^R between two SiC half-spaces [182]. It is seen that the flux is mostly exchanged at a frequency corresponding to the SiC surface phonon polariton.

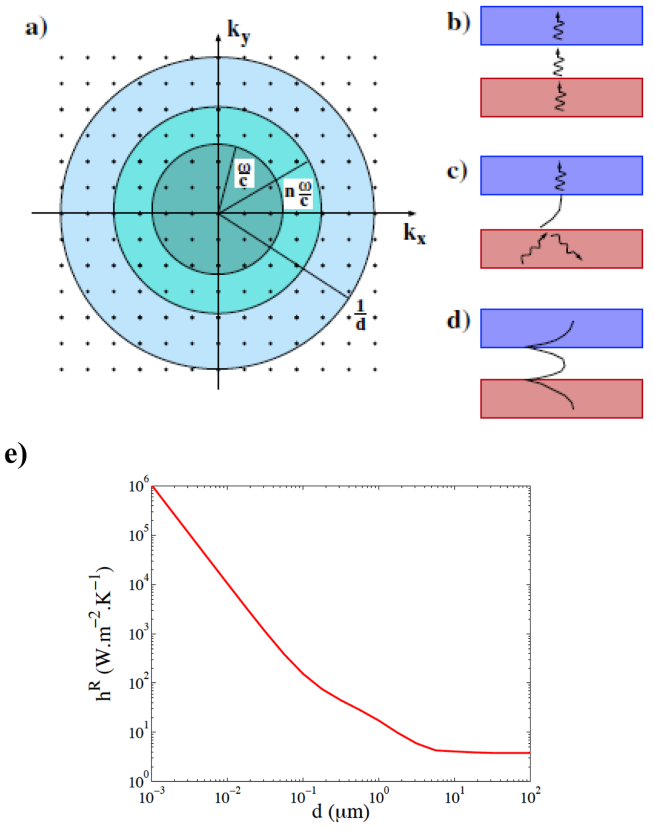

Figure 29. Schematic of the modes contributing to the radiative heat transfer. Modes with wave vectors $k_p < \omega/c$ correspond to propagating waves and modes with $k_p > \omega/c$ correspond to evanescent waves (reprint from 170, copyright 2010 by the American Physical Society). (*e*) h^R versus the gap width d between two SiC half-spaces [182]. The heat flux per unit area is given by $h^R\,\Delta T$ where ΔT is the temperature difference between the two surfaces.

Current and future challenges

How can we take advantage of this extraordinary large and quasimonochromatic heat flux for energy conversion? In what follows, we restrict the discussion to near-field TPVs, which has been proposed as a possible candidate [170, 173, 174] (see also section 15). Single-junction PV cells have an efficiency limited by the so-called SQ limit. The key issue is the mismatch between the narrow absorption spectrum of a single-junction PV cell and the broad incident spectrum of a blackbody: either the Sun or a secondary source at lower

temperature. Hence, IR photons with $h\nu < E_g$ are not absorbed, while photons with $h\nu > E_g$ lead to a loss of energy $h\nu - E_g$. TPVs is a concept that has been proposed to circumvent this limit. It amounts to illuminate the cell through a filter so that only energy at the right frequency is used, the rest being recycled in an isolated system.

Working with a *near-field TPV* system would have two key advantages: (i) the flux is increased by several orders of magnitude as compared to the far-field case so that the output power would be dramatically increased; (ii) the near-field thermal radiation can be quasimonochromatic so that the efficiency could be above the SQ limit. Furthermore, increasing the current in a junction results in a larger OC voltage so that the output electrical power is further increased. Alternatively, the larger flux for a given temperature difference may be a way to use energy from low-temperature sources, the so-called waste heat issue. Hence, near-field TPVs appears as a promising option [173–178]. What are the key challenges to fully benefit from the physics of near-field heat transfer? Fabrication and thermal management raise serious difficulties as the cell needs to remain at ambient temperature while being at a distance of around 100 nm from a hot surface. The second key issue is the design of a quasimonochromatic source at a frequency matching the cell band gap (see sections 15–17).

Advances in science and technology to meet challenges

The heat flux has been measured in the nanometric range [171, 172] between a sphere and a plane. Fabricating a system with two planar surfaces separated by a submicrometer distance is a challenge. The feasibility of a planar system has been demonstrated in the micrometer size regime by the company MTPV [175]. In this range, the gain in flux is limited to one order of magnitude, and there is almost no benefit regarding the efficiency. The design and modeling of the thermal management of the system will play a critical role in the final performance of the system [176].

An important feature of the near-field TPV cell is its potential to generate quasimonochromatic fluxes and, therefore, to increase the efficiency [177]. It has been shown that an ideal surface wave resonance producing a quasimonochromatic flux could generate efficiencies on the order of 35%. Yet, this would be obtained at unrealistically short distances on the order of less than 10 nm. In addition, there is no obvious material providing a phonon resonance at the required frequency. Using a quasimonochromatic emitter is not necessarily the best option. Finding the best near-field emitter is an open question. It could be either a new material or a metasurface with appropriate engineered resonances. This issue is all the more challenging as the system needs to operate reliably over a long time at temperatures above 1000 K.

Another challenge is related to the development of the PV cell. As the flux is due to evanescent waves, the absorption takes place very close to the surface. As a rule of thumb, if the gap has a width d, then, the absorption takes place within a distance d of the interface. In other words, the cell is very sensitive to surface defects and to e–h recombination processes taking place close to the interface [178]. This calls for the development of efficient surface passivation processes. Optimizing the detector is also an open question. It has recently been suggested to use graphene to tailor the detector [179, 180] or the flux [181].

Concluding remarks

Radiative heat transfer can be increased by orders of magnitude in the near field. It also provides the opportunity to tailor the spectrum with a potential benefit for the energy-conversion efficiency. A near-field TPV energy converter could be extremely compact and could operate at relatively low temperatures offering new avenues to harvest waste heat. Yet, designing a practical device raises a number of challenges. Many groups have now reported experimental measurements of the flux with different geometries in the near field. The challenge is now to move on to design practical devices operating with gaps on the order of 100 nm in order to take full advantage of the potential.

17. High-temperature nanophotonics: from theory to real devices and systems

Ivan Celanovic and Marin Soljacic

Massachusetts Institute of Technology

Status

While tailoring optical properties of solid state materials at room and cryogenic temperatures have been the focus of extensive research (see sections 5–8), tailoring optical properties of materials at very high temperatures is still a nascent field. Being able to engineer optical properties beyond what naturally occurring materials exhibit and maintaining these properties over high temperatures and over the device lifecycle has the promise to profoundly influence many fields of energy conversion, i.e., solar-thermal, TPV, radioisotope TPV, IR sources, and incandescent light sources [183–185]. Indeed, the opportunities for game-changing applications that would benefit immensely from high-temperature nanophotonic materials are vast, yet challenges remain formidable (see also sections 13, 15, 16).

In general, high-temperature nanophotonic structures enable us to control and to tailor spontaneous emission by virtue of controlling the photonic DOS (see section 1). These structures enable engineering spectral and/or directional thermal emission/absorption properties where it appears that the current state-of-the-art materials exhibit better control over spectral than directional properties. Indeed, the importance of tailoring both spectral and directional emission properties can be understood through the lens of specific applications.

TPVs energy-conversion devices require spectrally broadband, yet omnidirectional, thermal emission (usually 1–2.5 μm) with a sharp cutoff corresponding to the band gap of the PV diode [184]. Solar absorbers, for solar-thermal and solar TPVs (STPVs) need high absorptivity over the solar broadband spectrum but only within a very confined spatial angle [185–187]. Furthermore, many IR sources require both spectrally and angularly confined thermal emission properties [188] (see also sections 13, 15).

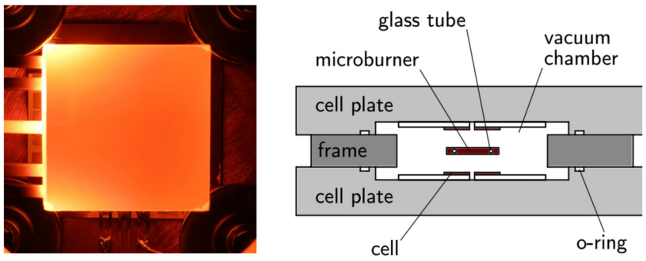

Figure 30. Micro-TPV MIT generator prototype; left: image of 2 × 2 cm reactor during operation; right: cross-sectional drawing of the prototype system.

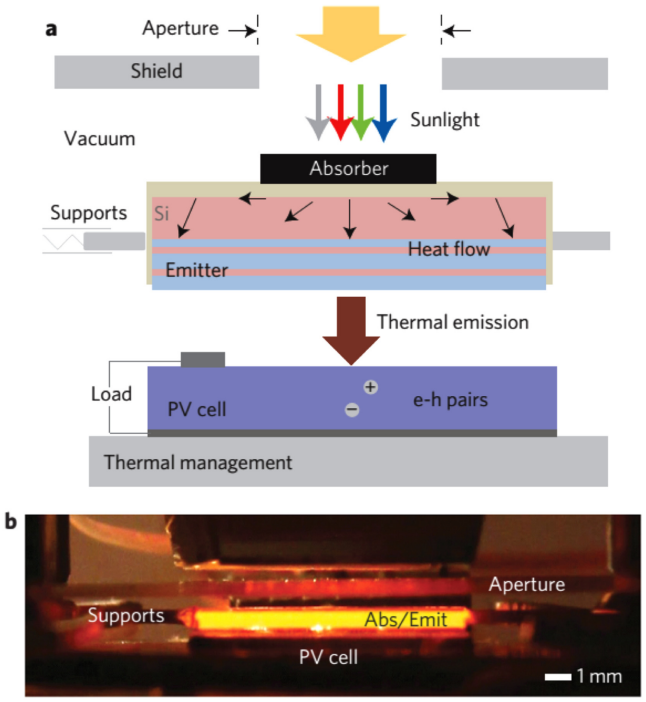

Figure 31. Operating principle and components of the STPV. Sunlight is converted into useful thermal emission and, ultimately, electrical power via a hot absorber–emitter. Schematic (*a*) and optical image (*b*) of our vacuum-enclosed devices composed of an aperture/radiation shield, an array of multiwalled nanotubes as the absorber, a 1D PhC, and a 0.55 eV band-gap PV cell (adopted from [187]).

Current and future challenges

Numerous challenges arise when trying to design nanophotonic materials with precisely tailored optical properties that can operate at high temperatures (>1100 K) over extended periods of time including the thermal cycling, such as TPV portable generators, shown in figure 30, and STPV shown in figures 31, 32. These challenges can broadly be categorized in two groups: material selection and fabrication challenges and design and optimization challenges (given the performance and operating condition constraints). Material selection and fabrication challenges include proper material selection and purity requirements to prevent melting, evaporation, or chemical reactions; severe minimization of any material interfaces to prevent thermomechanical problems, such as delamination; robust performance in the presence of surface diffusion; and long-range geometric precision over large areas with severe minimization of very small feature sizes to maintain structural stability. Indeed, there is a body of work that approached the design of high-T nanophotonics.

Two types of materials are most often considered for high-temperature nanophotonics, namely, refractory metals and dielectrics. Refractory metals have extremely high melting temperatures and are, hence, stable at high temperatures. The down side of these materials is that they tend to chemically react with O and other elements (i.e., C) at high temperatures. However, they have a relatively high reflectivity in deep IR making them amenable for 2D and 3D PhC-selective emitters. Dielectrics, such as SiO_2, HfO_2 are often considered for dielectric and metalodielectric PhCs since they tend to be

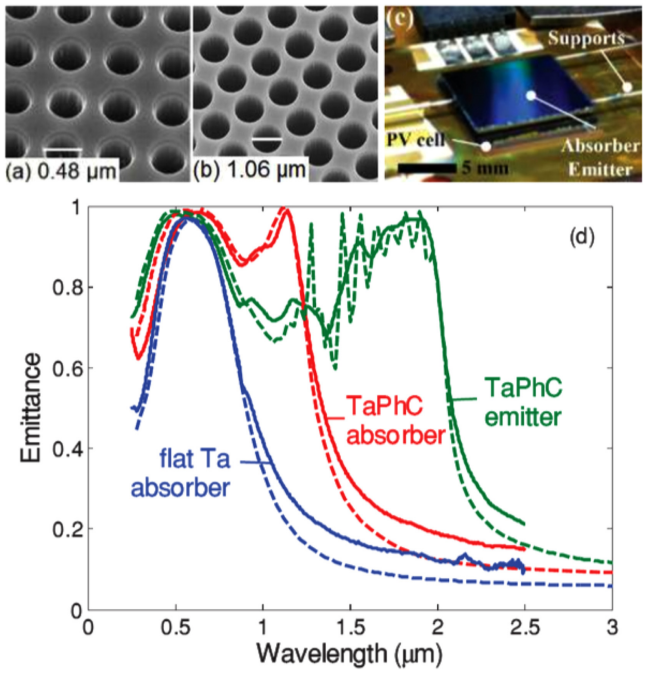

Figure 32. SEM images of fabricated (*a*) PhC absorber and (*b*) PhC emitter. (i) Photograph of a STPV setup absorber/emitter sample mounted on top of a PV cell. (*d*) Normal emittance determined from reflectance measurements at room temperature (solid lines) and simulated normal emittance (dashed lines) of the fabricated PhC emitter, PhC absorber, and flat Ta absorber.

less reactive at high temperatures and are standard microfabrication materials. Interface minimization is another aspect of design that has to be taken into account due to thermally induced stresses and potential reactions and interdiffusion. Hence, the simpler the interfaces the better. Surface diffusion is especially pronounced for metallic PhC, 2D and 3D due to relatively high diffusion constants that tend to drive diffusion around sharp features, hence, degrading optical performance. Finally, nano- and microfabricating structures that maintain long-range geometric precision and geometrical parameters at high-*T* remain a fabrication, a design constraint, and a challenge.

Advances in science and technology to meet challenges

Two key opportunities toward practical high-temperature nanophotonic devices remain: new and more robust material systems and fabrication processes; and even higher level of control of directional and spectral properties (i.e., even more selective emission/absorption, both spectrally and directionally). In terms of materials and fabrication challenges: demonstrating high-*T* photonic devices with tens of thousands of hours operational stability at temperatures above 1000 K; mastering materials and fabrication processes to fabricate metalodielectric photonic structures; developing passivation and coatings for refractory metallic structures that will be oxidatively and chemically stable in noninert environments.

In terms of achieving the next level of control of directional and spectral properties, several key challenges remain: angularly selective broadband absorbers; spectrally highly selective broadband wide-angle emitters, spectrally highly selective broadband narrow band emitters, and near-field highly resonant energy transfer.

Concluding remarks

The main driver for high-performance high-temperature nanophotonic materials are energy-conversion applications, such as: solar-thermal, TPVs, radioisotope TPV, IR, and incandescent light sources. These applications would benefit greatly from robust and high-performance high-*T* nanophotonic materials. Indeed, more work is needed that is strongly grounded in the experimental and application worlds. Real life constraints need to be brought into the design process in order to inform the theoretical and exploratory work. In the end, fresh and innovative thinking in terms of new theoretical approaches is always critical, and it drives the field forward. However, it needs to be well targeted and directly coupled to experimental and application work to provide rapid evaluation of advanced concepts and ideas.

18. Endothermic-PL: optical heat pump for next generation PVs

Assaf Manor and Carmel Rotschild

Technion, Israel Institute of Technology

Status

Single-junction PV cells are constrained by the fundamental SQ efficiency limit of 30%–40% [23] (see section 1). This limit is, to a great extent, due to the inherent heat dissipation accompanying the quantum process of electrochemical potential generation. Concepts, such as STPVs [189, 190] aim to harness these thermal losses by heating a selective absorber with solar irradiation and coupling the absorber's thermal emission to a low-band-gap PV cell (see sections 13–17). Although, in theory, such devices can exceed 70% efficiency [191], thus far, no demonstration above the SQ limit was reported. This is mainly due to the requirement to operate at very high temperatures.

In contrast to thermal emission, PL is a nonequilibrium process characterized by a nonzero chemical potential, which defines an enhanced and conserved emission rate [6] (see section 1). Recently, the characteristic of PL as an optical heat pump at high temperatures was theoretically and experimentally demonstrated [192]. In these experiments, PL was shown to be able to extract thermal energy with minimal entropy generation by thermally induced blueshift of a conserved PL rate.

Here, we briefly introduce and thermodynamically analyze a novel thermally enhanced PL (TEPL) device for the conversion of solar energy beyond the SQ limit at moderate operating temperatures. In such a device, high solar photon current is absorbed by a low-band-gap thermally insulated PL material placed in a photon-recycling cavity. Due to the rise in its temperature, the blueshifted PL generates energetic photons in rates that are orders of magnitude higher than thermal emission at the same temperature. The PL is harvested by a high-band-gap PV cell, yielding enhanced voltage and efficiency (see the detailed description below).

In addition, we present proof-of-concept experiments for TEPL operating at a narrow spectral range where sub-band-gap photons are harvested by a GaAs SC. Future challenges in this new direction include: i. Material research (see sections 5–8) for expending the overlap between the absorption line shape and the solar spectrum while maintaining high QE. ii. Optimizing the band gaps with respect to the absorbed spectrum and operating temperature. iii. Optimizing the photon-recycling efficiency (see sections 4, 15). iv. Exploring the fundamentals of endothermic PL. The low operating temperatures associated with the minimal entropy generation together with overcoming future challenges may open the way for practical realization of high-efficiency next-generation PV.

Current and future challenges

Figure 33(*a*) depicts the conceptual design of the TEPL-based solar energy converter. A thermally insulated low-band-gap PL absorber completely absorbs the solar spectrum above its band gap and emits TEPL toward a higher-band-gap PV cell, maintained at room temperature. Such a device benefits from both the high photon current of the low-band-gap absorber and the high PV voltage.

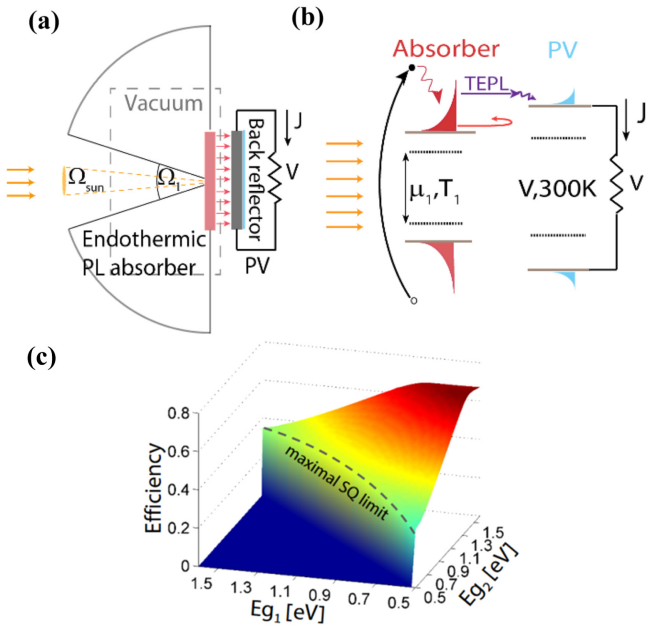

Figure 33. (*a*) The device's scheme. (*b*) The absorber and PV energy levels with the currents flow. (*c*) The maximal efficiency versus E_{g1} and E_{g2}.

For minimizing radiation losses, a semiellipsoidal reflective dome recycles photons by reflecting emission at angles larger than the solid angle Ω_1 [193]. In addition, the PV's backreflector [194] reflects sub-band-gap photons to the absorber. Figure 33(*b*) shows the absorber and PV energy levels, where μ_1 and T_1 define the absorber's thermodynamic state and its emission. In the detailed analysis of such a device, the PL absorber satisfies the balance of both energy and photon rates between the incoming and the outgoing radiation currents, while the PV satisfies only the rate balance due to the dissipated thermal energy required to maintain it at room temperature. By setting the PV's voltage, we solve the detailed balance and find the thermodynamic properties T and μ as well as the system's I–V curve and its conversion efficiency (see section 1). The analysis for various absorber and PV band-gap configurations shows a maximal theoretical conversion-efficiency limit of 70% for band-gap values of 0.5 and 1.4 eV under ideal conditions of photon recycling and thermal insulation (figure 33(*c*)). More importantly, the expected operating temperatures at such ideal conditions are below 1000 °C, about half of the equivalent temperature required in STPV.

When approaching the experimental proof of concept, we need to address the challenges of realizing a TEPL-based solar converter. First, high QE must be maintained at high temperatures. This limits the use of semiconductors due to nonradiative recombination mechanisms, which reduces QE with temperature. In contrast, rare-earth emitters, such as neodymium (Nd) and ytterbium, are known to maintain their QE at high temperatures as their es are localized and are insulated from interactions [195]. Although they have superior QEs, the use of rare earths as PL absorbers raises another challenge: the poor overlap between the solar spectrum and their absorption

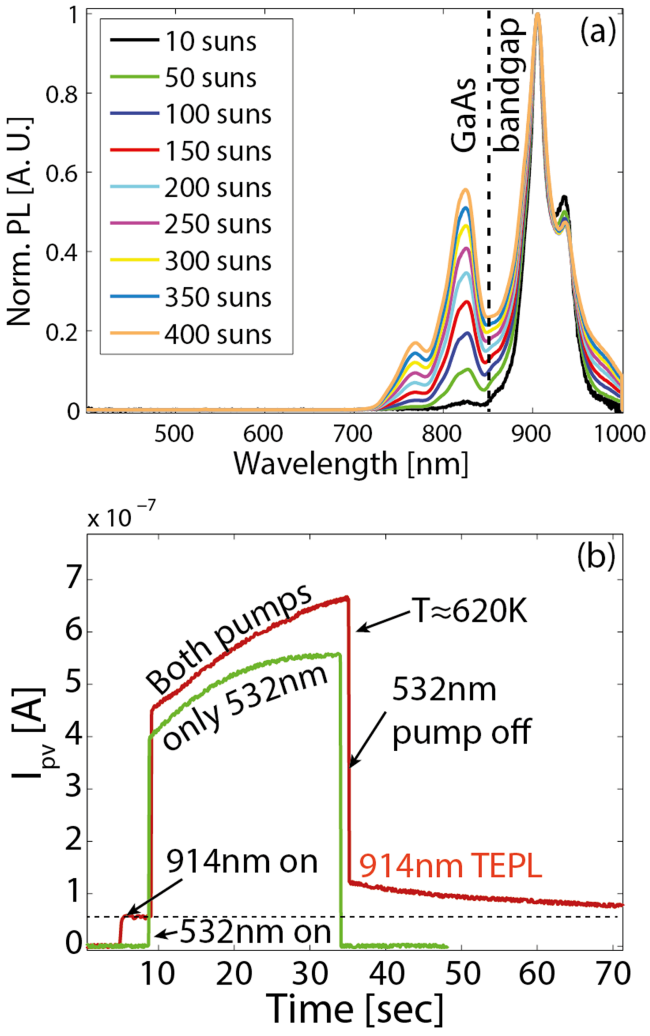

Figure 34. (*a*) PL evolution with pump power. (*b*) PV current versus time.

line shape. Within these limits, as a proof of concept for the ability to harvest sub-band-gap photons in a TEPL device, we experiment with a Nd^{3+}:SiO_2 absorber coupled to a GaAs PV. The sample is placed in vacuum conditions (10^{-4} mbars), pumped by a 914 nm (1.35 eV) laser. This pump is a sub-band gap with respect to the GaAs SC (1.44 eV). At room temperature, the 914 nm induces a PL spectrum between 905 and 950 nm. The temperature does not rise since each emitted photon carries similar energy to the pump photons. An additional 532 nm pump, which matches the Nd^{3+} absorption line, is used to mimic an average solar photon in order to increase both temperature and PL photon rate. The first experiment is performed only with the 532 nm pump in order to measure the pump power that is required for a significant blueshift. Figure 34(*a*) shows the PL spectrum evolution with the absorbed pump intensity, indicated in suns (one sun = 1000 W m^{-2}). At the pump power of 400 suns, the PL exhibits a significant blueshifting from 905 to 820 nm, which can be harvested by the GaAs PV. Figure 34(*b*) shows the time dependence of the PV current under dual pump lasers. At first, an increase in current is observed when only the 914 nm pump is switched on as a result of a room-temperature blueshift (red line at $t = 5$). Then, the 532 nm pump is switched on (red line at $t = 10$), and the current gradually rises due to the rise in temperature. When the sample reaches 620 K, the 532 nm pump is switched off, leaving only the 914 nm pump. The current, then, drops to a level two times higher than its initial value at $t = 5$. This demonstrates how the heat generated in the thermalization of the 532 nm pump is harvested by blueshifting of 914 nm sub-band-gap photons. The green line shows the PV's current time dependence when only the 532 nm pump is on with insignificant thermal current when both pumps are off.

Advances in science and technology to meet challenges

A future demonstration of efficient TEPL -conversion devices requires advances in material science, development of tailored optics, and an understanding the fundamentals of PL. The presented proof of concept demonstrates the ability to harvest sub-band-gap photons in TEPL, yet this demonstration can operate only at a narrow spectral range due to the typical absorption lines of rare earths. The challenge of expending the absorption spectrum while maintaining high QE requires the use of laser technology knowhow where a broad incoherent pump is coupled to a narrow emitter with minimal reduction in QE. Such sensitization may include the development of cascaded energy transfer [196] between rare earths and transition metals. Another challenge is replacing the Nd^{3+} absorber with a lower-energy gap material for enhancing photon rate and overall efficiency. In addition to the material research, realization of an efficient device requires the development of high-quality photon-recycling capabilities. This includes clever optical engineering with tailored narrow bandpass filters and cavity structures. Finally, focusing on the fundamental science, our experiments on endothermic PL [192] show a discontinuity in the entropy and chemical potential at a critical temperature where the PL abruptly becomes thermal emission. It is fascinating to explore the thermodynamic properties of this discontinuity.

Concluding remarks

Based on our recent experimental observations showing that PL at high temperatures is an efficient optical heat pump, we propose and analyze a solar energy converter based on TEPL. In addition, we experimentally demonstrate the TEPL's ability to harvest sub-band-gap radiation. Finally, the roadmap for achieving efficiency in such devices is detailed. We describe the expected challenges in material research, optical architecture, and fundamental science. We believe that successfully overcoming these challenges will open the way for disruptive technology in PVs.

Acknowledgments

This report was partially supported by the Russell Berrie Nanotechnology Institute (RBNI) and the Grand Technion Energy Program (GTEP) and is part of The Leona M and Harry B Helmsley Charitable Trust reports on Alternative Energy series of the Technion and the Weizmann Institute of Science. We also would like to acknowledge partial support by the Focal Technology Area on Nanophotonics for Detection. A. Manor thanks the Adams Fellowship program for financial support.

19. Harnessing the coldness of the Universe by radiative cooling to improve energy efficiency and generation

Aaswath Raman, Linxiao Zhu, and Shanhui Fan

Stanford University

Status

With the rise of PVs, we have made significant progress in exploiting a powerful and renewable source of thermodynamic heat, the Sun (see sections 2–14). However, our society has, thus far, largely ignored another ubiquitous resource that is equally important from a thermodynamic and energy-conversion point of view: the cold darkness of the Universe. Exploiting and harnessing this resource represents an important frontier for both energy and photonics research in the coming decade with the potential to dramatically improve the efficiency of any existing energy-conversion process on Earth.

This resource can be accessed due to a feature of Earth's atmosphere: between 8 and 13 μm, it can be transparent to electromagnetic waves. Thus, a significant fraction of thermal radiation from a sky-facing terrestrial object (at typical temperatures ~300 K) is not returned to it from the sky, effectively allowing such a surface radiative access to the Universe. Beginning in the 1960s, researchers investigated exploiting this concept, known as radiative cooling, at night using black thermal emitters [197]. Moreover, it was noted early on that the spectral features of the atmosphere's transparency meant that a spectrally selective thermal emittance profile should allow a radiative cooler to reach lower temperatures [198]. Subsequent work, thus, tried to find materials with suitable emissivity profiles or to engineer selective emitters based on a thin-film approach [199, 200]. While over the last two decades, research interest in this topic declined, some recent work also examined the use of photonic nanoparticle effects for radiative cooling [201]. However, all of these efforts focused on radiative cooling at night, and until recently, radiative cooling during the day remained an open challenge.

Current and future challenges

If radiative cooling is to play a role in energy efficiency, it is critical that it be accessible precisely at hours when the need for a colder cold sink is greatest: the day. Achieving radiative cooling during the day requires being able to maintain strong thermal emission, ideally selective to the atmospheric transparency window, while reflecting nearly all incident sunlight (figure 35). Our theoretical proposal [202] showed that daytime radiative cooling was, indeed, possible, and our recent experiment demonstrated [203] a performance of 5 °C below ambient steady-state temperatures and 40 W m^{-2} cooling power at air temperature in clear sky conditions (figure 36). It is important to note, however, that this performance is strongly dependent on the IR properties of the atmosphere, which are, in turn, influenced by humidity and cloud cover. Under dry hot conditions, better performance can be achieved with the same radiative cooler form [203]. In less favorable conditions, the net positive radiative flux at IR wavelengths lessens, and an even higher solar reflectance is needed to achieve meaningful cooling power during the day. To further improve performance in all conditions and to enable useful cooling powers even in humid climates, achieving near-unity emissivity within the window is also important. While this is challenging, a recent paper demonstrated daytime cooling in

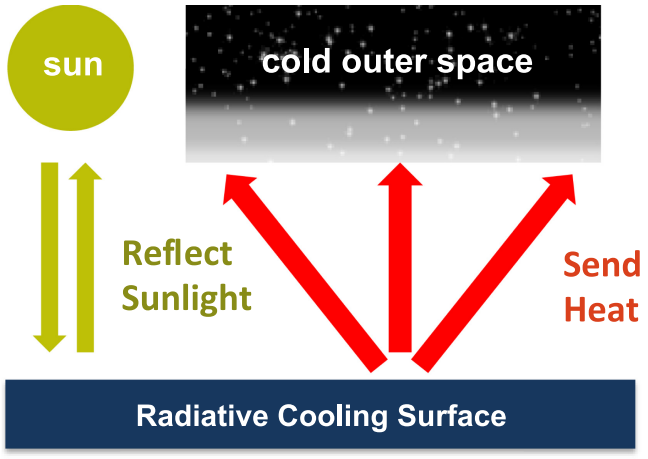

Figure 35. Schematic of how a surface can cool itself radiatively below air temperature. Strong selective thermal emission in the mid-IR must be achieved while also reflecting nearly all incident sunlight.

Figure 36. Outdoor test of a daytime radiative cooling surface. A test stand that insulates and minimizes parasitic heat gain is essential to maximize performance. A unique feature of radiative cooling experiments is the need to perform tests outdoors.

challenging atmospheric conditions, offering cause for optimism [204].

Effectively using radiative cooling also entails minimizing parasitic heating from the environment. This is a non-trivial challenge given the constraints of operating under the Sun, and the lack of cheap and rigid IR-transparent materials that could serve as a window for the large areas typically needed. Making practical use of such surfaces for cooling also requires engineering systems that can efficiently transfer heat loads to the sky-facing surfaces while minimizing other heat gains. Radiative cooling systems will be particularly sensitive to such gains given that cooling powers available will typically be $<100\,\mathrm{W\,m^{-2}}$.

In the demonstrations of daytime radiative cooling shown, so far, the sunlight is reflected and goes unused. One challenge is, thus, to make use of this sunlight while preserving the cooling effect. In this spirit, we recently proposed the use of radiative cooling to cool SCs [205] by engineering the thermal emissivity of a top surface above the PV material while transmitting the same amount of sunlight through it. This was one example of the broader vision of enabling and improving energy generation in addition to efficiency. Related to this, there was also a recent proposal to make use of the imbalance between outgoing and incoming IR-thermal emission from sky-facing objects directly for energy conversion [206]. In both cases, experimental demonstrations pose challenges and are fruitful areas for further research.

A*dvances in Science and Technology to Meet Challenges*—A variety of photonic approaches can be leveraged to achieve both the spectral and the angular selectivities desirable for radiative cooling (see sections 1, 13, 15–17). A recent metamaterial-based design, for example, experimentally achieved extremely strong and selective emissivity within the atmospheric window [207].

Creative interdisciplinary research recently showed how the geometric shape and arrangement of hairs on Saharan silver ants not only increase their solar reflectance, but also increase their thermal emissivity in the mid-IR, enabling their survival through cooling in very hot environments [208]. Such research opens up possibilities for biologically inspired metasurface designs that can achieve some of the same effects sought for radiative cooling during the day.

A key challenge and opportunity with radiative cooling will be to balance the need for low costs for what is inherently a large-area technology with the higher performance potentially achievable with more complex designs. While [203] showed that good performance can be achieved with a non-periodic 1D photonic structure, recent advances in imprint lithography make more complex designs tractable given sufficient performance gains.

Concluding remarks

Radiative cooling allows access to a thermodynamic resource of great significance that we have, thus far, not exploited in our energy systems: the dark Universe. By effectively harnessing it during the day, we are not only able to access a universal heat sink precisely when it is most needed, but also able to demonstrate that such systems can have a ‘capacity factor’ of 24 h a day—distinguishing this technology from PVs. These demonstrations, however, are just the first building block in what we believe is a worthwhile and game-changing broader project: engineering all terrestrial energy systems to take advantage of this dark resource to improve their efficiency and potentially directly generate energy as well. Improvements in spectral control of thermal emission through metamaterial and metasurface concepts could, thus, rapidly translate to improved performance both for direct cooling and for indirectly improving the efficiency or generation ability of any terrestrial energy system.

20. Entropy flux and upper limits of energy conversion of photons

Gang Chen

Massachusetts Institute of Technology

Status

The entropy of photons has been studied by many researchers in the past [209, 21, 6] (see also section 1) (1), but there are still unsettled questions. Understanding the entropy of photons will help set the correct upper limits in the energy conversion using photons from SCs to light-emitting diodes to optical refrigeration. We will use blackbody radiation as an example to lead the discussion. Considering an optical cavity of volume V at temperature T, the temperature and entropy (S) of photons inside the cavity obey the relation: $TS = 4U/3$, where $U(=4V\sigma T^4/c)$ is the internal energy of the blackbody radiation field inside the cavity, σ is the Stefan–Bolzmann constant, and c is the speed of light. While this relation is well established, the trouble arises when one considers the thermal emission from a black surface with emissive power $J_b = \sigma T^4$ W m^{-2} with the corresponding entropy flux J_s,

$$J_s = \frac{4}{3}\sigma T^3 = \frac{4}{3}\frac{J_b}{T}. \tag{2}$$

This expression does not follow the familiar definition for entropy flow across a boundary: Q/T if the heat flow Q is set equal to the emissive power J_b.

Current and future challenges

The entropy flux as defined in equation (2) is valid and the inequality between J_s and J_b/T is fundamentally due to the nonequilibrium nature of thermal radiation leaving a surface [20, 210]. Consider that an object at temperature T receives heat Q at one boundary by conduction and emits as a blackbody thermal radiation via surface A, the rate of entropy generation in the process is, according to the second law of thermodynamics,

$$\dot{S}_g = AJ_s - \frac{Q}{T} = \frac{1}{3}A\sigma T^4. \tag{3}$$

If emission generates entropy, the reverse process should not work: an external blackbody radiation source is directed at an object, delivering radiant power $Q = A\sigma T^4$. This same amount of power cannot be conducted out since, otherwise, the process will lead to entropy reduction. The key to show this, indeed, is the case of the Kirchoff law. We assume that the object's surface facing the incoming radiation is black. According to Kirchoff's law, the object will also radiate back to the incoming radiation source (we will assume a view factor of unity to simplify the discussion), so the net heat that can be conducted out is: $Q = A\sigma(T_h^4 - T^4)$. Entropy generated in the object is, then, $\dot{S} = \frac{Q}{T} + \frac{4}{3}A\sigma T^4 - \frac{4}{3}A\sigma T_h^4$. This function is always positive, reaching a minimum when $T = T_h$ (and $Q = 0$). Hence, the heat that can be conducted out is less than the radiant power that comes in (unless $T = 0$ K).

At first sight, the idea that thermal emission from a surface generates entropy might be surprising. Careful examination, however, reveals that thermal emission from a surface is a sudden expansion of photon gas bearing a similarity to the irreversible sudden expansion of gas molecules from a pressurized container to vacuum. Of course, there are also differences since photons normally do not interact with each other while molecules do. Hence, if a perfect photon reflector is placed in the path of the emitted photons to completely reflect back all photons leaving the black surface, there is no heat transfer and no entropy generation. In this case, photons at the emission surface are at an equilibrium state, and their temperature can be well defined, and, hence, no entropy is generated. In the case of molecules expanding into a vacuum, it will be difficult to completely reflect back all molecules as they scatter each other, and, hence, entropy will eventually be generated.

A standard way to make a black surface is a small opening on a large cavity. Immediately outside the opening, photons only occupy isotropically the half-space since no other photons come in. The local temperature of photons cannot be defined, and correspondingly, one should not expect, then, that J_b/T gives the entropy flux. If one is forced to use the local photon energy density to define a local equivalent photon temperature, this equivalent equilibrium temperature will be lower than T_h [211] (see section 1). In this sense, it is not surprising that the entropy flux as given by equation (3) is larger than J_b/T_h.

Although some researchers did use equation (2) for the entropy flux, they sometimes introduce a photon-flux temperature T_f equaling the ratio of J_b/J_s in the thermodynamic analysis of heat engines based on photons. Landsberg and Tonge [21] used the concept of photon-flux temperature to derive the maximum efficiency of a heat engine at temperature T receiving thermal radiation from a heat source at temperature T_h as $\eta_L = 1 - \frac{4}{3}\frac{T}{T_h} + \frac{1}{3}\left(\frac{T}{T_h}\right)^4$. This efficiency is called the Landsberg efficiency and has been derived by different researchers [210–212]. As we will see later, although the Lansberg and Tonge result is correct with proper interpretation (i.e., T equals the ambient temperature), their derivation did not, in fact, consider the ambient temperature (except in an alternative availability argument). We will re-derive below the Landsberg limit and show a higher limit when the radiation source is not from the Sun.

Our model considers a thermal emitter coupled to a heat reservoir at temperature T_h, heat engine at temperature T (our results are valid if T is time varying, but we will not include time here for simplicity), and a cold reservoir at T_c as shown in figure 37(a). We assume the surfaces involved in the radiative heat transfer between the heat reservoirs are blackbodies. The key is to recognize that when a heat engine absorbs thermal radiation, it also radiates back to the thermal emitter according to Kirchoff's law as illustrated in figure 37(a). Correspondingly, the net rate of entropy flowing into the heat engine is $S_{\text{in}} = \frac{4}{3}A\sigma(T_h^3 - T^3)$. The maximum power is reached when this entropy is rejected to the cold reservoir T_c without additional entropy generation in the heat engine and the heat rejection process. The rate of heat rejection is, then, $Q_c = T_c S_{\text{in}} = \frac{4}{3}AT_c\sigma(T_h^3 - T^3)$. The power output can be

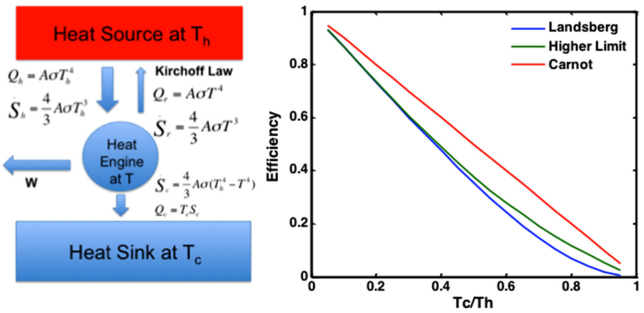

(a) (b)

Figure 37. (*a*) A heat engine operating between a heat source at T_h and a heat sink T_c. Heat transfer between the engine and heat source is coupled via thermal radiation. Kirchoff's law dictates that some photons, their associated energy, and entropy are sent back to the heat source, (*b*) comparison of three different efficiencies, the Carnot, the Landsberg, and efficiency $\eta 2$, which is higher than the Landsberg efficiency.

obtained from the first law of analysis for the heat engine,

$$W = Q_h - Q_r - Q_c = A\sigma T_h^4\left(1 - \frac{4}{3}\frac{T_c}{T_h}\right) - A\sigma\left(T^4\frac{4}{3}T_c T^3\right).$$

The above expression is maximum when $T = T_c$,

$$W_{\max} = A\sigma T_h^4\left(1 - \frac{4}{3}\frac{T_c}{T_h}\right) + \frac{1}{3}A\sigma T_c^4. \quad (4)$$

We can define two efficiencies using the above analysis. One is based on the radiant energy leaving the heat reservoir,

$$\eta_1 = \frac{W_{\max}}{A\sigma\ \Delta t\ T_h^4} = 1 - \frac{4}{3}\frac{T_c}{T_h} + \frac{1}{3}\left(\frac{T_c}{T_h}\right)^4. \quad (5)$$

This expression is the Lansberg efficiency. This efficiency definition is appropriate for solar radiation. However, if the thermal emission comes from a terrestrial heat source, such as in a TPV device (see sections 15–18), the heat supplied to the heat reservoir should be the difference of radiated and absorbed radiation by the reservoir $Q = \mathrm{A}\sigma(T_h^4 - T_c^4)$, and the efficiency should be defined as

$$\eta_2 = \frac{W_{\max}}{Q} = 1 - \frac{4}{3}\frac{T_c}{T_h} + \frac{1}{3}\left(\frac{T_c}{T_h}\right)^4\left[1 - \left(\frac{T_c}{T_h}\right)^4\right]^{-1}. \quad (6)$$

This efficiency is higher than the Landsberg efficiency. Thus, although the Landsberg efficiency is appropriate for solar radiation and is often considered as an upper limit for thermal radiation-based energy-conversion systems, a higher limit exists when terrestrial heat sources are used as the photon source.

Advances in science and technology to meet challenges

Our discussion, so far, has been limited to the blackbody radiation. We believe that the same strategy can be applied to search for the upper limits of all other photon-mediated energy-conversion processes involving nonblack objects, emission from SCs, light-emitting diodes, lasers, photosynthesis, optical UC, optical refrigeration [19, 213], near-field radiation heat transfer, near-field to far-field extraction, etc. For analyzing these processes, one should bear in mind two key results obtained from past studies. First, a general expression for the entropy of photons in a quantum state, whether they are at equilibrium or not, is $S_1 = k_B[(1+f)\ln(1+f) - f\ln f]$, where f is the number density of photons in the quantum state. From this expression, one can obtain entropy flux leaving a surface by considering the velocity of photons and summing up all their quantum states [21]. The other key result is photons possess an effective chemical potential when the radiation field is created via recombination of excited states at different chemical potentials (see sections 1, 4, 18), although purely thermally radiated photons do not have a chemical potential ($\mu = 0$) since their numbers are not fixed. This fact is used in analyzing photon-based energy-conversion processes and devices, such as PV cells [24], light-emitting diodes, photosynthesis, etc. However, there does not seem to be studies starting from the entropy-flux consideration to arrive at the maximum efficiency of energy-conversion processes. The SQ limit [23] for the PV cell, for example, is based on consideration of the balance of photon and charge number densities.

Concluding remarks

To summarize, thermal emission from a surface is a nonequilibrium process involving entropy generation. For blackbody radiation, the entropy flux expression, i.e., equation (2), is valid. By considering the entropy flux of photons, one can arrive at proper upper limits for different photon-based energy-conversion devices. More research along this direction can stimulate further advances in photon-based energy conversion.

Acknowledgments

The author thanks S. Boriskina, V. Chiloyan, B. L. Liao, W. C. Hsu, J. Tong, and J. W. Zhou for helpful discussions. This work was supported, in part, by the 'Solid State Solar-Thermal Energy Conversion Center (S^3TEC), an Energy Frontier Research Center funded by the U.S. Department of Energy, Office of Science, Office of Basic Energy Sciences under Award No. DE-SC0001299/DE-FG02-09ER46577 (for TPV applications) and by DOE-BES Award No. DE-FG02-02ER45977 (for extracting photons from the near field to the far field).

References

[1] Planck M 1914 *Theory Heat Radiat* (Philadelphia: F. Blakiston Son & Co.)
[2] Landau L and Lifshitz E 1980 *Statistical Physics, : 1. Institute of Physical Problems* (Moscow: USSR Academy of Sciences)
[3] Levi A F J 2006 *Appl Quantum Mech*
[4] Chen G 2005 *Nanoscale Energy Transport and Conversion: A Parallel Treatment of Electrons, Molecules, Phonons, and Photons* (New York: Oxford University Press)
[5] Klaers J, Schmitt J, Vewinger F and Weitz M 2010 Bose–Einstein condensation of photons in an optical microcavity *Nature* **468** 545–8
[6] Wurfel P 1982 The chemical potential of radiation *J. Phys. C: Solid State Phys.* **15** 3967–85
[7] Stuart H R and Hall D G 1997 Thermodynamic limit to light trapping in thin planar structures *J. Opt. Soc. Am.* A **14** 3001–8
[8] Callahan D M, Munday J N and Atwater H A 2012 Solar cell light trapping beyond the ray optic limit *Nano Lett.* **12** 214–8
[9] Boriskina S V, Ghasemi H and Chen G 2013 Plasmonic materials for energy: from physics to applications *Mater. Today* **16** 375–86
[10] Tong J K, Hsu W-C, Huang Y, Boriskina S V and Chen G 2015 Thin-film 'Thermal Well' emitters and absorbers for high-efficiency thermophotovoltaics *Sci. Rep.* **5** 10661
[11] Yu Z, Raman A and Fan S 2010 Fundamental limit of nanophotonic light trapping in solar cells *Proc. Natl. Acad. Sci. USA* **107** 17491–6
[12] Joulain K, Mulet J-P, Marquier F, Carminati R and Greffet J-J 2005 Surface electromagnetic waves thermally excited: radiative heat transfer, coherence properties and casimir forces revisited in the near field *Surf. Sci. Rep.* **57** 59–112
[13] Yablonovitch E 1982 Statistical ray optics *J. Opt. Soc. Am.* **72** 899–907
[14] Wurfel P 2005 *Physics of Solar Cells: From Principles to New Concepts* (Weinheim: Wiley-VCH Verlag GmbH & Co. KGaA)
[15] Bohren C F 1983 How can a particle absorb more than the light incident on It? *Am. J. Phys.* **51** 323–7
[16] Bohren C F and Huffman D R 1983 *Absorption and Scattering of Light by Small Particles* (New York: Wiley)
[17] Landau L 1946 On the thermodynamics of photoluminescence *J. Phys.* **10** 503–6
[18] Pringsheim P 1929 Zwei bemerkungen über den unterschied von lumineszenz und temperaturstrahlung *Z. Phys.* **57** 739–46
[19] Sheik-Bahae M and Epstein R I 2007 Optical refrigeration *Nat. Photon.* **1** 693–9
[20] Green M 2006 Energy, entropy and efficiency ed T Kamiya *et al Third Generation Photovoltaics* (Berlin, Heidelberg: Springer) vol 12, pp 21–34
[21] Landsberg P T and Tonge G 1980 Thermodynamic energy conversion efficiencies *J. Appl. Phys.* **51** R1–20
[22] Carnot N L S 1824 *Reflections Motive Power Heat* (Paris: Bachelier)
[23] Shockley W and Queisser H J 1961 Detailed balance limit of efficiency of P-N junction solar cells *J. Appl. Phys.* **32** 510
[24] Henry C H 1980 Limiting efficiencies of ideal single and multiple energy gap terrestrial solar cells *J. Appl. Phys.* **51** 4494–500
[25] Ross R T and Nozik A J 1982 Efficiency of hot-carrier solar energy converters *J. Appl. Phys.* **53** 3813
[26] Green M A, Emery K, Hishikawa Y, Warta W and Dunlop E D 2015 Solar cell efficiency tables (version 45) *Prog. Photovolt., Res. Appl.* **23** 1–9
[27] Boriskina S V, Tong J K, Ferry V E, Michel J and Kildishev A V 2015 Breaking the limits of optical energy conversion *Opt. Photonics News* **26** 50–3
[28] Miller O D, Yablonovitch E and Kurtz S R 2013 Strong internal and external luminescence as solar cells approach the Shockley–Queisser limit *IEEE J. Photovolt.* **2** 303–11
[29] International Technology Roadmap for Photovoltaic (ITRPV) 20156th Edn (www.itrpv.net) April
[30] Neuhaus D-H and Münzer A 2007 Industrial silicon wafer solar cells *Adv. OptoElectron* **2007** 24521
[31] Green M A *et al* 2016 Solar cell efficiency tables (version 47) *Prog. Photovolt.* **24** 3–11
[32] Green M A 2009 The path to 25% silicon solar cell efficiency: history of silicon cell evolution *Prog. Photovolt.* **17** 183–9
[33] Blakers A W *et al* 1989 22.8% efficient silicon solar cell *Appl. Phys. Lett.* **55** 1363–5
[34] Lammert M D and Schwartz R J 1977 The interdigitated back contact solar cell: a silicon solar cell for use in concentrated sunlight *IEEE Trans. Electron Devices* **24** 337–42
[35] Swanson R M *et al* 1984 Point-contact silicon solar-cells *IEEE Trans. Electron Devices* **31** 661–4
[36] Taguchi M *et al* 2000 HIT^{TM} cells—high-efficiency crystalline Si cells with novel structure *Prog. Photovolt.* **8** 503–13
[37] Masuko K *et al* 2014 Achievement of more than 25% conversion efficiency with crystalline silicon heterojunction solar cell *IEEE J. Photovolt.* **4** 1433–5
[38] Mailoa J P *et al* 2015 A 2-terminal perovskite/silicon multijunction solar cell enabled by a silicon tunnel junction *Appl. Phys. Lett.* **106** 121105
[39] Mokkapati S and Catchpole K R 2012 Nanophotonic light trapping in solar cells *J. Appl. Phys.* **112** 101101
[40] White T P *et al* 2014 Tandem solar cells based on high-efficiency c-Si bottom cells: top cell requirements for >30% efficiency *IEEE J. Photovolt.* **4** 208
[41] Allen T *et al* 2014 Reactive ion etched black silicon texturing: a comparative study *In IEEE Photovoltaic Specialists Conf. (Denver)*
[42] De S *et al* 2009 Silver nanowire networks as flexible, transparent, conducting films: extremely high DC to optical conductivity ratios *ACS Nano* **3** 1767
[43] Jacobs D A, Catchpole K R, Beck F J and White T P 2016 A re-evaluation of transparent conductor requirements for thin-film solar cells *J. Mater. Chem.* A **4** 4490–96
[44] Lal N *et al* 2014 Optics and light trapping for tandem solar cells on silicon *IEEE J. Photovolt.* **4** 1380
[45] Barugkin C *et al* 2015 Light trapping efficiency comparison of Si solar cell textures using spectral photoluminescence *Opt. Express* **23** A391–400
[46] Miller O D, Yablonovitch E and Kurtz S R 2013 Intense internal and external fluorescence as solar cells approach the Shockley-Queisser efficiency limit *J. Photovolt.* **2** 303–11 (http://arxiv.org/abs/1106.1603, http://dx.doi.org/10.1109/JPHOTOV.2012.2198434)
[47] Ross R T 1967 Some thermodynamics of photochemical systems *J. Chem. Phys.* **46** 4590–3
[48] Green M A 2012 Radiative efficiency of state-of-the-art photovoltaic cells *Prog. Photovolt., Res. Appl.* **20** 472–6
[49] Lush G and Lundstrom M 1991 Thin film approaches for high efficiency III-V cells *Sol. Cells* **30** 337
[50] Hanna M C, Beard M C and Nozik A J 2012 Effect of solar concentration on the thermodynamic power conversion efficiency of quantum-dot solar cells exhibiting multiple exciton generation *J. Phys. Chem. Lett.* **3** 2857–62

[51] Schaller R and Klimov V 2004 High efficiency carrier multiplication in PbSe nanocrystals: implications for solar energy conversion *Phys. Rev. Lett.* **92** 186601

[52] Padilha L A, Stewart J T, Sandberg R L, Bae W K, Koh W K, Pietryga J M and Klimov V I 2013 Aspect ratio dependence of auger recombination and carrier multiplication in PbSe nanorods *Nano Lett.* **13** 1092–9

[53] Aerts M, Bielewicz T, Klinke C, Grozema F C, Houtepen A J, Schins J M and Siebbeles L D A 2014 Highly efficient carrier multiplication in PbS nanosheets *Nat. Commun.* **5**

[54] Cirloganu C M, Padilha L A, Lin Q, Makarov N S, Velizhanin K A, Luo H, Robel I, Pietryga J M and Klimov V I 2014 Enhanced carrier multiplication in engineered quasi-type-II quantum dots *Nat. Commun.* **5** 4148

[55] Kramer I J and Sargent E H 2014 The architecture of colloidal quantum dot solar cells: materials to devices *Chem. Rev.* **114** 863–82

[56] Semonin O E, Luther J M, Choi S, Chen H Y, Gao J B, Nozik A J and Beard M C 2011 Peak external photocurrent quantum efficiency exceeding 100% via MEG in a quantum dot solar cell *Science* **334** 1530–3

[57] Beard M C, Luther J M, Semonin O E and Nozik A J 2013 Third generation photovoltaics based on multiple exciton generation in quantum confined semiconductors *Acc. Chem. Res* (doi:10.1021/ar3001958)

[58] Timmerman D, Valenta J, Dohnalova K, de Boer W and Gregorkiewicz T 2011 Step-like enhancement of luminescence quantum yield of silicon nanocrystals *Nat. Nanotechnol.* **6** 710–3

[59] Cate S, Sandeep C S S, Liu Y, Law M, Kinge S, Houtepen A J, Schins J M and Siebbeles L D A 2015 Generating free charges by carrier multiplication in quantum dots for highly efficient photovoltaics *Acc. Chem. Res.* **48** 174–81

[60] Luque A, Marti A and Stanley C 2012 *Nat. Photon.* **6** 146

[61] Okada Y *et al* 2015 *Appl. Phys. Rev.* **2** 021302

[62] Sakamoto K, Kondo Y, Uchida K and Yamaguchi K 2012 *J. Appl. Phys.* **112** 124515

[63] Lantratov V M, Mintairov S A, Blokhin S A, Kalyuzhnyy N A, Ledentsov N N, Maximov M V, Nadtochiy A M, Pauysov A S, Sakharov A V and Shvarts M Z 2010 *Adv. Sci. Technol.* **74** 231

[64] Sogabe T, Shoji Y, Ohba M, Yoshida K, Tamaki R, Hong H-F, Wu C-H, Kuo C-T, Tomić S and Okada Y 2014 *Sci. Rep.* **4** 4792

[66] Tomić S, Jones T S and Harrison N M 2008 *Appl. Phys. Lett.* **93** 263105

[67] Sugaya T, Amano T, Mori M, Niki S and Kondo M 2010 *Jpn. J. Appl. Phys.* Part 1 **49** 030211

[67] Okada Y, Yoshida K, Shoji Y and Sogabe T 2013 *IEICE Electron. Express* **10** 20132007

[68] Ekins-Daukes N J and Schmidt T W 2008 *Appl. Phys. Lett.* **93** 063507

[69] Olsson P, Domain C and Guillemoles J-F 2009 *Phys. Rev. Lett.* **102** 227204

[70] Basore P A, Chug D and Buonassisi T 2015 Economics of future growth in photovoltaics manufacturing *Proc. 42nd IEEE PV Specialists Conf.* pp 1–4

[71] Wadia C, Alivisatos A P and Kammen D M 2009 Materials availability expands the opportunity for large-scale photovoltaics deployment *Environ. Sci. Technol.* **43** 2072

[72] Siebentritt S and Schorr S 2012 Kesterites–a challenging material for solar cells *Prog. Photovolt., Res. Appl.* **20** 512

[73] Green M A, Ho-Baillie A and Snaith H J 2014 The emergence of perovskite solar cells *Nat. Photon.* **8** 506

[74] Materials Genome Initiative Strategic Plan (December 2014); (https://whitehouse.gov/mgi)

[75] Zakutayev A, Caskey C M, Fioretti A N, Ginley D S, Vidal J, Stevanovic V, Tea E and Lany S 2014 Defect tolerant semiconductors for solar energy conversion *J. Phys. Chem. Lett.* **5** 1117

[76] https://materialsproject.org; http://aflowlib.org; http://materials.nrel.gov

[77] Stevanovic V, Zakutayev A and Lany S 2014 Composition dependence of the band gap and doping in Cu_2O-based alloys as predicted by an extension of the dilute-defect model *Phys. Rev. Appl.* **2** 044005

[78] Zakutayev A, Perry N H, Mason T O, Ginley D S and Lany S 2013 Non-equilibrium origin of high electrical conductivity in gallium zinc oxide thin films *Appl. Phys. Lett.* **103** 232106

[79] Rühle S, Anderson A Y, Barad H-N, Kupfer B, Bouhadana Y, Rosh-Hodesh E and Zaban A 2012 All-Oxide Photovoltaics *K. Phys. Chem. Lett.* **3** 3755

[80] Novoselov K S *et al* 2004 Electric field effect in atomically thin carbon films *Science* **306** 666–9

[81] Mak K F *et al* 2010 Atomically thin MoS2: a new direct-gap semiconductor *Phys. Rev. Lett.* **105** 136805

[82] Tran V, Soklaski R, Liang Y and Yang L 2014 Layer-controlled band gap and anisotropic excitons in few-layer black phosphorus *Phys. Rev.* B **89** 235319

[83] Lee H S, Min S W, Chang Y G, Park M K, Nam T, Kim H, Kim J H, Ryu S and Im S MoS2 nanosheet phototransistors with thickness-modulated optical energy gap *Nano Lett.* **12** 3695

[84] Bernardi M, Palummo M and Grossman J C 2013 Extraordinary sunlight absorption and 1 nm-thick photovoltaics using two-dimensional monolayer materials *Nano Lett.* **13** 3664

[85] Lee C-H *et al* 2014 Hone & Philip Kim: atomically thin p–n junctions with van der Waals heterointerfaces *Nat. Nanotechnol.* **9** 676–81

[86] Lee G-H *et al* 2013 Flexible and transparent MoS2 field-effect transistors on hexagonal boron nitride-graphene heterostructures *ACS Nano* **7** 7931–6

[87] Wi S, Kim H, Chen M, Nam H, Guo L J, Meyhofer E and Liang X 2014 Enhancement of Photovoltaic response in multilayer MoS2 induced by plasma doping *ACS Nano* **8** 5270–81

[88] Britnell L *et al* 2013 Strong light–matter interactions in heterostructures of atomically thin films *Science* **340** 1311

[89] Tahersima M H and Volker J 2015 Sorger: enhanced photon absorption toward 2D material-based spiral solar cell *Nanotechnology* **26** 344005

[90] Atwater H A and Polman A 2010 Plasmonics for improved photovoltaic devices *Nat. Mater.* **9** 205–13

[91] Wang Y, Plummer E W and Kempa K 2011 Foundations of plasmonics *Adv. Phys.* **60** 799–898

[92] Green M A and Pillai S 2012 Harnessing plasmonics for solar cells *Nat. Photon.* **6** 130–2

[93] Ross R T and Nozik A J 1982 Efficiency of hot-carrier solar energy converters *J. Appl. Phys.* **53** 3813–8
Nozik A J 2002 Quantum dot solar cells *Physica* E **14** 115–20

[94] Kempa K *et al* 2009 Hot electron effect in nanoscopically thin photovoltaic junctions *Appl. Phys. Lett.* **95** 233121

[95] Brongersma M L, Halas N J and Nordlander P 2015 Plasmon-induced hot carrier science and technology *Nat. Nanotechnol.* **10** 25–34

[96] Clavero C 2014 Plasmon-induced hot-electron generation at nanoparticle/metaloxide interfaces for photovoltaic and photocatalytic devices *Nat. Photon.* **8** 95–103

[97] Kempa K 2013 Plasmonic protection of the hot-electron energy *Phys. Status Solidi RRL* **7** 465–8
Kong J *et al* 2015 Toward a hot electron plasmonic solar cell *Opt. Express* (accepted) (doi:10.1364/OE.23.0A1087)

[98] Ye F, Burns M J and Naughton M J 2015 Embedded metal nanopatterns as a general scheme for enhanced broadband

light absorption *Phys. Status Solidi* A **212** 561–5
Ye F, Burns M J and Naughton M J 2012 Embedded metal nanopatterns for near-field scattering-enhanced optical absorption *ibid* **209** 1829–34
[99] Moddel G and Grover S (ed) 2013 *Rectenna Solar Cells* (New York: Springer) pp 398
[100] Yesilkoy F, Potbhare S, Kratzmeier N, Akturk A, Goldsman N, Peckerar M and Dagenais M 2013 A mid-IR antenna integrated with a geometrically asymmetrical metal-insulator-metal rectifying diode ed G Moddell and S Grover *Rectenna Solar Cells* (New York: Springer) pp 163–88
[101] Grover S and Moddel G 2011 Applicability of metal/insulator/metal (MIM) diodes to solar rectennas *IEEE J. Photovolt.* **1** 78
[102] Miskovsky N M, Cutler P H, Mayer A, Weiss B L, Willis B, Sullivan T E and Lerner P B 2012 Nanoscale devices for rectification of high frequency radiation from the infrared through the visible: a new approach *J. Nanotechnol.* 19
[103] Nguyen H Q, Cutler P H, Feuchtwang T E, Huang Z-H, Kuk Y, Silverman P J, Lucas A A and Sullivan T E 1989 Mechanisms of current rectification in an STM tunnel junction and the measurement of an operational tunneling time *IEEE Trans. Electron Devices* **36** 2671–8
[104] Dagenais M, Choi K, Yesilkoy F, Chryssis A N and Peckerar M C 2010 Solar spectrum rectification using nano-antennas and tunneling diodes *Proc. SPIE* **7605** article #76050E
[105] Grover S, Joshi S and Moddel G 2013 Quantum theory of operation for rectenna solar cells *J. Phys. D: Appl. Phys.* **46** 136106
[106] Joshi S and Moddel G 2013 'Efficiency limits of rectenna solar cells: theory of broadband photon-assisted tunneling *Appl. Phys. Lett.* **102** 083901
[107] Mashaal H and Gordon J M 2011 Fundamental bounds for antenna harvesting of sunlight *Opt. Lett.* **36** 900–2
[108] Vos A D 1980 Detailed balance limit of the efficiency of tandem solar cells *J. Phys. D: Appl. Phys.* **13** 839
[109] Cotal H *et al* 2009 III-V multijunction solar cells for concentrating photovoltaics *Energy Environ. Sci.* **2** 174–92
[110] Imenes A G and Mills D R 2004 Spectral beam splitting technology for increased conversion efficiency in solar concentrating systems: a review *Sol. Energy Mater. Sol. Cells* **84** 19–69
[111] Sheng X *et al* 2014 Printing-based assembly of quadruple-junction four-terminal microscale solar cells and their use in high-efficiency modules *Nat Mater* **13** 593–8
[112] Derendorf K *et al* 2013 Fabrication of GaInP/GaAs//Si solar cells by surface activated direct wafer bonding *IEEE J. Photovolt.* **3** 1423–8
[113] Polman A and Atwater H A 2012 Photonic design principles for ultrahigh-efficiency photovoltaics *Nat Mater* **11** 174–7
[114] Marion W and Wilcox S 1994 Solar radiation data manual for flat-plate and concentrating collectors *Natl. Renewable Energy Lab*
[115] Kosten E D, Kayes B M and Atwater H A 2014 Experimental demonstration of enhanced photon recycling in angle-restricted GaAs solar cells *Energy Environ. Sci.* **7** 1907–12
[116] Ganapati V, Chi-Sing H and Yablonovitch E 2015 Air gaps as intermediate selective reflectors to reach theoretical efficiency limits of multibandgap solar cells *IEEE J. Photovolt.* **5** 410–7
[117] Sheng X *et al* 2015 Device architectures for enhanced photon recycling in thin-film multijunction solar cells *Adv. Energy Mater.* **5** 1400919
[118] Eisler C N *et al* 2014 Multijunction solar cell efficiencies: effect of spectral window, optical environment and radiative coupling *Energy Environ. Sci.* **7** 3600–5
[119] Yoon J *et al* 2011 Flexible concentrator photovoltaics based on microscale silicon solar cells embedded in luminescent waveguides *Nat. Commun.* **2** 343
[120] Bronstein N D *et al* 2013 Luminescent solar concentration with semiconductor nanorods and transfer-printed micro-silicon solar cells *ACS Nano* **8** 44–53
[121] Bronstein N D, Yao Y, Xu L, O'Brien E, Powers A S, Ferry V E, Alivisatos A P and Nuzzo R G 2015 Quantum dot luminescent concentrator cavity exhibiting 30-fold concentration *ACS Photonics* **2** 1576–83
[122] Perlin J 2013 *Let It Shine: The 6000-Year Story of Solar Energy* (Novato, CA: New World Library)
[123] Lu H *et al* 2013 High-yield synthesis of silicon carbide nanowires by solar and lamp ablation *Nanotechnology* **24** 335603
[124] Gordon J M, Feuermann D, Huleihil M, Mizrahi S and Shaco-Levy R 2003 Surgery by sunlight on live animals *Nature* **424** 510
[125] Rabl A 1985 *Active Solar Collectors And Their Applications* (New York: Oxford University Press)
[126] Winston R, Miñano J C and Benítez P 2005 *Nonimaging Optics* (Oxford: Elsevier)
[127] Chaves J 2008 *Introduction To Nonimaging Optics* (Boca Raton, FL: CRC Press)
[128] Gordon J M 2010 Aplanatic optics for solar concentration *Opt. Express* **18** A41–52
[129] Kotsidas P, Modi V and Gordon J M 2011 Gradient-index lenses for near-ideal imaging and concentration with realistic materials *Opt. Express* **19** 15584–95
[130] Mashaal H and Gordon J M 2014 Basic limit for the efficiency of coherence-limited solar power conversion *Opt. Lett.* **39** 5130–3
[131] Ji S, Yin K, Mackey M, Brister A, Ponting M and Baer E 2013 Polymeric nanolayered gradient refractive index lenses: technology review and introduction of spherical gradient refractive index ball lenses *Opt. Eng.* **52** 112105
[132] Mojiri A, Taylor R, Thomsen E and Rosengarten G 2013 Spectral beam splitting for efficient conversion of solar energy: a review *Renew. Sustain. Energy Rev.* **28** 654–63
[133] Imenes A G and Mills D R 2004 Spectral beam splitting technology for increased conversion efficiency in solar concentrating systems: a review *Sol. Energy Mater. Sol. Cells* **84** 19–69
[134] Atwater H, Polman A, Kosten E, Callahan D, Spinelli P, Eisler C, Escarra M, Warmann E and Flowers C 2013 Nanophotonic design principles for ultrahigh efficiency photovoltaics *Nobel Symp. 153 Nanoscale Energy Convert* vol 15191 pp 17–21(New York: AIP)
[135] Hu Q, Xu D-H, Zhou Y, Peng R-W, Fan R-H, Fang N X, Wang Q-J, Huang X-R and Wang M 2013 Position-sensitive spectral splitting with a plasmonic nanowire on silicon chip *Sci. Rep.* **3** 3095
[136] Boriskina S V, Lee S Y K, Amsden J J, Omenetto F G and Dal Negro L 2010 Formation of colorimetric fingerprints on nano-patterned deterministic aperiodic surfaces *Opt. Express* **18** 14568–76
[137] Boriskina S V, Tong J K, Hsu W-C, Weinstein L, Huang X, Loomis J, Xu Y and Chen G 2015 Hybrid optical-thermal devices and materials for light manipulation and radiative cooling *Proc. SPIE 9546, Act. Photonic Mater.* **VII** 95461U
[138] Shen Y, Ye D, Celanovic I, Johnson S G, Joannopoulos J D and Solja I , M 2014 Optical broadband angular selectivity *Science.* **343** 1499–501
[139] Branz H (http://arpa-e.energy.gov/sites/default/files/documents/files/FOCUS_ProgramOverview.pdf)
[140] Boriskina S V and Chen G 2014 Exceeding the solar cell shockley-queisser limit via thermal up-conversion of low-energy photons *Opt. Commun.* **314** 71–8

[141] Chen G *et al* 2015 Internally-heated thermal and externally-cool photovoltaic cascade solar system for the full solar spectrum utilization *US 0053266 A1* (2015)
[142] Ni G *et al* 2015 Volumetric solar heating of nanofluids for direct vapor generation *Nano Energy* **17** 290–301
[143] Ross R T and Nozik A J 1982 Efficiency of hot-carrier solar energy converters *J. Appl. Phys.* vol 535 p 3813
[144] White T P and Catchpole K R 2012 Plasmon-enhanced internal photoemission for photovoltaics: theoretical efficiency limits *Appl. Phys. Lett.* **101** 073905
[145] Boriskina S V, Zhou J, Hsu W-C, Liao B and Chen G 2015 Limiting efficiencies of solar energy conversion and photo-detection via internal emission of hot electrons and hot holes in gold *Proc. SPIE 9608, Infrared Remote Sens. Instrum.* vol XXIII p 960816 (Bellingham,WA: SPIE Optical Engineering Press)
[146] Briggs J A, Atre A C and Dionne J A 2013 Narrow-bandwidth solar upconversion: case studies of existing systems and generalized fundamental limits *J. Appl. Phys.* **113** 124509
[147] Schulze T F and Schmidt T W 2014 Photochemical upconversion: present status and prospects for its application to solar energy conversion *Energy Environ. Sci.* **8** 103–25
[148] Fischer S, Favilla E, Tonelli M and Goldschmidt J C 2015 Record efficient upconverter solar cell devices with optimized bifacial silicon solar cells and monocrystalline BaY_2F_8:30% Er^{3+} upconverter *Sol. Energy Mater. Sol. Cells* **136** 127–34
[149] Naik G V and Dionne J A 2015 Photon upconversion with hot carriers in plasmonic systems *Appl. Phys. Lett.* **107** 133902
[150] Sellers D G, Polly S J, Zhong Y, Hubbard S M, Zide J M O and Doty M F New nanostructured materials for efficient photon upconversion *IEEE J. Photovolt.* **5** 224–8
[151] Fischer S, Martín-Rodríguez R, Fröhlich B, Krämer K W, Meijerink A and Goldschmidt J C 2014 Journal of Luminescence *J. Lumin.* **153** 281–7
[152] Monguzzi A, Bianchi F, Bianchi A, Mauri M, Simonutti R, Ruffo R, Tubino R and Meinardi F 2013 High efficiency up-converting single phase elastomers for photon managing applications *Adv. Energy Mater.* n/a–n/a (doi:10.1002/aenm.201200897)
[153] Zou W, Visser C, Maduro J A, Pshenichnikov M S and Hummelen J C 2012 Broadband dye-sensitized upconversion of near-infrared light *Nat. Photon.* **6** 560–4
[154] Wang P, Li Z, Salcedo W J, Sun Z, Huang S and Brolo A G 2015 2. Experimental section *Phys. Chem. Chem. Phys.* **17** 16170–7
[155] Huang Z, Li X, Mahboub M, Hanson K M, Nichols V M, Le H, Tang M L and Bardeen C J 2015 Hybrid molecule–nanocrystal photon upconversion across the visible and near-infrared *Nano Lett.* **15** 5552–7
[156] Bermel P *et al* 2010 Design and global optimization of high-efficiency thermophotovoltaic systems *Opt. Express* **18** A314–34
[157] Kolm H H 1956 Solar-battery power source *Tech. Rep., MIT Lincoln Laboratory. Quarterly Progress Report, Group* **35** 13
[158] Fraas L, Ballantyne R, Hui S, Ye S-Z, Gregory S, Keyes J, Avery J, Lamson D and Daniels B 1999 Commercial GaSb cell and circuit development for the midnight sun® TPV stove *Fourth NREL conference. on thermophotovoltaic generation of electricity* vol. 460 no. 1 pp 480–7(New York: AIP)
[159] Wanlass M W, Ahrenkiel S P, Ahrenkiel R K, Carapella J J, Wehrer R J and Wernsman B 2004 Recent advances in low-bandgap, inp-based gainas/inasp materials and devices for thermophotovoltaic (TPV) energy conversion *In Thermophotovoltaic Generation of Electricity: Sixth Conference on Thermophotovoltaic Generation of Electricity: TPV6* vol. 738 no. 1 pp 427–35(New York: AIP)
[160] O'Sullivan F, Celanovic I, Jovanovic N, Kassakian J, Akiyama S and Wada K 2005 Optical characteristics of 1D Si/SiO2 photonic crystals for thermophotovoltaic applications *J. Appl. Phys.* **97** 033,529
[161] Chan W R, Bermel P, Pilawa-Podgurski R C N, Marton C H, Jensen K F, Senkevich J J, Joannopoulos J D, Soljacic M and Celanovic I 2013 Toward high-energy-density, high-efficiency, and moderate-temperature chip-scale thermophotovoltaics *Proc. Natl. Acad. Sci. USA* **110** 5309–14
[162] Zhou Z, Chen Q and Bermel P 2015 Prospects for high-performance thermophotovoltaic conversion efficiencies exceeeding the shockley-queisser limit *Energy Conversion Manage.* **97** 63–9
[163] Gee J M, Moreno J B, Lin S-Y and Fleming J G 2002 Selective emitters using photonic crystals for thermophotovoltaic energy conversion *In Twenty-ninth IEEE Photovolt. Spec. Conf.*
[164] Yu Z, Sergeant N P, Skauli T, Zhang G, Wang H and Fan S 1730 Enhancing far-field thermal emission with thermal extraction *Nat. Commun.* **4**
[165] Sakr E, Zhou Z and Bermel P 2014 High efficiency rare-earth emitter for thermophotovoltaic applications *Appl. Phys. Lett.* **105** 111107
[166] Hargreaves C M 1969 Anomalous radiative transfer between closely-spaced bodies *Phys. Lett.* A **30** 491–2
[167] Biehs S A, Rousseau E and Greffet J J 2010 Mesoscopic description of radiative heat transfer at the nanoscale *Phys. Rev. Lett.* **105** 234301
[168] Polder D and van Hove M 1971 Theory of radiative heat transfer between closely spaced bodies *Phys. Rev.* B **4** 3303
[169] Xu J B, Lauger K, Moller R, Dransfeld K and Wilson I H 1994 Heat transfer between two metallic surfaces at small distances *J. Appl. Phys.* **76** 7209–16
[170] Mulet J-P, Joulain K, Carminati R and Greffet J-J 2002 Enhanced radiative transfer at nanometric distances *Microscale Thermophys. Eng.* **6** 209–22
[171] Shen S, Narayanaswamy A and Chen G 2009 Surface Phonon polaritons mediated energy transfer between nanoscale gaps *Nano Lett.* **9** 2909–13
[172] Rousseau E, Siria A, Jourdan G, Volz S, Comin F, Chevrier J and Greffet J-J 2009 Radiative heat transfer at the nanoscale *Nat. Photon.* **3** 514–17
[173] DiMatteo R S, Greiff P, Finberg S L, Young-Waithe K A, Choy H K H, Masaki M M and Fonstad C G 2001 Enhanced photogeneration of carriers in a semiconductor via coupling across a nonisothermal nanoscale vacuum gap *Appl. Phys. Lett.* **79** 1894
[174] Narayanaswamy A and Chen G 2003 Surface modes for near field thermophotovoltaics *Appl. Phys. Lett.* **82** 3544
[175] DiMatteo R *et al* 2004 Micron-gap ThermoPhotoVoltaics (MTPV) *AIP Conf. Proc.* **738** 42
[176] Francoeur M, Vaillon R, Mengüç M P *et al* 2011 Thermal impacts on the performance of nanoscale-gap thermophotovoltaic power generators *IEEE Trans. Energy Convers.* **26** 686–98
[177] Laroche M, Carminati R, Greffet J-J *et al* 2006 Near-field thermophotovoltaic energy conversion *J. Appl. Phys.* **100** 063104
[178] Park K, Basu S, King W P and Zhang Z M 2008 Performance analysis of near-field thermophotovoltaic devices considering absorption distribution *J. Quant. Spectrosc. Radiat. Transfer* **109** 305–16
[179] Ilic O, Jablan M, Joannopoulos J D, Celanovic I and Soljačić M 2012 Overcoming the black body limit in plasmonic and graphene near-field thermophotovoltaic systems *Opt. Express* **20** A366–84

[180] Svetovoy V B and Palantzas G 2014 Graphene-on-silicon near-field thermophotovoltaic cell *Phys. Rev. Appl.* **2** 034006
[181] Messina R, Antezza M and Ben-Abdallah P 2012 Three-body amplification of photon heat tunneling *Phys. Rev. Lett.* **109** 244302
[182] Mulet J-P 2003 Ecole centrale Paris *Thesis Title* Modélisation du rayonnement thermique par une approche électromagnétique
[183] Fleming J G, Lin S Y, El-Kady I, Biswas R and Ho K M 2002 All-metallic 3D photonic crystals with a large photonic band-gap *Nature* **417** 52–5
[184] Chan W R *et al* 2013 High energy density, high efficiency, moderate-temperature chip-scale thermophotovoltaics *Proc. Natl Acad. Sci. USA* **110** 5309–14
[185] Rinnerbauer V, Ndao S, Yeng Y X, Chan W R, Bermel P, Senkevich J, Joannopoulos J D, Soljacic M and Celanovic I 2012 Recent developments in high-temperature photonic crystals *Energy Environ. Sci.* **5** 8815–23
[186] Shen Y, Ye D, Celanovic I, Johnson S G, Joannopoulos J D and Soljacic M 2014 Optical broadband angular selectivity *Science* **343** 1499
[187] Lenert A, Bierman D M, Nam Y, Chan W R, Celanovic I, Soljacic M and Wang E N 2014 Nanophotonic solar thermophotovoltaics for high-performance solar power generation *Nat. Nanotechnol.* **9** 126–30
[188] Zoysa M D *et al* 2012 Conversion of broadband to narrowband thermal emission through energy recycling *Nat. Photon.* **6** 535–9
[189] Wurfel P and Ruppel W 1980 Upper limit of thermophotovoltaic solar-energy conversion *IEEE Trans. Electron Devices* **27** 745–50
[190] Swanson R M 1979 A proposed thermophotovoltaic solar energy conversion system *IEEE Proc.* **67** 446
[191] Würfel P 2008 *Physics of Solar Cells: From Principles to New Concepts* (Hoboken, NJ: Wiley)
[192] Manor A, Martin L L and Rotschild C 2015 On the conservation of photon rate in endothermic-photoluminescence and its transition to thermal emission, Accepted for publication in *Optica*
[193] Braun A, Katz E A, Feuermann D, Kayes B M and Gordon J M 2013 Photovoltaic performance enhancement by external recycling of photon emission *Energy Environ. Sci.* **6** 1499–503
[194] Yablonovitch E, Miller O D and Kurtz S R 2012 The opto-electronic physics that broke the efficiency limit in solar cells *In 2012 38th IEEE Photovoltaic Specialists Conf. (PVSC)*
[195] Torsello G, Lomascolo M, Licciulli A, Diso D, Tundo S and Mazzer M 2004 The origin of highly efficient selective emission in rare-earth oxides for thermophotovoltaic applications *Nat. Mater.* **3** 632–7
[196] Rotschild C, Tomes M, Mendoza H, Andrew T L, Swager T M, Carmon T and Baldo M A 2011 Cascaded energy transfer for efficient broad-band pumping of high-quality, micro-lasers *Adv. Mater.* **23** 3057–60
[197] Trombe F 1967 Perspectives sur l'utilisation des rayonnements solaires et terrestres dans certaines régions du monde *Rev. Gen. Therm.* **6** 1285
[198] Catalanotti S *et al* 1975 The radiative cooling of selective surfaces *Sol. Energy* **17** 83–9
[199] Granqvist C G and Hjortsberg A 1980 Surfaces for radiative cooling: silicon monoxide films on aluminum *Appl. Phys. Lett.* **36** 139
[200] Berdahl P, Martin M and Sakkal F 1983 Thermal performance of radiative cooling panels *Int. J. Heat Mass Transf.* **26** 871–80
[201] Gentle A R and Smith G B 2010 Radiative heat pumping from the Earth using surface phonon resonant nanoparticles *Nano Lett.* **10** 373–9
[202] Rephaeli E, Raman A and Fan S 2013 Ultrabroadband photonic structures to achieve high-performance daytime radiative cooling *Nano Lett.* **13** 1457–61
[203] Raman A P, Anoma M A, Zhu L, Rephaeli E and Fan S 2014 Passive radiative cooling below ambient air temperature under direct sunlight *Nature* **515** 540–4
[204] Gentle A R and Smith G B 2015 A subambient open roof surface under the mid-summer sun *Adv. Sci. advs.* 201500119
[205] Zhu L, Raman A, Wang K X, Anoma M A and Fan S 2014 Radiative cooling of solar cells *Optica* **1** 32–8
[206] Byrnes S J, Blanchard R and Capasso F 2014 Harvesting renewable energy from Earth's mid-infrared emissions *Proc. Natl. Acad. Sci. USA* **111** 3927–32
[207] Hossain M M, Jia B and Gu M 2015 A metamaterial emitter for highly efficient radiative cooling *Adv. Opt. Mat.* **3** 1047–51
[208] Shi N N, Tsai C-C, Camino F, Bernard G B and Yu N 2015 Keeping cool: enhanced optical reflection and heat dissipation in silver ants *Science* aab3654
[209] Landau L and Lifshitz E 1980 *Statistical Physics, Part 1.*
[210] Petela R 1964 Exergy of heat radiation *J. Heat Transfer* **86** 187–93
[211] Chen G 2005 *Nanoscale Energy Transport and Conversion* (Oxford: Oxford University Press)
[212] Mashaal H and Gordon J M 2014 Basic limit for the efficiency of coherence-limited solar power conversion *Opt. Lett.* **39** 5130–3
[213] Mungan C E 2003 Thermodynamics of radiation-balanced lasing *J. Opt. Soc. Am.* B **20**

QUERY FORM

JOURNAL: Journal of Optics

AUTHOR: S Boriskina *et al*

TITLE: Roadmap on optical energy conversion

ARTICLE ID: joptaa0bbf

The layout of this article has not yet been finalized. Therefore this proof may contain columns that are not fully balanced/ matched or overlapping text in inline equations; these issues will be resolved once the final corrections have been incorporated.

SQ1
Please be aware that the colour figures in this article will only appear in colour in the online version. If you require colour in the printed journal and have not previously arranged it, please contact the Production Editor now.
